NCAR/TN-488+STR
NCAR TECHNICAL NOTE

April 12, 2012

Thermodynamic Profiling Technologies Workshop Report to the National Science Foundation and the National Weather Service

Editors and Co-Chairs
R.M. Hardesty
R.M. Hoff

Contributing Authors
R.M. Hoff
R.M. Hardesty
F. Carr
T. Weckwerth
S. Koch
A. Benedetti
S. Crewell
N. Cimini
D. Turner
W. Feltz
B. Demoz
V. Wulfmeyer
D. Sisterson
T. Ackerman
F. Fabry
K. Knupp

Principal Investigators
R.E. Carbone
R.J. Serafin

Co-sponsored by the National Science Foundation and the U.S. National Weather Service, Office of Science and Technology.

Any opinions, findings, conclusions, or recommendations expressed in this publication are those of the authors and do not necessarily reflect the views of either the National Science Foundation or the National Weather Service.

National Center or Atmospheric Research
P.O. Box 3000
Boulder, Colorado 80307-3000

NCAR/TN-488+STR
NCAR TECHNICAL NOTE
April 12, 2012

Thermodynamic Profiling Technologies Workshop Report to the National Science Foundation and the National Weather Service

Editors and Co-Chairs

R. Michael Hardesty — NOAA Earth System Research Laboratory Chemical Sciences Division
Raymond M. Hoff — University of Maryland, Baltimore County

Contributing Authors

Raymond M. Hoff — University of Maryland, Baltimore County
R. Michael Hardesty — NOAA Earth System Research Laboratory Chemical Sciences Division
Fred Carr — University of Oklahoma
Tammy Weckwerth — National Center for Atmospheric Research Earth Observing Laboratory
Steven Koch — NOAA Earth System Research Laboratory Global Systems Division
Angela Benedetti — European Centre for Medium-Range Weather Forecasts
Suzanne Crewell — Universität zu Köln
Domenico Cimini — IMAA-CNR Istituto di Metodologie per l'Analisi Ambientale (IMAA), Department of Earth and Environment of the Italian National Research Council (CNR)
David Turner — NOAA National Severe Storms Laboratory
Wayne Feltz — University of Wisconsin at Madison, Cooperative Institute for Meteorological Satellite Studies (CIMSS) Space Science and Engineering Center (SSEC)
Belay Demoz — Howard University
Volker Wulfmeyer — Universität Hohenheim
Doug Sisterson — Argonne National Laboratory
Tom Ackerman — University of Washington
Frederick Fabry — McGill University
Kevin Knupp — University of Alabama in Huntsville

Principal Investigators

Rit E. Carbone — National Center for Atmospheric Research
Robert J. Serafin — National Center for Atmospheric Research Earth Observing Laboratory

Co-sponsored by the National Science Foundation and the U.S. National Weather Service, Office of Science and Technology.

Any opinions, findings, conclusions, or recommendations expressed in this publication are those of the authors and do not necessarily reflect the views of either the National Science Foundation or the National Weather Service.

National Center or Atmospheric Research
P.O. Box 3000
Boulder, Colorado 80307-3000

Foreword

The Thermodynamic Profiling Technologies Workshop was convened on 12-14 April 2011 to assess the merits of ground-based remote sensing technologies applicable to highly resolved observations and analyses of temperature and moisture in the lower troposphere over land. Such observations are central to some of the most important research and operational goals in atmospheric and Earth system studies, mesoscale numerical weather prediction, and monitoring of regional climate variability. The Workshop was also motivated by the recommendations of the NRC study *Observing Weather and Climate from the Ground Up; A Nationwide Network of Networks* (2009, available at http://www.nap.edu/catalog.php?record_id=12540), several of which dealt with observational priorities in the low troposphere.

Workshop Objectives

- Identify currently available and potentially suitable profiling technologies, singly or in combination, that show promise to meet or exceed "reasonable" performance requirements and potentially attractive cost-performance trade-offs for a national multi-use network.
- Identify what, if any, additional technological advancements may be necessary to achieve satisfactory performance or a more cost effective lifecycle solution for: a) the national multi-use network; and b) specialized research applications.
- Identify the potential for additional-variable sensing opportunities (wind, O_3, SO_2, CO, or $PM_{2.5}$) that might be accomplished and/or complemented in whole or in part by the thermodynamic observing system.
- Provide a set of guiding principles with regard to profiling network performance, operations, and forecast impact attributes.
- Describe and prioritize a focused set of "testbed" activities, objectives, timetable, and metrics for success. In general, testbeds should address technology performance, operational practices, and the forecast sensitivity to improved observations.
- Identify educational opportunities related to the development, testing and deployment of a national profiling network, and advanced research systems.
- Provide input regarding NSF's support for new research instrument developments and inform students and researchers of opportunities for enhancement of observational technologies.

Participants included national and international experts from academia, research laboratories, and industry (see Appendix A). The format of the workshop, which extended over two and one-half days, included invited overview talks, panel discussions, and significant opportunities for community input during open discussion periods.

This report summarizes presentations and discussions from each of the workshop sessions. Issues addressed in the report include motivation for the workshop, overview of the major technologies available for observing thermodynamic profilers, and a discussion of how technologies could be incorporated into a workshop. Recommendations on the next step are presented.

Thermodynamic Profiling Technologies Workshop

Contents

SUMMARY OF MAJOR WORKSHOP FINDINGS

Following is a list of major points and conclusions from the workshop based on the oral presentations and major discussion sessions:

- The requirements for thermodynamic profiles are highly dependent on the specific applications. Among the more demanding performance requirements are those intended to improve forecasts of convective initiation and storm strength. For this application it was generally agreed that temperature profile measurements are needed to better than 1°C accuracy, while moisture profiles should be better than 1 g kg^{-1}. The desired vertical resolution was 50-100 m. Such measurements are likely attainable with currently-available or future technologies, albeit at variable spatial resolution. Adding wind profiles alongside thermodynamic profiles has been shown to improve forecasts of convective activity, suggesting co-location of thermodynamic and wind profiling capabilities. Knowledge of the fine scale structure of boundaries improved knowledge of moisture convergence, which then can be derived from timeseries analysis of continuous vertical profiles. Such analyses would also benefit substantially from horizontal gradient information provided by horizontal scanning.

- Microwave radiometers (MWR) can be used to measure temperature, humidity, and integrated cloud amounts. Ground-based temperature and water vapor profiling are characterized by weighting functions at the different frequencies that decrease continuously with height and limit vertical resolution (which is ~50m near the surface and decreases to 300m aloft) with ~ 2-3 degrees of freedom. Liquid water path can also be observed. Microwave radiometer profilers have been commercially available for more than a decade. Commercial microwave radiometers use statistical algorithms to provide temperature and humidity. Retrievals can be enhanced through the use of additional information provided by e.g., cloud radar and ceilometer or numerical weather prediction model output (e.g., one-dimensional variational retrieval, 1DVAR). Vertical scanning provides enhanced boundary layer temperature profiling but does not improve water vapor profiling. Microwave radiometers provide unattended measurements of water vapor at high temporal resolution, although absolute calibration still poses challenges. Retrievals are independent of the occurrence of clouds although heavy precipitation can affect measurements. Significant synergy exists between MWR, lidars and passive IR retrievals. Currently about one hundred MWR systems are operating continuously worldwide, although coordination among these systems is limited. Interference from wireless communications is becoming an increasing problem.

- Infrared radiometry for temperature and moisture profiling has an extensive heritage. Commercially-available instruments are hardened and well-proven. Retrieval techniques include "onion peeling" and the one-dimensional variational method (1DVAR). Automated calibration methods enable measurement of radiance to better than 1%. Ground-based instruments provide best spatial resolution extremely close to the surface, with resolution degrading at higher elevations. Current IR technologies are capable of retrieving qT profiles to 3-4 km with ~4-8 degrees of freedom. Presence of clouds above the instruments can adversely affect the measurement, although co-located measurements from a ceilometers or lidar can mitigate the effect. Measurements are not possible during precipitating conditions. Deployment configuration would focus on zenith-pointing; no significant advantage is gained by scanning. Pairing an infrared radiometer with a microwave instrument would improve the initial guess and enable combined retrievals, but would increase cost. Additional research to improve spectroscopy and addressing the benefits of combined retrievals would be beneficial. Costs of these systems would be a few hundred thousand dollars, installed.

- Differential absorption lidar (DIAL) is a candidate technology for a water vapor profiling network. The technique has been extensively applied and validated, mostly for research applications. State of the art research systems can measure water vapor concentrations to ranges of several km with better than 5% accuracy and range resolution of 100 m or so. Automated DIAL systems have not been demonstrated, however recent research has indicated the potential of compact solid-state instruments incorporating diode laser sources and flared amplifiers for automated profiling. Cost for such a system would likely be a few hundred $K. Support for research and development to encourage technology advancement associated with small systems would be extremely useful. By employing a low-cost, compact DIAL, continuous, lower troposphere water-vapor profiling with high absolute accuracy (error < 5 %) should be possible without need for calibration. Such a system should be able to obtain measurements with spatial/temporal resolutions of 50-300m and 15-30 min during daytime and nighttime, respectively up to 3-6 km.

- Water-vapor and temperature Raman lidar systems are capable of measurements to heights of ~4 km in daytime and ~10 km at night with about 30m vertical resolution over 1 minute time steps. State of the art systems have errors <5% in q and < 1°C. Raman instruments have demonstrated continuous automated monitoring of water vapor at the Department of Energy CART

site in Oklahoma and at the Swiss Meteorological Service site in Payerne, Switzerland. Data from the Payerne lidar are being transmitted to the MeteoSwiss service for assimilation into forecast models. Raman systems utilize powerful lasers and large telescope apertures, and also require an integrated water vapor measurement for calibration, all of which tends to increase costs. A Raman system for automated water vapor profiling will likely cost several hundred $K to more than $1M. Analysis of returns in the rotational Raman band can be applied to measure temperature profiles, although utility of Raman lidar temperature data for assimilation into models has not been demonstrated.

- Other methods can also provide information on thermodynamic profiles, but are likely more limited in their suitability as sensors in operational networks. Use of the Global Navigation Satellite Systems as a signal source and low orbiting satellites as receivers to estimate changes in refractive index can provide some profile information, albeit at poor horizontal resolution. Ground-based GPS receivers can also be used to estimate refractive index induced changes along the path between the receiver and individual GNSS satellites. Application of meteorological radars to observe horizontal variations in refractive index near the surface computed from the radar returns from hard targets can provide maps of refractive index variations to ranges of about 40 km. Another technique, DIfferential Attenuation Radar (DIAR) makes use of differential attenuation by water vapor at two wavelengths to derive humidity information. However, DIAR sampling depends on the presence of a distribution of background targets at various ranges to recover water vapor profile information, so the profile depth of retrieved water vapor may be limited, particularly in precipitation-free conditions. Radio-acoustic sounding (RASS) can measure virtual temperature profiles, but strong wind and the irritating effects of acoustic noise on nearby people are issues. Overall, comprehensive integration of different methods that optimize observations with differing resolutions, advantages and disadvantages, and measurement methodologies (e.g., scanning versus fixed) was viewed by workshop participants as a highly desirable and probably necessary feature for comprehensive observations.

- Testbeds allow for testing of scientific theories, computational tools, and new technologies. Testbeds can be used to compare instruments, such as remote sensing systems, to determine a best methodology, and/or to evaluate the accuracy of a model or process. The primary users of a network of thermodynamic profilers will be the National Weather Service and associated forecasters that develop early warning, although researchers and model developers will also have a significant interest. A testbed can be established at a single location or mobile. Because different observations may be more or less useful for improving forecasts in different parts of the country, a flexible mobile testbed could be altered for specific regions. However, moving the testbed will eliminate the availability of continuous long-term data at a single location. All testbed data should ideally be saved and archived for research value. A testbed should be designed and budgeted to incorporate change, and should include a role for associated field campaigns to provide insights into important processes. An important aspect of a testbed is the development of clientele to promote synergisms among users and researchers.

- A proposed testbed or network should take into account the availability of other thermodynamic information such as soundings by balloon and airplanes (e.g., ACARS, TAMDAR), satellite-borne sensors (GNSS receivers, IR, and MW profilers, etc.), wind profilers, radars (radars provide the 0°C level and can detect wind shear levels that are associated with temperature and moisture gradient layers). Work to optimally combine testbed data with observations from other sources will be an important component in evaluating the impact of the testbed instruments.

SECTION 1. MOTIVATION

In 2009, a Committee of the National Academy's Board on Atmosphere and Climate assessed the current national needs for improved measurements of the lower atmosphere, particularly the lowest 2-3 kilometers where the vertical structure of the atmosphere is determined by land-surface exchange of moisture and energy, orography, and turbulence. The report from this panel (NRC, 2009) recognized the importance of measurements in this region of the atmosphere to five areas of societal needs (energy security, public health and safety, transportation, water resources, and food production) and determined that there were commonalities that could be better addressed by a modernized observing system, relying primarily on remote sensing techniques that have been developed over the last half century. While these suggested observations involved the measurement of traditional meteorological variables, they also included measurements of a wide range of atmospheric trace gases and particles. Here we examine the state-of-the-art of current measurements of temperature and water vapor as fundamental indicators of the thermodynamic structure of the Planetary Boundary Layer (PBL) and suggest a path forward for national agencies to start addressing these observational needs. We term these measurements "Thermodynamic Profiling of the Troposphere" or TPT.

1.1 Other Recent Assessments of TPT Needs

A 1998 workshop on remote sensing of lower-tropospheric water vapor highlighted standard and emerging technologies (Weckwerth et al., 1999). Table 3 of that paper summarizes water vapor instrument performance and remains largely valid today. The workshop identified scientific research requirements for improved moisture measurements from the planetary boundary layer, atmospheric chemistry, hydrology, tropical convection, severe weather, climate, and polar research communities. While radiosondes and passive remote sensors have been available for some time, the broad requirements for improved moisture measurements still remain today. The recommendations of the 1998 workshop included a charge to improve and develop active and passive remote sensing techniques to obtain four-dimensional fields of water vapor. There was also a call for field campaigns for water vapor measurement validation.

The 1998 water vapor workshop partially motivated the International H_20 Project (IHOP_2002; Weckwerth et al., 2004) which was conducted in the U.S. Southern Great Plains in late spring, 2002. IHOP_2002 brought together many standard and state-of-the-art water vapor, temperature, and wind sensors to better understand warm-season convective precipitation. One of the four primary goals of IHOP_2002 was to utilize the varied moisture sensors to determine the future optimal mix of operational water vapor measurement strategies to better predict warm-season rainfall. Additionally, IHOP_2002 participants worked toward better quantification of measurement accuracy, precision, and performance limitations. This led to detailed intercomparisons between water vapor lidars and radiosondes and enhanced the confidence level of water vapor remote sensors (e.g., Behrendt et al., 2007a; 2007b). One of the remaining outstanding goals of IHOP_2002 is to assimilate the varied water vapor data to create four-dimensional moisture fields for research and forecasting applications.

Conclusions from the IHOP_2002 experiment showed that the water vapor observations, along with wind and temperature measurements and radar observations, have potential for assimilation into numerical models. Data assimilation from IHOP_2002 has shown a positive impact on quantitative precipitation forecasting (QPF) skill (Wulfmeyer et al., 2006, Liu and Xue, 2008). Additionally the improved measurements have led to better understanding of convection initiation processes (Murphey et al., 2006; Miao and Geerts, 2007; Wakimoto and Murphey, 2010) and in the difficulties in NWP forecasting skill (Wilson and Roberts, 2006).

There has been significant progress in assessing the relationships between land surface heterogeneities and boundary layer moisture distribution (Martin and Xue 2006). IHOP_2002 demonstrated that a mix of operational ground-based and satellite-borne moisture sensing instruments and assimilation techniques are essential for improving forecasts of convective rainfall. The Lindenberg Campaign for Assessment of Humidity and Cloud Profiling Systems and its Impact on High-Resolution Modeling (LAUNCH-2005) operated a triangle of three water-vapor Raman lidar systems. Using the MM5 4DVAR, Grzeschik et al. (2008) demonstrated a significant positive impact of these systems on the analysis of the water-vapor field, which lasted about 12 h.

In 2007, the Department of Energy contributed the ARM Mobile Facility (AMF), which operated many of the same sensors as IHOP_2002 to a large observational study in Europe called the Convective Orographically-induced Precipitation Study (COPS; Wulfmeyer et al., 2008, 2011). The overarching objective of COPS is to "advance the quality of forecasts of orographically induced convective precipitation by 4-dimensional observations and modelling of its life cycle." COPS has been endorsed as a Research and Development Project (RDP) of the World Weather Research Program (WWRP), which will ensure that COPS technologies will emerge into a more operational setting. A strong backbone of COPS was extensive water-vapor remote sensing synergy at different supersites and a strong collaboration with forecast centers for quasi-operational COPS data assimilation (DA) studies (Zus et al., 2008; Yan et al., 2009; Schwitalla et al., 2011; Bauer et al., 2011). Water-vapor lidar demonstrated a strong impact on the analysis

for better prediction of convection and precipitation by means of 3DVAR in combination with a 3-h rapid update cycle. It is time now for the U.S. to similarly begin to move some of the research results generated in these large experiments into an operational environment where on-going measurements can be routinely used to improve forecast skill in numerical models.

Table 1.1 summarizes the primary requirements for measurements at a variety of scales.

1.2 Research Needs for Thermodynamic Profiling Systems

Thermodynamic profilers are subdivided in this report into passive and active remote sensors, by wavelength of the measurement, and combined with in-situ measurements from the ground and on aircraft (so called hybrid techniques). Many sensors are already operational, e.g., the ACARS, radar wind profilers, GPS, and the WSR-88D (NEXRAD) radar network. The Aircraft Meteorological Data Relay (AMDAR) and Aircraft Communication Addressing and Reporting System (ACARS) have been demonstrated in operational global data assimilation use (Cardinali et al., 2003), into the European regional forecast systems, and are now routinely assimilated into the NWS forecast system. Radar wind profilers are utilized in a network of nearly 100 units in the U.S. to give winds throughout the troposphere. The NEXRAD network is central to understanding precipitation and clouds throughout the troposphere.

During the workshop, reports from convection and boundary layer experts emphasized that the atmospheric boundary layer (ABL) contains a multitude of phenomena with sharp spatial and temporal gradients that impose stringent requirements for observational resolution and accuracy of all measurements in this region if these phenomena are to be understood and predicted well. For example, horizontal convective rolls (HCRs) affect fine-scale stability and convergence structure, which can influence the location of convection initiation (Weckwerth, 2000). Convection initiation can also be triggered or modulated by cold fronts (e.g., Koch and Clark, 1999), gravity and solitary waves, undular bores (Karyampudi et al., 1995) and outflow boundaries (gust fronts, e.g., Wilson and Schreiber, 1986). Land-surface heterogeneity and orography play an essential role in the formation of convergence zones leading to a strong variability in the temporal-spatial intensity of precipitation (Wulfmeyer et al., 2011). The small-scale wind and stability variations are not well-sampled within these potential convection initiation precursors. There remains a great deal to be understood about nocturnal boundary layer behavior, especially under what conditions it can be partially or completely mixed out. Additionally, observations capable of improving the understanding of elevated convection initiation and maintenance are scarce (e.g., Marsham et al., 2011). Improvement in parameterization of surface and boundary layer processes for numerical models requires more detailed (and sustained) measurements. And, because models can predict ABL variables in great spatial/temporal detail, observations are needed to verify these estimates and show where the greatest modeling improvements are necessary.

Table 1-1. Observational requirements (from WMO, ESA, USWRP, and EUMETSAT sources).

Parameter	Turbulence	Weather Forecasting	Initiation of Convection	Regional Climate	Global Climate
Horizontal Resolution (m)	30	200-3000	300	10000	50000
Vertical Resolution in ABL (m)	30	30-150, Increasing with Height	50-100	50-300, Increasing with Height	500
Vertical Resolution in Free Troposphere (m)	---	~500	500	~500	500-1000
Repeatability, s	1	900	600	3600 (1h)	21600 (6h)
Precision %WV °K	 5 0.2	 10 0.2	 10 0.2	 10 0.2	 10 0.2
Bias %WV °K	 ---	 5 0.2	 5 0.2	 1-2 0.1	 1-2 0.1
Timeliness	---	10 m (nowcasting)	---	---	---
Coverage	Vertical Profiling	2D, 3D (radius<10 km)	2D, 3D (radius>10 km)	100 x 100 km	Global
Data Assimililation	---	Observational Error Covariance Matrix	Observational Error Covariance Matrix	---	---

Table 1-2. Measurements of a given atmospheric variable per hour over a 10*10 km area, roughly comparable to the size of a convective cell. For this exercise, a typical surface station would be counted as reporting information for 5 variables (P, T, T_d, winds, and precipitation).

Data Source	Number of Observations
Upper air observation of any variable using planes, radiosondes, GPS…	≈ 0–10 (0–8 about thermodynamics)
Surface observations of any variable	≈ 0–10 (0–4 about thermodynamics)
Geostationary satellite (per channel)	≈ 25
Radial velocity, assuming 10% echo coverage	≈ 2,500
Radar reflectivity	≈ 25,000

At the mesoscale, there is a mismatch between the resolution of information available on precipitation (primarily using radar) and that obtained on the thermodynamic variables that ultimately dictate the evolution of storm systems: every hour, over a size comparable to that of a convective cell (100 km^2), radar provides of the order of 25,000 measurements of precipitation and winds, while there is considerably less information for thermodynamic variables, especially in the lower atmosphere away from the surface (Table 1.2). With at best only a couple of temperature or humidity measurements throughout the volume and life cycle of a thunderstorm cell, a proper forecast is impossible.

For temperature and humidity information, the NRC report suggested that the U.S. could be covered by sensors spaced on the scale of current radiosonde synoptic measurements (~150 km), which could require up to 400 sites nationally. This call for a large number of new, sophisticated stations has certainly raised eyebrows and has demonstrated that an important first step is to prove that measurements on this scale will improve our current forecasting capability commensurate to the cost of such implementation. This cannot be assessed by a local scale field project such as IHOP_2002 or COPS. It can be assessed by a short term demonstration project on a larger scale but such an assessment on a national scale is likely to be cost prohibitive when the infrastructure cost of the demonstration is a major impediment. To that end, the workshop was drawn to the potential for one or more regional demonstrations, to be justified below.

1.3 Operational Needs for Thermodynamic Profilers

"Operational" refers both to the data needs of forecasters, media, and first responders in order to convey crucial and timely information to the public, and to the provision of sufficient initial conditions to NWP models to enable prediction of ABL and convective phenomena. For the former, the greatest need is increased temporal resolution over the 12hr rawinsonde period for thermodynamic data in the ABL. In North America, the 00Z and 12Z launch times for these rawinsondes are particularly ill-suited to determine the maximum and minimum diurnal cycle excursions of the ABL (measurements are made at 4-7 a.m. and p.m. local standard time in the continental U.S.) Satellites and radars can provide 5-minute (and possibly higher) resolution of winds, clouds, and rain. However, high-frequency, high-resolution thermodynamic observations are important for monitoring/now-casting important tropospheric characteristics such as inversion strength, transient waves important to nighttime convection, PBL height, freezing level, CAPE, and convergence zones.

For NWP, early studies on the sensitivity of initiation and mode of convection to initial temperature and moisture values provided by Crook (1996) suggested that we need to measure them to within 1 K and 1 g kg^{-1}, respectively (Ducrocq et al., 2000; Dierer et al., 2009; Li et al., 2011; Lin et al., 2011). The requirements for initiation may not be as stringent in regions of moderate to strong mesoscale forcing, however the requirements for mode of convection may still require such precision (Ziegler et al., 2010). Forecasts of convection and ABL structure are also sensitive to fine-scale vertical gradients of wind and stability (Richardson et al., 2007). Most importantly, unlike large-scale motions for which wind-pressure relationships can evolve information on unobserved fields from observations of one or the other, there are no such balances on the convective scale, requiring wind and thermodynamic measurements to be made simultaneously and with similar spatial and temporal resolution.

Use of satellite data has become central to the operational observing system. As was pointed out, however, in the NRC study (2009), satellite sounders have limited or no resolution for the lower troposphere. Although cloud cover is one factor in this inability to see into the PBL, the primary limitation is physical; the weighting functions for sounding are too broad to be able to resolve structures in the PBL.

1.4 Climate Needs for Thermodynamic Profilers

In order to understand how local and regional climates will respond to increased heating from greenhouse gases, it is vital to have the proper measurements to monitor potential changes. Tem-

perature and moisture responses in the troposphere will depend on the fluxes of these quantities into and through the ABL via turbulence and moisture convection. While even most surface networks are deficient in their ability to measure such fluxes, the situation is especially dire above the surface, where there exist only a few research towers that collect such data. Given the high spatial variability of topography, soil and vegetation cover, etc., a national network of lower tropospheric sensors is needed for sufficient monitoring and understanding of changes in thermodynamic properties resulting from the evolving climate.

Climate modification from radiative gas forcing or aerosols is likely to be reflected in the thermodynamic properties in the lower troposphere. Changes in the surface energy balance will change both the ABL profile as well as the height of the ABL. There is a need for ABL climatologies to be developed to observe how the ABL stability, moisture, and depth is responding to warmer temperatures and increased transpiration. The thermodynamic profile will respond to increased humidity in the boundary layer by decreasing the lapse rate and CAPE will increase with stronger surface latent heat fluxes. Additional water in the lower atmosphere is a predicted feature of the warming of the atmosphere but the feedbacks between cloud formation and precipitation in an atmosphere with both increased temperature and increase condensation nuclei from pollution sources is not well understood. This has led the IPCC to call climate response of aerosols in a warming climate one of the least well known forcing agents for climate. The multitude of potential confounding influences is daunting. Increased temperature and drying in boreal forests has begun to show a signature in increased forest fires in northern boreal regions (Turetsky et al., 2011). Those fires produce absorbing aerosols in the lower free troposphere and there are indications that those aerosols heat the free troposphere, creating elevated inversions or suppressing convection. McMillan et al. (2010) conjectured that this suppression of convection may have resulted in a strengthened inversion and worsening of a major pollution episode in Houston, Texas, from fire plumes which were generated in California.

The increased capacity for the lower atmosphere to hold water will create changes to the cloud cover of the planet as well as perturb the precipitation-evaporation balance of the planet. Our understanding of the water and energy cycles which have been derived over the last 100 years may need modification in a climate which on average is warmer than the past. These changes and their effects on circulation are possible to measure now at very high resolution with lower tropospheric profilers (see sections below) and improvement in long-term, systematic observations at these scales will help refine predictions of humidity and precipitation from climate models. Climate measurements from satellites require continuity between the relatively short lifetimes of instruments in orbit; ground-based sensors with sufficient QA/QC can bridge gaps between satellite profilers and sounders.

1.5 Will Such TPT Data Be Used?

The previous local scale experiments that combine these state of the art observations indicate that data are now available at spatial and temporal scales which will add value to quantitative forecasts. There is strong evidence (particularly emphasized by satellite observations and ACARS/AMDAR measurements) that the operational data assimilation systems will ingest these data if they are both widespread and routinely available. Statements were made at the workshop that it is too expensive to begin ingestion of observations from systems that are only going to be available for a short period of time or are not sufficiently spatially distributed to cover the entire forecast domain. The step to prove that such data will improve forecasts can be demonstrated by Observing Systems Experiments (OSEs) and Observing Systems Simulation Experiments (OSSEs). Both of these techniques are an investment to decrease the cost and decrease the risk of implementing operational systems. We will discuss these in the next section.

The NRC Report (2009) identified nearly a dozen other sectors that potentially would use such data, if available. Power line icing in winter, effects of fog on air, rail and mobile transportation, roadway winter conditions, evapotranspiration and the effects on surface/groundwater, convective initiation in mesocyclones, etc., are applications that rely on precise, relatively local prediction of changes in temperature and humidity. In each case, these sectors identified significant cost outlays from the lack of poor advance knowledge of essentially predictable events that affected corporate effectiveness and public welfare. The obvious link between weather and aircraft safety drove much of the observing system of the 20th century and the 21st century should expand observations where weather awareness benefits other important societal needs.

1.6 Use of OSE and OSSE in Observing System Impact Assessments

Deploying a new network of sensors is expensive, and thus there is a desire to understand what benefits a new network might provide relative to the expense of establishing the new observation system. Two numerical modeling techniques commonly used to determine the value of an observing system or a particular variable to an analysis or forecast are observing systems experiments (OSE) and observing systems simulation experiments (OSSE). OSEs, often called "data denial experiments," systematically add or deny existing data sets to a control forecast and assess the differences.

OSEs have several advantages:

- Real data are used with appropriate error covariance estimates without the need of their artificial simulation.
- The new observations are assimilated in addition to many routine observations (depending on the sophistication of

the forecast system) giving real insight in the impact of additional observations.

- State-of-the-art DA systems can be applied and compared, e.g., variational or ensemble-based techniques.
- The impact of additional observations is measured using skill score analysis of independent data sources.
- Real existing cases are verified with respect to forecast accuracy taking into account the limitation of the forecast system.

OSEs are possible if new observing systems are operated with sufficient spatial density and duration. However, for demonstrating forecast impact, it is not necessary to operate the remote sensing systems over a large domain. As soon as interesting cases on convection initiation and precipitation are occurring downstream, DA studies can be performed and the forecast impact measurement by appropriate skill scores.

Alternatively, an Observation System Simulation Experiment (OSSE) can be used for quantifying the cost versus benefit of a new observing system or a network of composited sensors. An advantage of the OSSE framework is the ability to verify the forecast and analysis against an absolute "truth." This is not possible with real data, as the state of the entire atmosphere is never accurately known. If the OSSE setup is sufficiently realistic, this capability for verification can be a powerful tool.

An OSSE can be used to evaluate different network configuration options and tradeoffs in design, including different types instruments that are deployed, instrument accuracy and noise characteristics, temporal sampling, and spatial distribution. OSSEs can also be applied to evaluate different processing and assimilation techniques, as well as other factors. OSSEs have been used for evaluating a wide range of new observational techniques to improve numerical weather prediction, atmospheric dispersion simulations, and other applications. A recent study investigated how different networks of ground-based boundary layer profilers would impact the forecast of convective precipitation during a cold-season event over the central United States (Otkin et al., 2011; Hartung et al., 2011; referred to hereafter as the OH papers).

An OSSE consists of several components: (1) a representation of the atmosphere called the Nature Run that plays the role of truth, usually a long, free numerical model forecast; (2) synthetic observations that are extracted from the Nature Run fields for all existing and proposed observing systems; (3) a data assimilation system for assimilating the synthetic observations into a forecast model, and (4) the numerical weather prediction model used for experimental forecasts. A schematic diagram of the OSSE process is illustrated in Figure 1.1.

The Nature Run is a typically a high resolution, both time and in space, simulation of a particular weather event by a numerical weather prediction model. The model can be run in a wide variety of ways, but the essential objective is that the model provides a realistic simulation of an actual weather event with the proper amount of variability and correlation among the different variables. It is not a requirement that the Nature Run provide an exact replication of the particular event, however, the Nature Run needs to be a relatively long-duration simulation, as it ultimately needs to cover the time window associated with the data assimilation period as well as the forecast period. In the OH papers, the Nature Run was 72 h long; in global OSSE studies, a very good period of time to use is approximately one year.

The second step in the process is to create synthetic observations from the Nature Run output. In the OH papers, this step included the generation of temperature and humidity profiles that would be retrieved from a network of AERI and microwave radiometers (MWR) and the wind profiles from a Doppler wind lidar (see below for instrument descriptions). It is critical that the simulated observations are as realistic as possible; thus the observations should include the both correlated and uncorrelated error, biases, and other instrumental characteristics. The first is particularly important, as many remotely sensed profiles (especially passive remote sensors) contain a significant amount of correlated error. This also places a requirement back upon the Nature Run, and in particular on the resolution of the Nature Run fields. For example, some remote sensors, such as the ground-based instruments simulated in the OH papers, have very small footprints (order 10s to 100s of meters) relative to the model domain size (order of 100s to 1000s of meters). Thus, to properly capture the variability that would be inherent in real observations by a real instrument, the Nature Run should ideally be at the resolution that the instrument is able to resolve. However, this results in an extremely computationally expensive Nature Run, and thus this tradeoff is typically made.

The third step in the process is the assimilation of these observations into a forecast model run. Early attempts at OSSEs such as described by Atlas (1997), often suffered from identical twin or fraternal twin problems, in which the same or similar models were used for both the Nature Run and forecast experiments. These twin model experiments suffer from insufficient model error that may bias conclusions about data impact. There are many ways that this can be avoided: using a different model entirely, changing the physics options used by the same model, coarsening the vertical and/or spatial resolution of the forecast model, initializing the forecast model with a different dataset, or some combination of these. Typically, the forecast model is allowed to spin up for some period of time, and then enters the assimilation period wherein the sim-

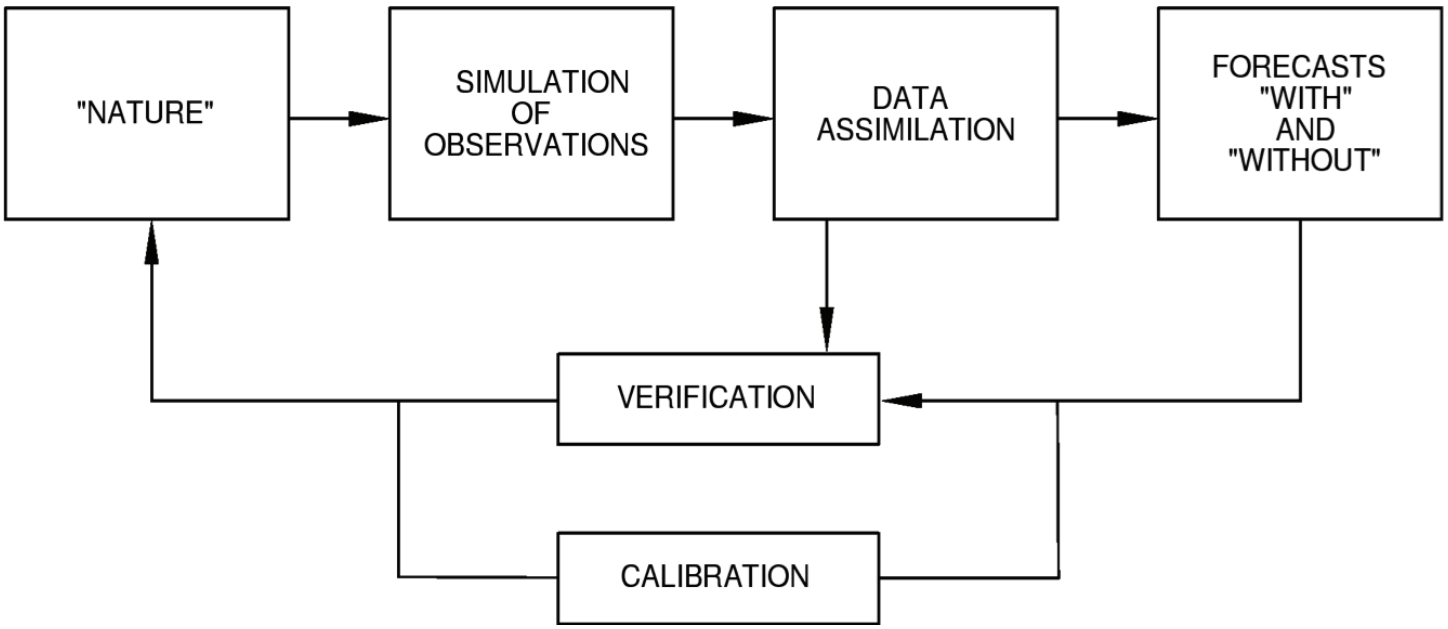

Figure 1-1. Schematic diagram of the Observing System Simulation Experiment process.

ulated observations from the Nature Run are incorporated using one of many assimilation techniques into the analysis. In the OH papers, the assimilation period was 24 h and the boundary layer profiles were assimilated hourly using an Ensemble Kalman Filter approach. It is necessary to calibrate the OSSE to ensure that the behavior of the system is sufficiently similar to the real world for the results of the OSSE to be meaningful. In previous OSSEs, calibration methods have included comparisons of observation minus analysis and observation minus background statistics for the OSSE in comparison to real data (Stoffelen et al., 2006) and comparison of observation impact through data denial experiments.

The final step is to run the forecast model in a forecast mode beyond the end of the assimilation period. These forecasts are then compared to the Nature Run, and provide a measure of how similar the forecast was to reality. In the OH papers, they demonstrated that a network of thermodynamic profilers and wind profilers provided a better forecast of accumulated precipitation then a network that consisted of either thermodynamic or wind profilers.

While OSSEs provide a relatively straightforward way to assess the impact of various observation and assimilation systems, care must be taken in the interpretation of the results. The Nature Runs for OSSEs are computationally expensive due to the requirement for high spatial and temporal resolution, both in terms of CPU power and storage space, and thus there are typically only a small number of cases performed. The poor statistical sampling of events or lack of calibration may result in one observation seemingly outperforming another, resulting in misleading conclusions. Another problem is that the choice of the data assimilation system may impact how the data are incorporated into the analysis, and thus change the results of the subsequent forecast. Also, the Nature Run may not properly represent the range of variability and needed realism for the particular case being tested in the OSSE. Thus, the Nature Run does not provide a true test of assimilation/forecast system; this includes the small-scale variability at the instrument footprint size.

Workshop participants agreed that OSE and OSSE studies have provided useful information on sensitivity of forecasts to different observing systems but many more such studies are needed if the "optimal mix" of future observing systems is to be determined. Various mesoscale OSE studies have shown value of radiosonde observations, global position systems (GPS), surface, profiler, aircraft, and infrared observational data. Particularly, lidar systems demonstrated a strong impact on QPF using airborne water-vapor DIAL systems during IHOP_2002 (Wulfmeyer et al., 2006), a network of ground-based water-vapor Raman lidar systems (Grzeschik et al., 2008) and airborne and ground-based lidar systems during COPS. Storm-scale models have assessed the contributions of NEXRAD V_R and Z data as well as the benefits of gap-filling radar (CASA) data over NEXRAD data alone. Many of the systems described later in this report, though, have yet to be fully assessed. Testbeds (see Section 6), with as many instrument systems as possible present, permit the use of OSEs to determine relative value of different

observations (and could provide a calibration dataset for OSSEs). However, testbeds may lack the spatial dimensions needed for assessment of forecasts longer than a few hours.

Verification studies demonstrate that both OSEs and OSSEs should be performed with convection-permitting resolution to ensure the reliability of the results. It is essential that all routine observations are assimilated in combination with the new observing system network and that a rapid-update cycle is applied similar to routine forecast systems so that the impact of the observations is optimally ingested and advected to a larger domain.

Recently, operational and research NWP centers have used their 4DVAR data assimilation systems to back out simultaneously the relative contributions to forecast error reduction by all observing systems in short-range forecasts, thus providing a more economical method to assess multiple (up to 30) systems (Cardinali, 2009). Lui and Kalnay (2009) have shown that ensemble Kalman filter DA techniques can also do this, but without the need for the linear assumption of the adjoint versions of 4DVAR. It is also possible to apply these techniques using a 3DVAR, e.g., that of the WRF system.

Satellite data (in global studies) appear to dominate in importance, but not if normalized to contribution per observation. Results may also vary according to verification metric and type of weather phenomena studied.

Without existing networks of the desired thermodynamic profiling capability, though, OSSEs are necessary. A complete OSSE would start with current and upcoming observations (e.g., satellite missions already in the pipeline) and then add in instruments that could potentially make up the new ground-based network. The OSSE should look at the value of the new observations for both "routine" forecast conditions as well as impact on "extreme events." This would allow the value of the new instruments to be placed in context with the observations that already exist, and would be helpful to understand the benefits of the new network. However, properly done OSSEs are expensive to calibrate and complete, and require a dedicated team to perform them. Such a team exists for satellite OSSE studies (JCSDA), but a national effort to examine the relative value of all possible observing systems is needed.

SECTION 2. MICROWAVE RADIOMETRY

Microwave radiometry is a passive technique that has been used for several decades to observe thermodynamic profiles in the troposphere (see Westwater, 1993; Westwater et al., 2005 for tutorials). Ground-based microwave radiometers (MWR) are instruments calibrated to measure the down-welling natural emission from the Earth's atmosphere. The quantity measured by an MWR is atmospheric radiance [W/(m^2·sr·Hz)], which is usually converted into brightness temperature (T_b) using Planck's law to adopt the intuitive units of Kelvin. The most common commercial units operate in the 20-60 GHz frequency (0.5 to 1.5 cm wavelength) range, in which atmospheric thermal emission comes from atmospheric gases (primarily oxygen and water vapor) and hydrometeors (mainly liquid water particles, because ice emission is negligible) (Figure 2.1). In the 20-60 GHz range, the Rayleigh scattering regime applies up to sizes of small raindrops and in general the scattering contribution is negligible up to light precipitation.

The atmospheric state (i.e., profiles of atmospheric pressure, temperature, humidity, and hydrometeor contents) determines the T_b being measured. If scattering is neglected the brightness temperature observed at frequency ν by a ground-based microwave radiometer pointing in zenith direction is given by

$$Tb_v = T_{cos} e^{-\tau(0,\infty)} + \int_0^{\infty} \alpha(z) \cdot T(z) \cdot e^{-\tau(z,\infty)} dz \qquad (2.1)$$

with the cosmic background temperature T_{cos}=2.7 K and the opacity

$$\tau(z_1,z_2) = \int_{z_1}^{z_2} \alpha(z) dz \qquad (2.2)$$

is the integral of the volume absorption coefficient α. The contribution of a certain atmospheric layer to the signal as observed by the instrument is described by so-called weighting functions. Unlike the infrared case, there is a small but measurable extraterrestrial source term and the Planck function reduces to a linear proportionality with temperature at the microwave limit.

Solving Equation 2.1, i.e., the *forward problem*, is straightforward, though very different atmospheric states may lead to similar T_b. When the measured T_b are processed to estimate atmospheric thermodynamic variables, such as temperature and humidity profiles, this process is called the *inverse problem*. The inverse problem is ill-posed, meaning that its solution is not unique nor stable. A priori knowledge of the atmospheric variable is needed to constrain the solution domain and find a meaningful solution to the inverse problem.

Typically, synthetic T_b derived via radiative transfer calculations from representative long-term radiosonde data sets for the specific geographic region are used to derive statistical algorithms via regression or neural network techniques (Löhnert and Crewell, 2003). These algorithms are simple to apply in real time but strongly rely on the underlying data set and cannot provide uncertainty estimates for an individual measurement. Optimal estimation methods (OE) solve the inverse problem in a physically consistent way, optimally coupling MWR observations with a priori background knowledge, as well as with other instruments' observations, accounting for their error characteristics (Cimini et al., 2011; Löhnert et al., 2004). OE has the advantage of associating a dynamical error characterization to the retrieved atmos-

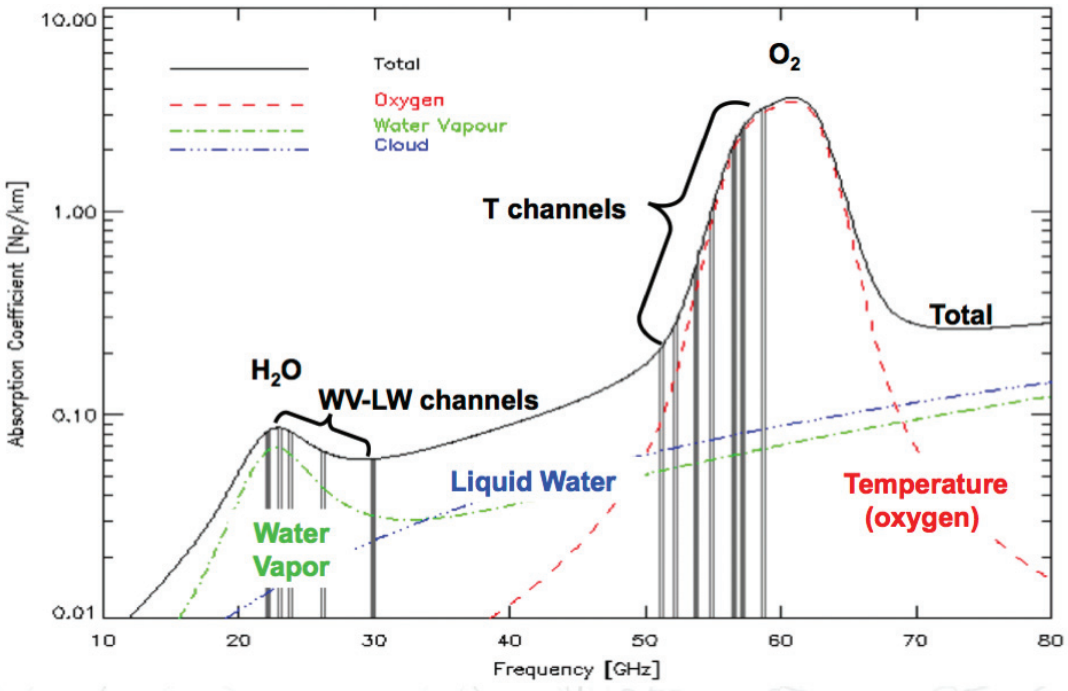

Figure 2-1. Atmospheric absorption as a function of oxygen, water vapor and cloud liquid. The spectral range of commercially available water vapor (WV; 20-30 GHz) and temperature (50-60 GHz) profilers is indicated.

pheric variables, at the expenses of more computations (iterative process).

2.1 Capability to Measure Temperature

Microwave profilers that measure several frequencies along the 60-GHz oxygen absorption complex are well established for observing the atmospheric temperature profile from the ground as well as from space. From the ground, observations are typically taken in zenith direction at about five to ten frequency channels from 50–60 GHz. Channels in the centre of the absorption band are highly opaque and the observed T_b is close to the environmental temperature. For frequencies further away from the center, the atmosphere is less opaque and the signal systematically stems from higher atmospheric layers. The root mean square (RMS) accuracy of this method is about 0.6 K close to the surface and degrades to about 1.5–2 K in the middle troposphere (Crewell et al., 2001; Güldner and Spänkuch, 2001; Liljegren et al., 2005).

For ground-based observations the weighting functions at the different frequencies all decrease continuously with height and limit the vertical resolution rather than the radiometric noise. The vertical resolution, which is often defined as the half-width of the vertical inter-level covariance function of the retrieval errors, decreases rapidly from about 500 m at a height of 300 m to 1 km at a height of 500 m (Liljegren et al., 2005). By observing the atmosphere under different angles, additional information about the temperature of the lowest kilometer can be gained. One-channel systems operating around 60 GHz have been developed (Kadygrov and Pick, 1998), which derive profile information from elevation scanning. By assuming horizontal homogeneity of the atmosphere, the observed radiation systematically originates from higher altitudes with increasing elevation angle. Because the T_b vary only slightly with elevation angle, the method requires a highly sensitive radiometer that is typically realized by using wide bandwidths up to 4 GHz. The resulting vertical resolution has been estimated using the Dirac delta function to decrease from 8 m at a height of 10 m to about 300 m at a height of 400 m and improve the accuracy bet-

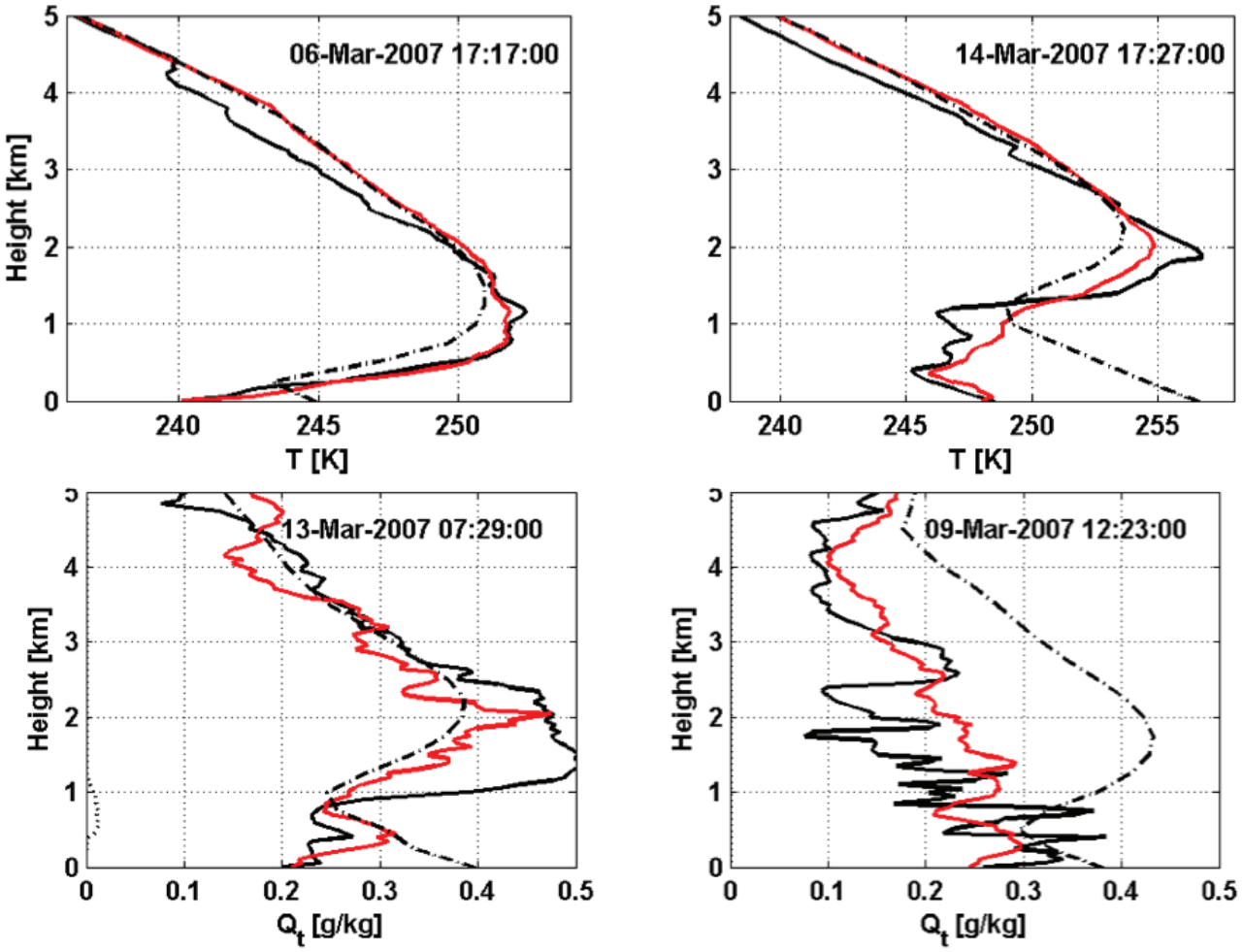

Figure 2-2. Profiles of temperature (top) and specific humidity (bottom) as forecasted by the NCEP global model (dash-dotted), as measured by a radiosonde (black solid), and as retrieved from a multi-channel MWR (red solid) at the ARM NSA site in Barrow, Alaska.

ter than 1 K by comparison with observations from a 300-m tower (Westwater et al., 1999). Because the use of a single highly opaque channel limits the information content to altitudes below 600 m, Crewell and Löhnert (2007) combined multi-channel and multi-angle observations and achieved a precision better than 0.5°K for the lowest 1500 m. In general this means that a surface inversion can be observed very well while elevated or multiple inversions are difficult to capture.

Figure 2.2 shows profiles of temperature taken at Barrow, Alaska, in 2007 (after Cimini et al., 2010).

2.2 Capability to Measure Water Vapor

Water vapor has distinct spectral features at 22.235 and 183 GHz. Dual channel ground-based MWR make use of the rotational line at 22.235 GHz to derive the vertically integrated water vapor (IWV). Within this method one channel measures at a frequency close to the line centre (around 24 GHz) where water vapor absorption is almost independent of height. In clear-sky conditions, the observed brightness temperature is approximately proportional to IWV. The second channel is located in a window region where water vapor and oxygen absorption are relatively low (for example 31.4 GHz). Because microwave emission of clouds increases approximately with the square of the frequency (Figure 2.1), the second channel can be used to characterize the cloud's contribution to the intensity observed at the first frequency. This combination is extremely powerful as the IWV and the liquid water path (LWP), which is the vertically integrated liquid water density, can be retrieved simultaneously. Specifications of the accuracy vary between 0.3 and 1 kg m^{-2} for IWV and 20 to 30 gm^{-2} for LWP. Sometimes microwave IWV measurements from the ground are used to scale radiosonde or water vapor lidar measurements (e.g., Turner et al., 2003 and Turner and Goldsmith, 1999). Improvements in accuracy can be made by using additional frequencies (i.e., 90 GHz) to further constrain the retrieval problem (Crewell and Löhnert, 2003).

Water vapor profiles are derived from microwave profilers that measure the atmospheric emission at several frequencies along the wings of pressure-broadened rotational lines. From the ground the 22.235 GHz line is usually used except at low humidity conditions where the strong 183 GHz water vapor line is more suitable (Cimini et al., 2010). With a pressure broadening of about 3 MHz/hPa tropospheric profiling can be realized with several channels spaced by a few GHz along the line.

Figures 2.3-2.4 show a MWR plots of temperature, water vapor, integrated water vapor, liquid water path, cloud base height, and profiles from the Whistler, Canada, site during the 2010 Winter Olympics.

2.3 State of the Technology

Because of the low radiances emitted by the atmosphere in the microwave range, radiometers need to amplify the signal received at the antenna by about 80 dB. High thermal stability is the key to stable amplification and therefore accurate MWR observations. Microwave profilers have been commercially available for more than a decade. Two different detection techniques are used. Solheim et al. (1998) developed a radiometer system that utilizes a stable frequency synthesizer as local oscillator to sequentially measure at different

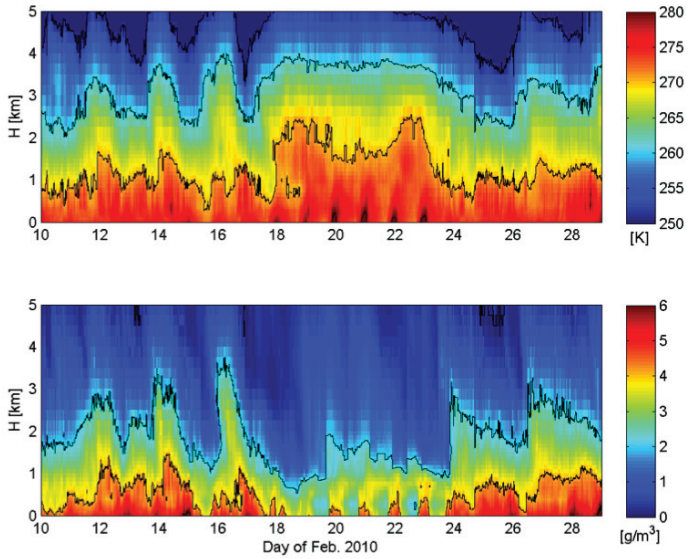

Figure 2-3. Temperature (top) and water vapor density (bottom) time-height cross section retrieved from multi-channel MWR all-weather observations in Whistler, Canada, during the 2010 Vancouver Winter Olympics.

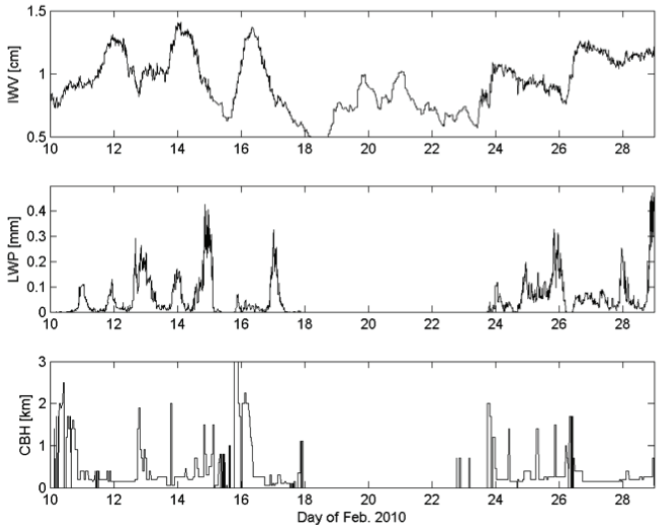

Figure 2-4. Time series of IWV (top), LWP (centre), and cloud base height (bottom) retrieved from multi-channel MWR all-weather observations in Whistler, Canada, during the 2010 Vancouver Winter Olympics.

frequencies in K-band (20-30 GHz) and V-band (50-60 GHz). In such a heterodyne receiver signal amplifying, filtering, and processing is done at a lower intermediate frequency (IF). This approach has the advantage that, depending on the user requirement, different sets of frequencies can be observed. As a trade-off, atmospheric variations, e.g., clouds, during frequency scanning might degrade the retrieval performance because all channels cannot be observed simultaneously. Rose et al. (2005) developed a MWR for the same frequency range using direct detecting techniques that allow parallel measurements at all frequency channels. The approach requires low noise amplifiers (LNA) that have become available for frequencies up to 100 GHz within the last decade. This system is purely passive and also avoids interference by radio signals (radio frequency interference) lower than the detection frequency.

The commercial systems employ GPS clocks, environmental temperature, humidity and pressure sensors, and optionally broadband infrared radiometers as well as azimuth scanners. Elevation scanning is performed via an internal mirror and also used within tipping curve calibration procedures (see Han and Westwater, 2000). Systems can run as stand-alone in the field requiring only power connection or being connected to an external PC and controlled via the internet or mobile phone network. Power consumption is moderate for the MWR alone but becomes significant (> 1kW) when heated blowers are operated to keep the radome as dry as possible during precipitation and dew formation.

Commercial MWR (Figure 2.5) make use of statistical algorithms to directly provide temperature and humidity profiles as well as higher order products like stability parameters. In addition to the different frequency channels further information on the environmental temperature, humidity or infrared temperature is sometimes input to the retrieval algorithms. Optimal Estimation Methods are typically applied in post-processing. Examples are the Integrated Profiling Technique (IPT), developed to couple MWR with cloud radar, ceilometer and other observations for temperature, humidity, and cloud water content profiling (Löhnert et al., 2004 and 2008) and the 1-dimensional Variational Retrieval (1DVAR), developed to couple MWR observations with NWP model output (analysis or forecast) for temperature, humidity,

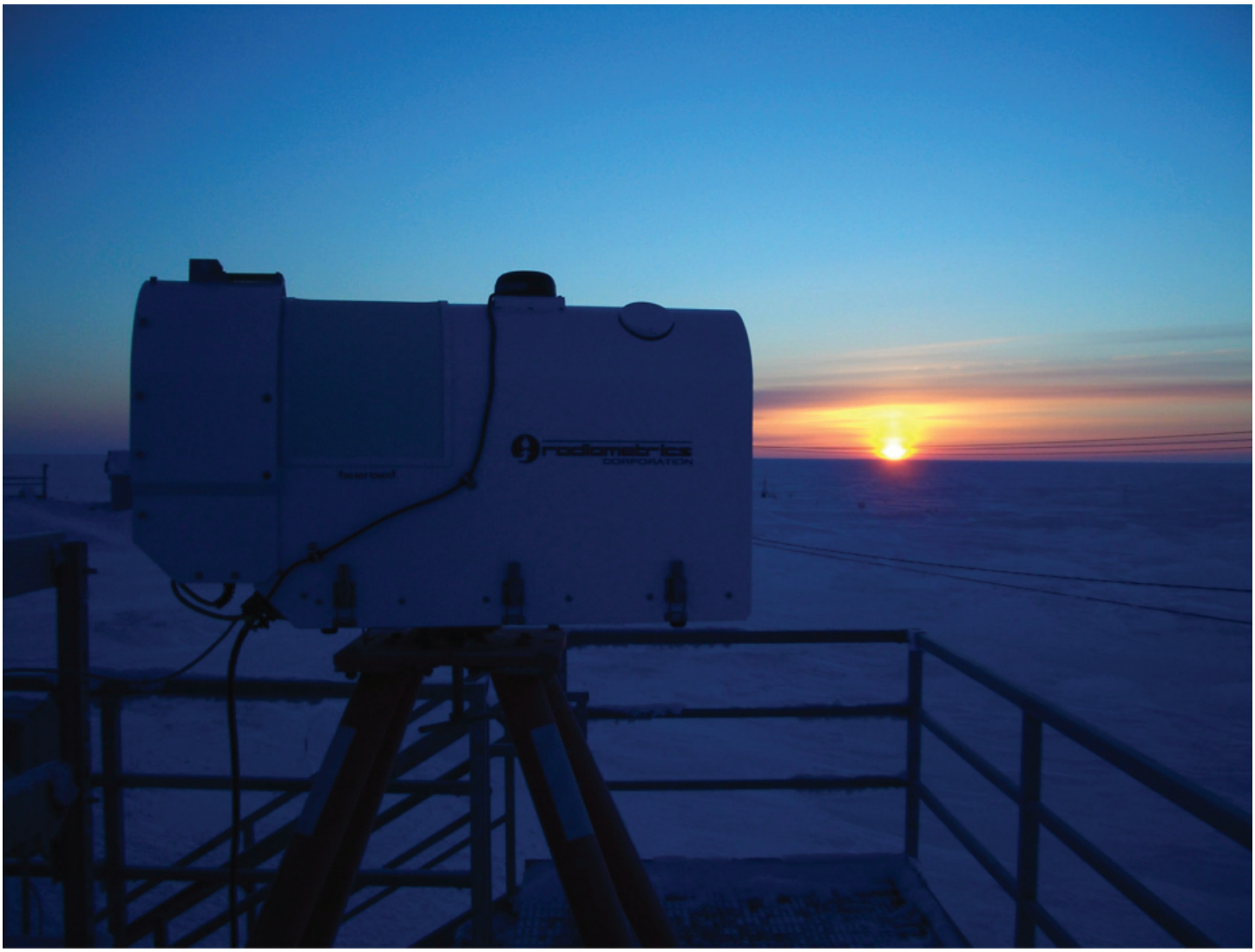

Figure 2-5. The ARM Radiometrics MWR at Barrow, Alaska.

and cloud water content profiling (Cimini et al., 2006, 2010, 2011; Hewison, 2006, 2007). The main advantage of 1DVAR with respect to other techniques is the use of the NWP output as a first guess, as usually the NWP output is more representative of the present atmospheric state than a climatological mean. The use of 1DVAR was demonstrated in all-weather conditions during the Vancouver 2010 Winter Olympics (Cimini et al., 2011), providing temperature and water vapor density profiles within 1 K and 0.5 g/m^3 from surface up to 10 km.

2.3.1 Strengths

From the ground, microwave radiometers can provide unattended measurements of water vapor and temperature at high temporal resolution (<30s) during all weather conditions except during precipitation when water on the antenna/radome emits microwave radiation and disturbs the measurement. Day and nighttime operation are equivalent because essentially no microwave radiation from the sun will scatter into the instrument's FOV. They are passive instruments requiring no transmitted power.

The accuracy of temperature and humidity profiles is more or less independent of the occurrence of clouds, except for cases of heavy precipitation where saturation effects may occur or the instrument is influenced by rainwater on the radome.

2.3.2 Weaknesses

While the noise level (<0.2 K) and the relative accuracy of MWR measured T_b is rather satisfactory, the absolute calibration still poses some challenges. Tipping curve calibrations (Han and Westwater, 2000) require homogeneous conditions which are in practice difficult to find. Liquid nitrogen (LN_2) calibrations suffer from uncertain knowledge of the liquid nitrogen refractivity and practical issues over handling, transportation, and operator safety.

The broad spectral features in the microwave region do not allow for a large number of wavelengths to be probed and, therefore, the number of degrees of freedom in the microwave retrieval is low (generally <2 independent pieces of information). This, as in infrared measurements, controls the number of levels that can be determined from the spectra.

Due to the increased use of wireless communication, Radio Frequency Interference (RFI) has become problematic not only at lower frequencies but even at protected frequencies, e.g., 24 GHz.

Radiation absorption by atmospheric gases and hydrometeors is quantitatively modelled while solving the forward problem and thus absorption model uncertainties affect all the retrieval methods based on synthetic T_b. Only retrieval methods based on historical dataset of MWR observations and simultaneous atmospheric soundings are not affected by absorption model uncertainties. The most relevant absorptions in the 20-60 GHz range come from water vapor, oxygen, and liquid water. Modifications of absorption models are continuously proposed based on laboratory data and MWR field observations (Cimini et al., 2004; Liljegren et al., 2005; Clough et al., 2006; Cadeddu et al., 2007; Payne et al., 2008; Turner et al., 2009). For water vapor, the absorption model uncertainties are approximately within 5% (Payne et al., 2008, 2011), which dominate the measurement error budget especially for high-humidity conditions. For oxygen, different absorption models agree very well (0.3%) at opaque channels (56-60 GHz), but show larger differences between them and with respect to MWR observations at more transparent channels (50-56 GHz). These uncertainties are quite consistent and can be effectively mitigated with bias removal solutions. Without any intervention, absorption model uncertainties in the 50-56 GHz range may bias temperature retrievals in the upper atmosphere, but have negligible effect in the boundary layer. For liquid water, the major uncertainties are related to supercooled water, i.e., liquid water at sub-freezing temperatures, because absorption models at these temperatures is primarily based on extrapolations from higher temperature regions. Partly due to lack of laboratory measurements for liquid water at low temperatures, the mass absorption coefficients calculated by different models at 31.4 GHz deviate by about 5% at 0°C and up to 50% at −30°C (Kneifel et al., 2010), but there have been some recent advances in this area (e.g., Cadeddu and Turner 2011). Nonetheless, liquid water path measurements at subfreezing temperatures should be interpreted with care.

2.4 Readiness for Deployment in a Network

MWR technology has matured so far that more than a hundred systems operate continuously worldwide. However, there is lack of coordination of MWR operations worldwide, causing underutilization of MWR data. Recent attempts that tried to address this issue include the LUAMI (Lindenberg Upper-Air Method Intercomparison) campaign and MWRnet. The LUAMI campaign was carried out to demonstrate the capabilities of MWRP systems for their use in operational meteorology, deploying a test network of MWRP supplying quality-proven data in real-time to a network hub at the DWD Atmospheric Observatory in Lindenberg. The temporary network of eight MWRP operated reliably and data were collected for one month. A common retrieval algorithm, a statistical regression based on MWRP observations and NWP model output, was applied to data from all the 8 MWRP; this method effectively removed absorption model and calibration issues, producing weak-biased retrievals with respect to NWP.

More recently, efforts are being made towards the establishment of a permanent international network of microwave radiometers (MWRnet, http://cetemps.aquila.infn.it/mwrnet/). The MWRnet

initiative started within the European Ground-based observations of essential variables for CLImate and METeorology (EG-CLIMET) Cooperation of Scientific and Technical research (COST) action, and proposed the following goals:

- Establishing the "best practice" for making MWR observations and retrievals;
- Defining procedures for optimum calibration and quality control;
- Developing common retrieval algorithm with error analysis (from observations to retrievals);
- Implementing metadata and data handling protocols;
- Facilitating the registration and access of well documented and quality controlled MWR observations and retrievals with errors; and
- Providing near-real-time MWR data and retrievals (with errors) for NWP Data Assimilation (DA) and Observation System Experiments (OSE).

MWRnet currently has about 40 members and more than 75 MWR worldwide (including dual-channel units, water vapor profilers, single-channel temperature profilers, multi-channel temperature profilers, and temperature/humidity profiling units), of which some 25 are located in Europe.

2.4.1 Deployment Scenarios

Due to their relatively mature state MWR could be deployed at many field sites that have viewing down to the horizon. The highest value can be expected if they are employed in synergy with other instruments.

Benefits/Drawbacks of Scanning:

Elevation scanning can be performed with all MWR requiring an unblocked view into at least one direction. As discussed in Section 2.1 (see also IR description, Section 3.2) this provides enhanced boundary layer profiling. As a trade-off about 1-2 min observation time in the zenith direction are lost.

For water vapor retrievals, elevation scanning is not beneficial and is also limited due to the high spatial and temporal variability of humidity. On the other hand, azimuth scans can characterize site representativeness (Kneifel et al., 2009), humidity and cloud variability. Another application is nowcasting by estimating water vapor gradients (Schween et al., 2011). Yet, no common scanning patterns have been defined. Scanning always leads to a reduction of zenith observation time.

Because elevation scanners are already integrated into the radiometer systems only azimuth turn tables are needed for complete scanning capability. They are available at a relatively low price (<10,000 €) and their control is already included in typical radiometer software. One typical scanning application is the tracking of GNSS satellites to verify slant wet delay estimates. The combination of several scanning radiometers is also proposed for tomography of water vapor (Padmanabhan et al., 2009) and cloud liquid (Huang et al., 2008).

Approximate Costs:

Currently there are at least two vendors of MWRs which offer single temperature or humidity profilers for less than $100,000 and combined humidity and temperature profilers for less than $160,000.

MWRs are also used for geodetic, astronomical, and propagation studies. With increasing demand, we can expect further miniaturization, lower maintenance levels, and lower cost in the future.

2.5 Synergy with Other Instruments

There is a large synergy between microwave and passive IR retrievals (See Section 1.2). Because MWRs can only provide limited information (~1 degree of freedom) on the vertical distribution of cloud liquid (Crewell et al., 2009) they are often combined with cloud radar and ceilometer measurements to simultaneously provide temperature, humidity, and cloud liquid water profiles (Löhnert et al., 2008).

2.5.1 Environmental Issues

Microwave radiometers have been run operationally for multiple years in a wide range of different environments, from the tropics (+40°C) to the Arctic (-35°C). The main limitation to these microwave radiometer observations is the need to keep liquid water off of the radome, as this could contribute a significant signal and hence contaminate the atmospheric retrievals. All MWRs are equipped with rain and dew mitigation techniques, typically in the form of hygroscopic windows, blowers, and heaters. Microwave hardware components are rather reliable over several years. Radiometer periphery is more likely to be subject of damage. Inspection by eye and cleaning of external components, i.e., IR mirror, is recommended every couple of months. The quality of the radome can be affected by birds, UV radiation, etc., requiring replacement roughly every year. Depending on their design heaters and blowers might be exchanged in the time frame of a few years.

2.5.2 Reliability

MWRs are running autonomously around the globe. With dependable power and internet connection to monitor performance the radiometers are generally run reliably and produce data.

The data quality depends on good calibrations and the detection of disturbances like precipitation, dew, icing, or birds.

2.6 Research Needed

Several areas of future research were identified for the already well-developed MWR technique. New techniques into all weather operation of the MWR are needed. The need to keep the radome free from hydrometeors and ice while not affecting the temperature of the dome is a challenge. The ability to quality-assure the results and identify meteorological features which affect the transmission in the microwave through the instrument structures is required. Adding a capability to replace LN_2 with unattended calibrations available for the instrument without user intervention would make the MWR more applicable to routine network operation.

On the scientific side, there is still a need to better understand the absorption of hydrometeors. Water and ice coexist in clouds and having laboratory measurements of microwave absorption of supercooled water would help understanding MWR retrievals in sub-freezing conditions. Further work is needed to understand how multiangle radiometric measurements could be better peeled through tomographic techniques, perhaps giving three-dimensional structures if azimuthal scans were available.

Research into the use of MWR with other techniques (Raman or DIAL H_2O, aerosol profiling, etc.) may provide synergies to better understand the fundamentals of microwave radiative transfer.

SECTION 3. INFRARED RADIOMETRY

3.1 Background

Spectrally resolved infrared (IR) radiation measurements contain a wealth of information about the thermodynamic structure of the atmosphere, as well as information on other components of the atmosphere that emit IR radiation (e.g., clouds, dust, aerosols). In a cloud and aerosol free atmosphere with only gaseous emission, the downwelling infrared radiance at the surface *I(0)* (with units of W / (m^2 sr cm^{-1})) at wavenumber *v* (with units of cm^{-1}) is given by

$$I_v^{\downarrow}(0,\mu) = \int_0^{\infty} B_v(T(z)) W_v^{\downarrow}(z) dz \qquad (3.1)$$

where *T(z)* is the temperature profile, *B* denotes Planck's function, and *W(z)* is the weighting function at height *z*. Essentially, Equation 3.1 is identical to Equation 2.1, except there is no extraterrestrial source of infrared radiation as a background as there is for the microwave region. In the microwave, the Planck function is proportional to temperature, but in the infrared, the exponential form of the function must be retained. The weighting function depends on the emission from level *z*, which is a function of the absorption cross-section β_a for the relevant gases at that level, multiplied by the transmission (t_v between that level and the surface divided by μ, the cosine of the viewing zenith angle:

$$W_v^{\downarrow}(z) = \beta_{\alpha,v}(z) \frac{t_v(0,z)}{\mu} \qquad (3.2)$$

If the downwelling IR radiation is measured at a sufficiently high spectral resolution as to accurately resolve individual absorption lines, then these observations can be inverted to provide water vapor and temperature (hereafter, qT) profiles. Due to pressure broadening of absorption lines of atmospheric gases, a spectral resolution of approximately 1 cm^{-1} is required for most surface locations (i.e., for pressures greater than 800 mb).

Information on the vertical profiles of qT exists in different regions of the IR spectrum. Typical IR spectrometer measurements include observations of the 15 μm and 4.3μm absorption band of carbon dioxide (CO_2) and the 6.7 μm vibration-rotation and the pure rotational (between 100 and 15 μm) water vapor (H_2O) absorption bands (Figure 3.1). CO_2 is, to first order, a well-mixed gas with a constant concentration with altitude. (This assumption is removed for retrievals of CO_2 profiles in a varying qT environment.) With this assumption, for surface-based measurements the IR radiation observed at a given wavelength in the CO_2 absorption band is primarily due to emissions from levels extending from the instrument to the altitude of interest, where the emission at a specific level is dependent on the temperature at altitude, as well as the transmission between that altitude and the instrument. Similarly, in the H_2O spectral region, the radiance observed at different frequencies is primarily a function of the water vapor concentration profile and the temperature profile.

3.2 Capability to Measure Temperature and Water Vapor Profiles

There are several techniques that can be used to retrieve qT profiles from ground-based IR spectroscopic observations. These include two broad classes of methods: statistical retrievals and physical retrievals. A statistical retrieval uses an a priori dataset to build statistical relationships between the spectral radiance and profiles of temperature and humidity. A wide variety of different statistical approaches could be used, and a primary advantage is that statistical methods are computationally very fast. However, a common drawback of these methods is that the qT profiles that are retrieved are not necessarily physically consistent with the radiance observations themselves (i.e., if the retrieved qT profiles were input into a radiative transfer model, the computed spectrum may not match the observed spectrum). Physical retrieval algorithms are iterative methods that adjust the qT profiles, starting with a first guess profile, until the computed radiance matches the observed spectrum. Physical methods are more accurate than statistical methods, but are typically much more computationally expensive.

The method that has been used for over a decade in ground-based IR profiling is the so-called "onion-peeling" approach (Smith et al., 1999; Feltz et al., 1998). This retrieval method takes advantage of the change in the opacity of the atmosphere from the center of the absorption band (where the absorption is highest, and thus the information in the observations is largely from the atmosphere closest to the instrument) to the weaker absorption on the edge of the gaseous absorption band where there is information from higher in the atmosphere. The onion peeling approach, simply stated, is that the opaque region of the CO_2 spectrum is used to determine the air temperature just above the instrument. The temperature at this level is fixed, and a slightly less opaque spectral region is investigated. The contribution to the downwelling spectrum from this region is due to both emission from the layer whose temperature was already determined as well as the region of the atmosphere just above. This allows the temperature of the slightly higher altitude to be determined. This process is repeated to provide the entire temperature profile, and a similar process is used to get the water vapor profile. Several features are apparent from this discussion. First, the information content in the observations is highest for height levels nearest to the instrument, and decreases with altitude away from the instrument. This results in lower spatial (vertical) resolution with altitude. Second, if there are any errors in the tempera-

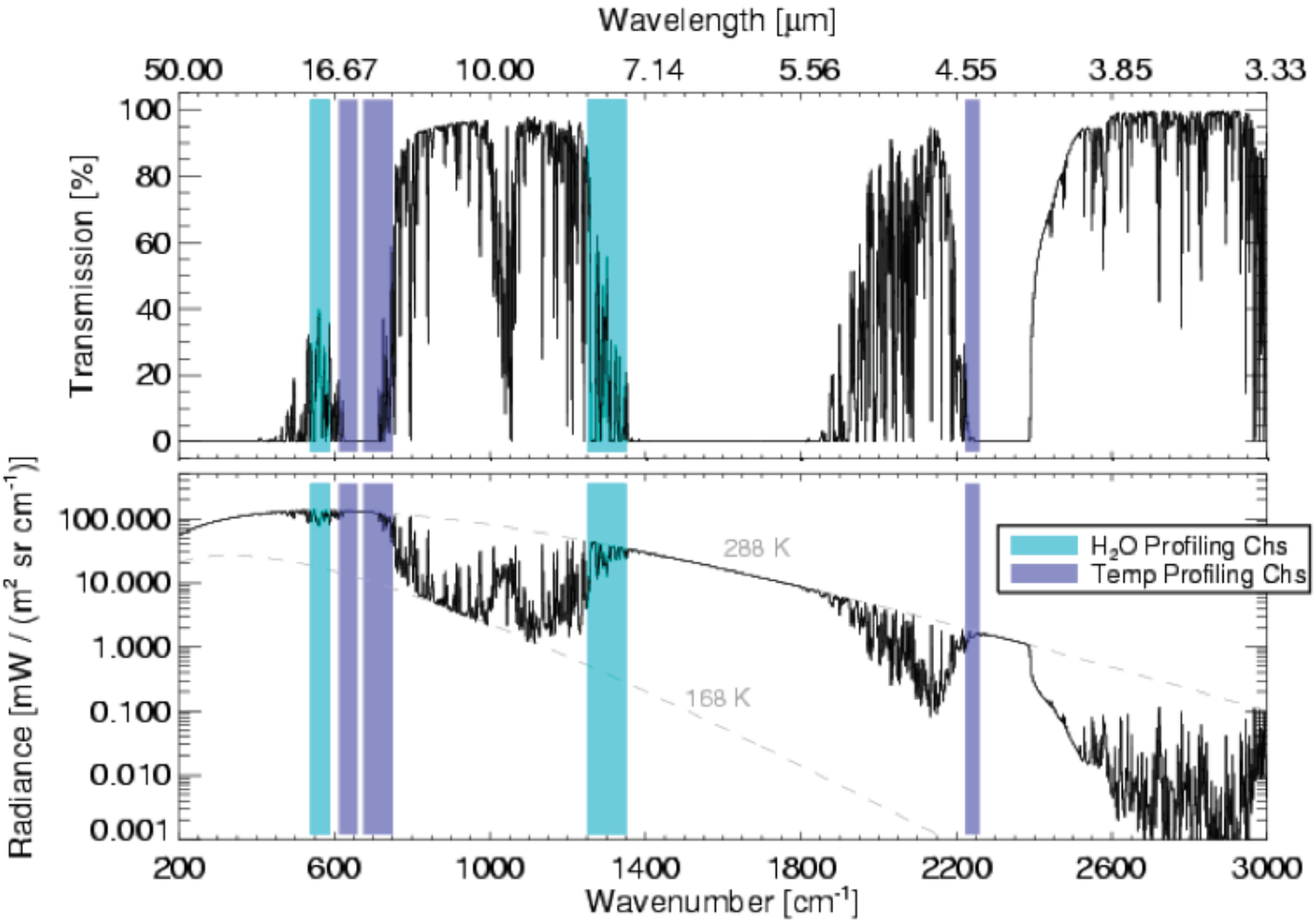

Figure 3-1. The atmospheric transmission (top) and downwelling radiance (bottom) computed for the U.S. Standard Atmosphere with a spectral resolution of 2 cm-1. The spectral regions typically used for profiling water vapor and temperature are indicated. Typical IR spectrometers measure radiance between 550 to 3000 cm-1.

ture (or water vapor concentration) at a lower level (perhaps due to instrument noise), the onion peeling technique will propagate this error into layers above that level. And lastly, this technique doesn't yield information on the error covariance matrix of the retrieved profiles, thereby making it difficult to both quantify the error and its correlation between different levels or to assimilate the data into a numerical model.

A second retrieval technique that helps to overcome the issues associated with the onion peeling technique is a 1-dimensional variational method, such as the Optimal Estimation (OE) approach (Rodgers, 2000). This iterative technique uses *a priori* information, together with the sensitivity of the forward model, to retrieve the entire profile of temperature and humidity simultaneously. The *a priori* information is used to help constrain the solution, because the problem is ill-defined (i.e., there are multiple different atmospheric profiles that would yield the same spectral radiance observations, given the random instrument noise). A significant advantage of OE is that the method propagates the covariance of the *a priori* and sensitivity of the forward radiative transfer model used in the retrieval to provide an uncertainty covariance matrix of the retrieved qT profiles, which is very beneficial for properly assimilation of these profiles. Furthermore, the framework provides quantitative values on the number of independent pieces of information in the observations, as well as where this information lies in the vertical (Löhnert et al., 2009).

3.3 State of the Technology

The Space Science and Engineering Center at the University of Wisconsin – Madison (UW) pioneered the technique of measuring downwelling IR spectral radiation in the early 1990s with their Atmospheric Emitted Radiance Interferometer (AERI) systems (Knuteson, et al., 2004a,b). These IR spectrometers are based around a Michelson Fourier Transform Spectrometer mated to detectors that have sensitivity to radiation between about 3 and 19 µm. This configuration provides data at a maximum unapodized

resolution of 0.5 cm^{-1}. The field of view of the AERI is 45 mrad. The detector temperature is maintained at cryogenic temperatures (order 75 °K) to improve the signal-to-noise ratio (SNR) of the data. Typically, multiple scans of the interferometer are accumulated to further improve the SNR and this results in a typical temporal resolution of 20 s per individual sky spectrum. A principal component based noise filter can be used to further enhance the SNR (Turner et al., 2006).

Accurate qT profile retrievals require that the calibration of the downwelling IR radiance observations be very accurate, and that any instrument artifacts have been removed. These IR spectrometers have a rotating scene mirror aligned to the optical axis of the instrument that allows the instrument to alternately view the sky or two calibration targets. These calibration targets are well-characterized blackbodies; one of which is kept at 60°C while the other floats at ambient temperature. The linearity of the detectors have been determined, and thus a linear calibration procedure is used to extrapolate the blackbody observations to the colder sky view in order to calibrate the measured sky radiance spectrum (Revercomb et al., 1988). Additional corrections have been applied to the data to account for instrument self-apodization and to spectrally calibrate the observations, all of which has resulted in an accuracy of AERI measurements better than 1% of the ambient radiance (Knuteson et al., 2004b). An automated hatch is used to protect the rotating scene mirror during precipitation (i.e., downwelling radiation from the sky is not measured during these conditions).

3.3.1 Strengths

There are several strengths associated with IR spectrometers. First, they offer relatively high information content on the vertical profile of water vapor and temperature related to other passive profilers (see section below on sensor synergy for details). For example, AERI observations have been used in a wide array of research projects, ranging from thermodynamic profiling studies (Feltz et al., 2003), cloud (Turner, 2005) and aerosol (Turner, 2008) studies, trace gas measurements (Yurganov et al., 2010), and spectroscopy (Tobin et al., 1999). AERI instruments have also been used at sea to make accurate measurements of the atmospheric state and sea surface temperature (Minnett et al., 2001). Furthermore, due to their calibration approach, both the absolute calibration and the sensitivity of the instrument is monitored, which makes these observations particularly well suited for long-term observations that can be used to develop climatologies and trend analyses (e.g., for climate). Finally, as IR instruments, they do not need solar radiation and can operate day and night.

3.3.2 Weaknesses

One limitation to qT profiling with ground-based IR spectrometers is the presence of clouds above the instrument. Clouds are extremely efficient emitters of IR radiation, and various properties of the cloud in the field of view of the spectrometer need to be known in order for the retrieval to accurately account for the cloud emission. Most current retrieval methods are designed for clear sky conditions within the narrow (e.g., 2° for an AERI) field-of-view of the instrument. Fortunately, the high temporal resolution allows these retrieval algorithms to provide profiles when there are breaks in the overhead cloud field. Retrievals of qT profiles in cloudy conditions from IR spectrometer data require information from other observations to help characterize the cloud contribution to the downwelling radiance. Cloud base height is perhaps the most critical cloud variable needed, and thus IR spectrometers should be paired with a ceilometer or other active remote sensor that is able to provide this information. Retrievals of thermodynamic profiles from ground-based IR observations in precipitating conditions are not possible.

Another limitation is the vertical resolution of the qT profiles. For example, while AERIs report temperature and humidity on 100m surfaces, the number of true independent pieces of information in the retrieval is based on the spectroscopy and wavelengths used in the retrieval. Because the weighting functions all peak at the surface for an upward looking IR radiometer, differences in wavelength do not give orthogonal weighting functions which is what one would desire for independent retrievals of qT with height. Thus, not all of the weighting functions are truly independent of each other (see discussion of Figure 3.4), which limits the ability to discriminate heights.

3.4 Readiness for Deployment in a Network

As one of the most widely used IR spectrometers, a long history of AERI observations exist, with nearly two dozen systems deployed world-wide, many of which are providing long-term (decadal length) climate-quality observations for the Atmospheric Radiation Measurement (ARM) program in the Arctic, mid-latitudes, and tropics (Ackerman and Stokes, 2003). A recent study that highlights the long, contiguous time-series of AERI observations investigated the downwelling radiance climatology and trends over a 14-year period in the central U.S. (Turner and Gero, 2011; Gero and Turner, 2011).

Current versions of commercial IR spectrometers are hardened, well-proven systems requiring little manual attention other than to visually inspect the cleanliness of the scene mirror periodically. For AERI, the two main components of the that require scheduled maintenance are the Stirling cooler, which is used to keep the detectors at cryogenic temperature and has a lifetime of 3-5 years, and the laser inside the interferometer, which is used to trigger the sampling of the data acquisition system and has

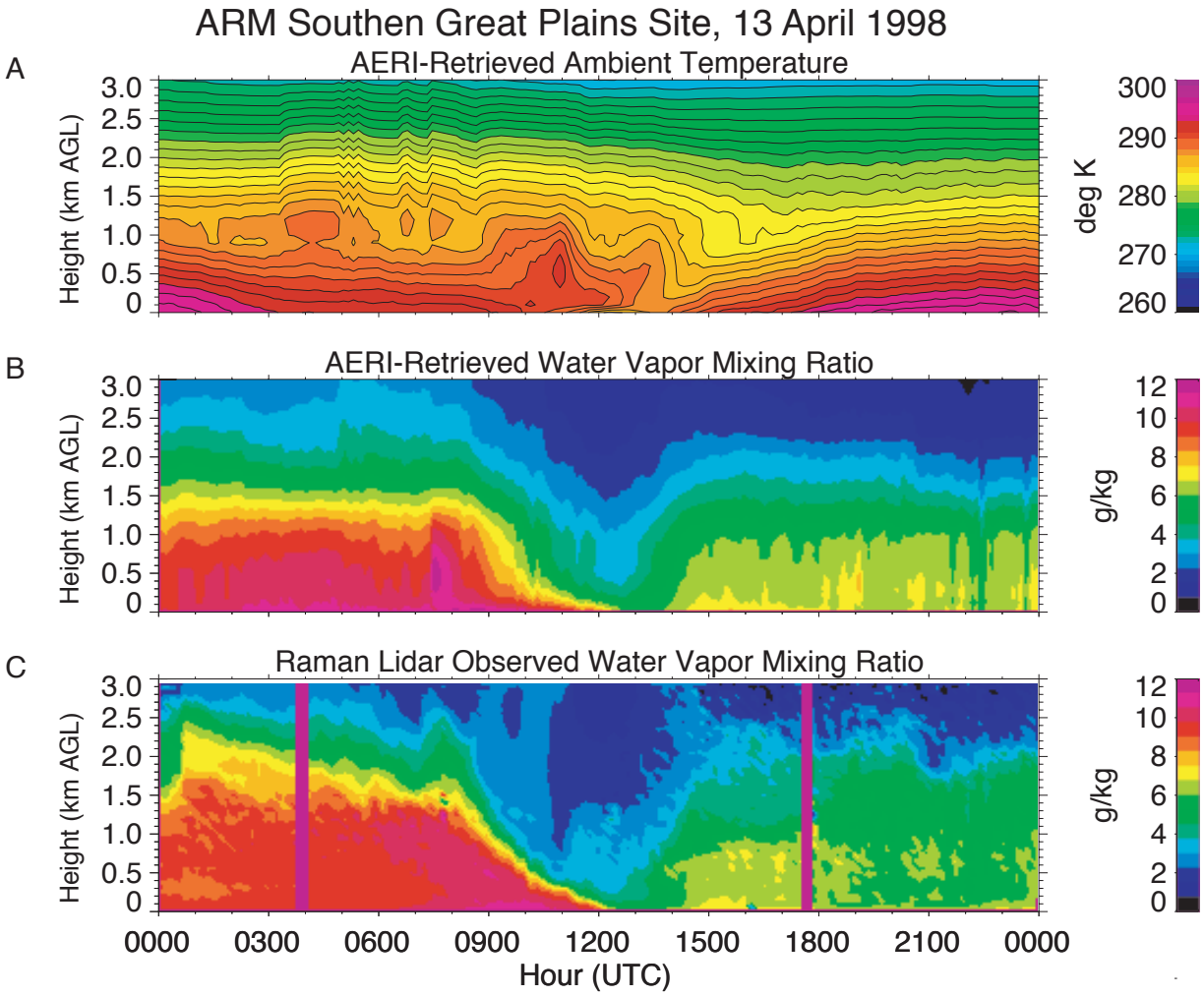

Figure 3-2. AERI-retrieved profiles of temperature (A) and water vapor (B), along with the water vapor measured by the co-located Raman lidar (C), at the ARM site during a dryline passage on 13 April 1998 (Turner et al. 2000).

a lifetime of five years. Thus, an IR spectrometer such as AERI is well-suited to be part of an operational network. Figure 3.2 shows the AERI product from ARM.

Currently, two separate vendors have developed and are marketing IR spectrometer systems. These systems have virtually identical specifications and capability as the UW AERIs. Both companies have several instruments that are currently operational around the world.

3.4.1 Deployment Scenarios

IR spectrometer systems are typically installed in a fixed building with the foreoptics installed through the wall (Figure 3.3a), but stand-alone configurations (Figure 3.3b) exist for both commercial vendors. Due to the opacity of the atmosphere at infrared wavelengths, these systems are typically configured to only view the atmosphere in the zenith direction, and thus have a narrow sky port.

3.4.2 Benefits / Drawbacks of Scanning

Due to opacity of the atmosphere in most mid-latitude locations, scanning the instrument will not add significant value. As such, these instruments are typically deployed in a zenith-only viewing mode.

3.4.3 Approximate Costs

The purchase price of commercially available IR spectrometer systems ranges from approximately $240K to $320K, but are anticipated to drop by at least 30% in the coming decade.

3.5 Synergy with Other Instruments

Data from a spectral microwave radiometer (MWR) that makes multiple measurements on the side of the 22.2 GHz water vapor absorption line and 60 GHz oxygen absorption feature can also be inverted to retrieve qT profiles. The MWR and IR spectrometer techniques are very complementary, yet there are some significant

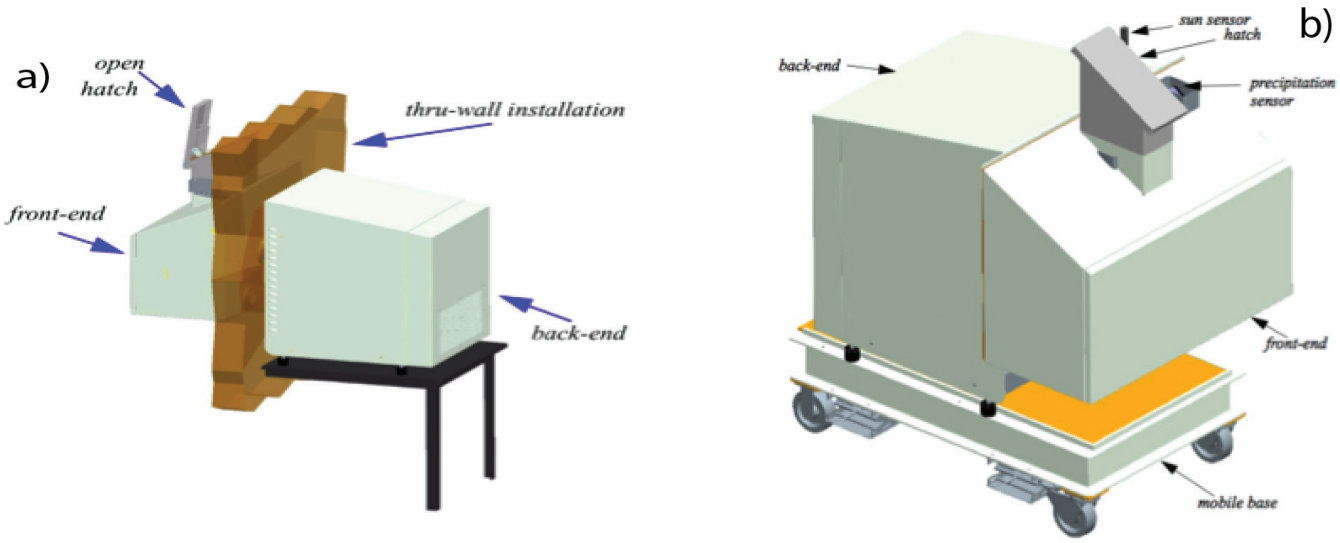

Figure 3-3. Two common deployment configurations for ground-based IR spectrometers: the through-wall (Figure 3.3a) and stand-alone (Figure 3.3b). (Images from the ABB AERI operations manual).

differences too. An analysis by Löhnert et al. (2009) demonstrated that the AERI instrument has 2-3 times more degrees of freedom of signal (i.e., independent pieces of information) in both the temperature and water vapor profile as compared to the MWR (Figure 3.4). However, in high PWV conditions the information content in the IR observations decreases slightly; for example, in dry conditions the degrees of freedom of signal is between 6-8 for the water vapor but decreases to less than 6 for higher water vapor conditions. The extra information improves the vertical resolution of the IR-retrieved profile relative to the MWR, thereby providing more accurate retrievals in many atmospheric conditions of features such as elevated temperature inversions, strong moisture gradients, etc.; these improvements allow for more accurate estimation of convective indices such as CAPE and CIN. Thermodynamic profiles and convective indices derived from AERI observations have been very useful in characterizing preconvective environments in a wide variety of case studies (Turner et al., 2000; Feltz et al., 2002, 2003; Wagner et al., 2008).

Pairing an IR spectrometer with a spectral MWR has many synergistic advantages. An IR spectrometer thermodynamic retrieval is sensitive to the first guess profile used in the physical retrieval, whereas the MWR retrieval is much less sensitive; thus, using the lower information content profile retrieved from the MWR as the first guess in the IR spectrometer retrieval process improves the likelihood of a successful retrieval from the spectrometer.

3.6 Environmental Issues

Some care needs to be taken in the deployment of an IR spectrometer. An AERI instrument needs to be run in a configuration where the interferometer is at laboratory temperatures and the front end (blackbodies and scene mirror) are in the ambient environment. This is typically achieved using one of two different methods (Figure 3.3a,b). The front end needs to be protected from precipitation as this preserves the lifetime of the gold plated scene mirror. An automated hatch uses rain sensors to detect the precipitation and closes the hatch; this does not affect the data quality as the atmosphere is generally quite opaque in precipitation conditions anyway and thus no thermodynamic profiling would be possible.

3.7 Reliability

IR spectrometers have been environmentally hardened to work operationally, and have demonstrated this over many years at a wide range of sites ranging from the Arctic (-35°C) to the tropics (+40°C). The length of the data record of several of these systems is longer than a decade. For an AERI instrument, three components typically require periodic service: (a) the scene mirror, which should be inspected monthly and cleaned or replaced when dirty; (b) the Stirling cooler, which typically has a lifetime of 3-5 years; and (c) the laser inside the interferometer, which has a lifetime of five years.

3.8 Research Needed

Current efforts are underway to develop a retrieval algorithm that uses both IR spectrometer and MWR data simultaneously to retrieve qT profiles in both clear and cloudy scenes. The former has already been demonstrated (Löhnert et al., 2009). Additionally, joint AERI / MWR retrievals of cloud properties have been shown to improve the accuracy of cloud liquid water path significantly (Turner, 2007). It is anticipated that the joint qT/cloud property retrieval algorithm will be very useful in cloudy scenes, with the

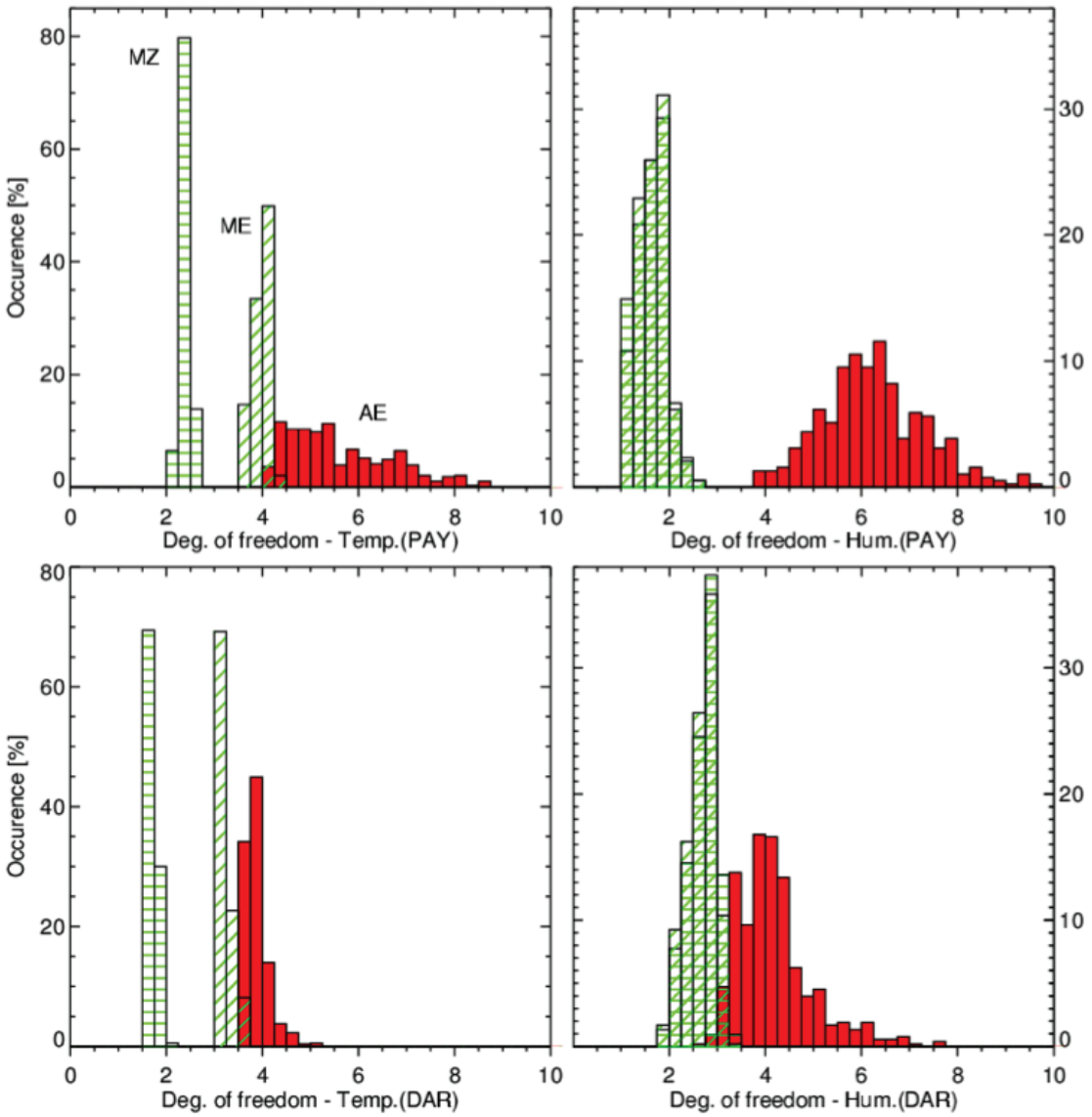

Figure 3-4. The distribution of degrees of freedom of signal in zenith spectral MWR observations, scanning MWR observations, and AERI observations for profiles of temperature (left) and water vapor (right) at a mid-latitude site (Payerne) and tropical site (Darwin); from Löhnert et al. (2009).

MWR providing the profile through the lower portion of the troposphere (even through the cloud, because the cloud opacity in the microwave is significantly smaller than the infrared opacity), whereas the IR spectrometer data will improve the accuracy and vertical resolution of the profile below the cloud.

Additional investigation is also needed to decrease uncertainties in the spectroscopy of various water vapor and carbon dioxide absorption lines in the IR spectrum.

3.9 Contributions for Air Quality Applications

IR spectrometers can contribute in two ways to air quality applications. First, due to their relatively high information content, IR spectrometers are able to better resolve the temperature inversion at the top of the boundary layer, which is important to understand whether pollutants will be trapped in the boundary layer or not. Secondly, various trace gases have absorption bands in the IR, and thus observations in these spectral regions can be used to infer the column amount of the trace gas. For example, significant amount of work has been done to retrieve the column amount of carbon monoxide (Yurganov et al., 2010).

SECTION 4. LIDAR

4.1 Active Remote Sensing Methodology

In contrast to a passive remote sensing system, an active system employs a transmitter that sends a short pulse of light into the atmosphere. Lidar has been demonstrated with wavelengths from <0.3-10 μm. Lidar has high range resolution determined by the ability to digitize the returned signal in time (~1.5-300 m) and the range itself is determined by measuring time of flight of the pulse between the transmitter to the scattering volume and returned to the detector.

The strength of the backscatter signal strongly depends on wavelength. For direct detection receivers used in thermodynamic profiling applications, the photon number N as a function of range R is given by the following equation

$$N(R) = CO(R)\frac{\beta(R)}{R^2}T(R) \tag{4.1}$$

where C is a system constant containing laser pulse energy and receiver area, O is the overlap function between the transmitted and received signal (generally unity beyond a few hundred meters), β is the backscatter coefficient of the atmosphere, and T the atmospheric transmission from the lidar site to the scattering volume and back.

Elastic systems (those that detect radiation at the same wavelength as the emitted radiation) are relatively simple. In an elastic lidar, β is determined by molecular and particle backscattering. Inversion of the lidar equation with respect to particle backscattering gives information about aerosol microphysical properties. A fundamental impediment to the solution to the above equation is the lack of knowledge of both the backscatter and attenuation (in the transmission term) at the same time. Examples of such systems are ceilometers used in a network setting by NOAA/NWS in the ASOS network of sites (close to 1000 sites in the U.S.). Because aerosols tend to be confined to the PBL, simple elastic systems have the ability to discern PBL height, but may or may not give quantitative profile information, depending on the configuration. Despite their potential value, ASOS ceilometer data are not archived at the present time.

In inelastic systems, such as Raman lidar, β must be replaced by the Raman backscattering coefficient that is proportional to the number density of the scattering molecule (N_2, O_2, H_2O) and the Raman backscattering cross section. Figure 4.1 demonstrates the relative intensity of backscatter signals. As the figure shows, Raman backscattering signals are two to three orders of magnitude smaller than elastic scattering. This has consequences with respect to the daytime performance of Raman lidar, as the solar background overwhelms the signal and limits the achievable range to below 4-5 km in the daytime by using narrow-band interference filters (see below for this discussion). On the other hand, Raman signals are easy to analyze and have been put to routine use at a number of national infrastructure sites (e.g., MeteoSwiss, DWD-Germany, DOE-USA, etc.).

For temperature and humidity retrievals with lidar, we distinguish below between Raman techniques and the differential absorption lidar (DIAL) method.

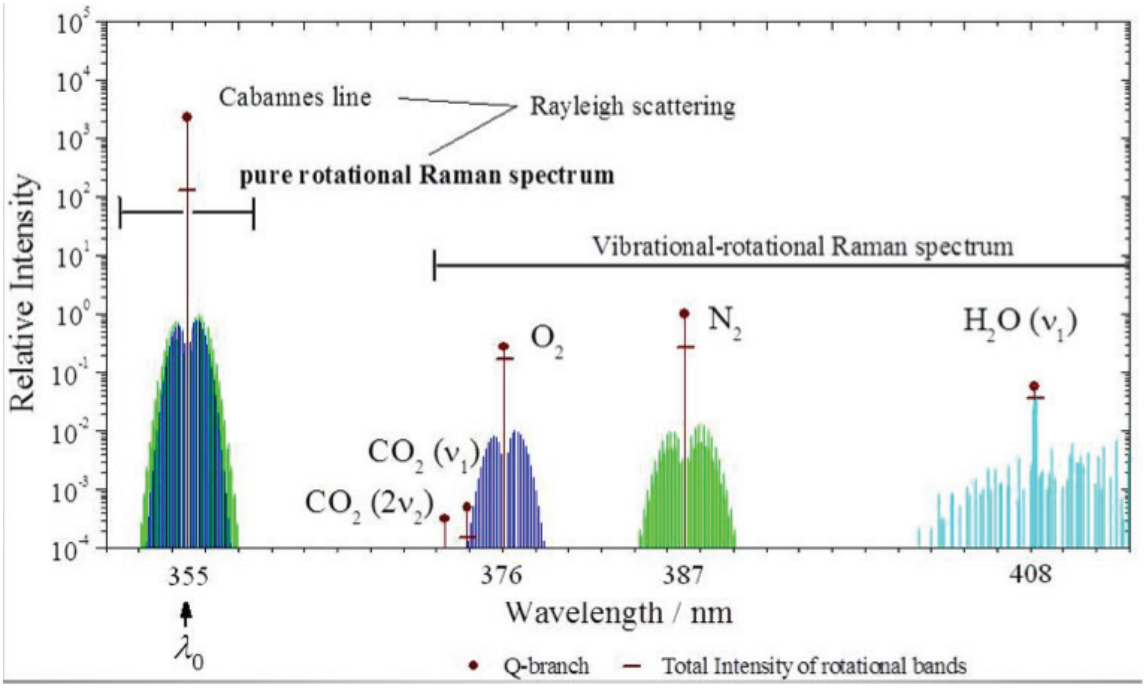

Figure 4-1. Relative intensity of elastic and inelastic scattering in the atmosphere.

4.2 Lidar-Based Temperature Profiling

The Rotational Raman Lidar (RRL) method for the measurement of atmospheric temperature was first suggested by Cooney (1972). The intensity of the pure rotational Raman spectrum of nitrogen is related to J, where J is the rotational quantum number of the transition, with higher quantum numbers more populated at higher temperature due to the Boltzmann density distribution. RRLs use this property and measure the ratio of backscatter signals, *Q*, at two suitable spectral regions in the Raman spectrum that have different temperature dependency. The temperature profile is determined by

$$T(R) = -\frac{2a^2}{b-\sqrt{b^2-4a[c-1\mathrm{n}Q(R)]}} \tag{4.2}$$

after calibration of the signal intensities with the coefficients *a*, *b*, and *c*. Usually these coefficients are determined by careful comparisons with radiosoundings. After calibration, the retrieval has excellent long-term stability. Care must be taken to block the elastic backscatter signal from swamping the rotational Raman channels (Behrendt and Reichardt, 2000). For daytime high-resolution RRL, the methodology to choose the channels has been described by Radlach et al. (2008). The noise error profile can be determined for each retrieval according to

$$\sigma_T = \frac{\partial T}{\partial Q} Q \sqrt{\left(\frac{\sigma_{RR1}}{I_{RR1}}\right)^2 + \left(\frac{\sigma_{RR2}}{I_{RR2}}\right)^2} \tag{4.3}$$

where 1,2 refer to the two spectral regions. Obviously, the system noise is mainly determined by solar background and backscatter signal Poisson statistics, which can directly be measured by the photon counting system. As signal statistics scale with laser power and receiver area (currently 10 W and 40 cm diameter in the Institute of Physics and Meteorology (IPM) system), these are the most appropriate means for further improvements of range and resolution.

Several ground-based and airborne lidar systems exist today and a thorough discussion can be found in the literature (Behrendt, 2005 gives an extensive survey). Using high quality filters, temperature measurements in optically thin cirrus were made possible (Behrendt and Reichardt, 2000). Most RRL profiling has utilized the 532nm wavelength of the Nd:YAG laser because of high laser power and receiver efficiency compared to ultraviolet (UV systems. The l^{-4} dependence of Raman scattering gives UV systems an advantage for daytime tropospheric profiling (Di Girolamo et al., 2004; see also Figure 4.2), providing narrow-band interference filters are used. Daytime profiling at this wavelength was also demonstrated using gratings and Fabry-Perot interferometer detection (Arshinov et al., 2005). State-of-the-art systems for daytime measurements are based on frequency-tripled Nd:YAG lasers so that this laser technology is fundamental for RRL. An RRL with high resolution during daytime was demonstrated by Radlach et al. (2008) at the IPM at the University of Hohenheim, and has also three-dimensional scanning capability.

High spectral resolution lidars (HSRL) have been used to measure tropospheric temperature profiles but with much more complication and difficulty (Hua et al., 2005). The HSRL technique resolves the temperature dependent linewidth of the Cabannes line, which is Doppler broadened. This requires much higher system stability and it is hard to reject the Mie scattering signal (Hair et al., 2001; Hua et al., 2005). As with the rotational Raman technique and state of the art interference filters, measurements in optically thin clouds are possible.

4.3 Lidar-Based Water Vapor Profiling

Lidar, with its ability to provide range-resolved profiles in a short time (seconds or minutes), can be used to make unique remote measurements of water vapor distributions. A number of lidar systems have been developed and demonstrated for water vapor measurements using either the differential absorption lidar (DIAL) technique or the Raman scattering approach.

4.3.1 The Raman Technique

The Raman technique for moisture profiling utilizes very weak light scattering from molecules at wavelengths shifted from the incident light. The Raman technique relies on measuring the rotational or vibrational-rotational component of Raman scattering from the atmosphere. The method generally requires the detection of laser radiation that is shifted to the longer wavelengths (Stokes shift) for the gas being probed.

In atmospheric water vapor profiling, the main molecules of interest are water vapor, nitrogen, and oxygen that have convenient, although weak, vibrational Raman shifts at approximately 3657, 2331, 1556 cm^{-1}, respectively (see Figure 4.2; Turner et al, 2002; Whiteman et al., 2003a,b, 2006). For a 355nm tripled Nd-YAG laser, this places the detected wavelength for water vapor at 407 nm in the visible and for a 532 nm doubled Nd-YAG laser, the line is at 607nm. Because these wavelengths have strong skylight background, this requires precision 0.1 - 0.3 nm bandwidth filters with high out-of-band light rejection for collecting the Raman scattered return during daytime.

If water-vapor N_H and Nitrogen N_N Raman scattering signals are used, their ratio is taken which becomes proportional to the water-vapor mixing ratio *m*

$$m(R) = C\Delta(R)\frac{N_H(R)}{N_N(R)} \tag{4.4}$$

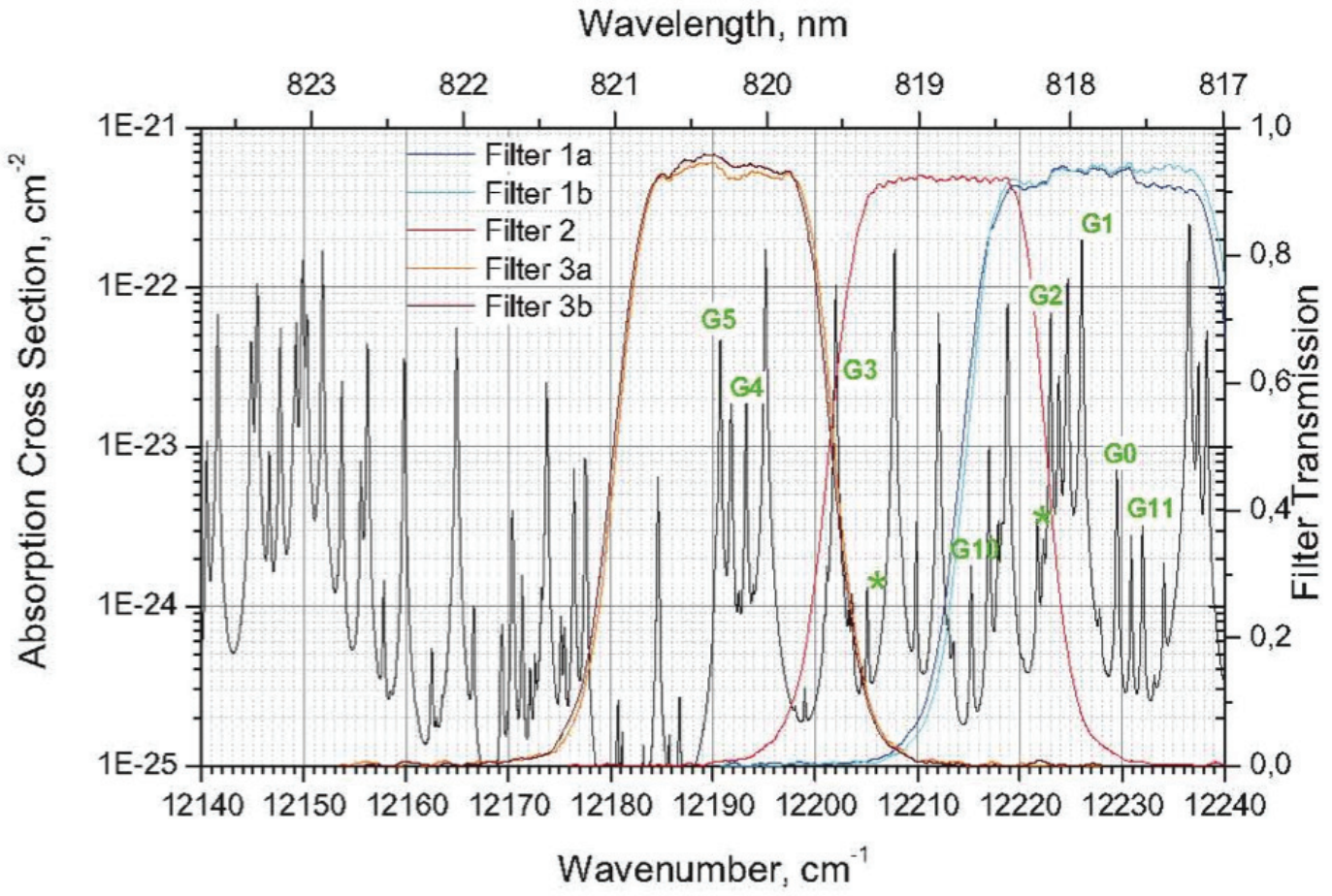

Figure 4-2. Suitable water-vapor absorption lines and offline frequencies for DIAL in the 820-nm wavelength region and corresponding filter bandwidths for the IPM system.

C is a system calibration constant and D is a correction for atmospheric extinction. Ansmann et al. (1992) and Whiteman et al. (1992) show that this correction can be determined with an error of < 5 %. Venable et al. (2011) have demonstrated the error can be further reduced to less than 3%. The advantage of such a system is that it is possible to combine a water-vapor channel with RRL channels so that qT profiles are retrieved, simultaneously, as is done successfully by a number of systems (DOE-ARM Raman lidar: Ferrare et al, 2006; MeteoSwiss aerological station at Payerne, Switzerland: Calpini et al., 2009; the NASA/GSFC system: Di Girolamo et al., 2004). The constant C is related to the Raman water vapor cross-section and can be calculated from first principles (Venable et al., 2011) or calibrated using column water vapor measurements from MWR or GPS observations (Turner et al., 2000; Russo, 2007; Adam, 2010). New methods, like that of the Howard University and NASA/GSFC lidar groups (Venable et al, 2011) have removed this requirement by using a NIST traceable light source to determine the calibration with less than 3% relative uncertainty. Note that above equation depends on the temperature sensitivity of the Raman cross-section, which is often neglected in the lower troposphere but becomes important in the upper troposphere. An extensive discussion of this is available in Whiteman (2003).

Also the error analysis is straightforward and can be performed as in RRL for each profile according to

$$\frac{\sigma m}{m} = \sqrt{\left(\frac{\sigma_H}{N_H}\right)^2 + \left(\frac{\sigma_N}{N_N}\right)^2} \tag{4.5}$$

The majority of the Raman lidars operating today use the Nd:YAG laser at wavelengths of 355nm, where daytime solar background is considerable. The Solar-Blind Raman lidar avoids the daytime background pollution of the Raman signal by operating at 248 nm wavelength, where solar background is negligible. However, the range of this system is limited to less than a km because of the high absorption caused by ozone. For short distances, solar blind Raman lidars can provide a highly detailed and fast sampling rate that would allow flux calculations (Eichinger et al., 1993). A spatial resolution of about 1.5m can be achieved (Eichenger et al., 1999).

4.3.2 DIAL

The DIAL lidar technique utilizes two laser wavelengths to determine the range-resolved profile of atmospheric water vapor num-

ber density or relative humidity (Bösenberg, 1998; Wulfmeyer, 1998; Wulfmeyer and Bösenberg, 1998). The online wavelength is tuned to a water-vapor absorption line while the offline wavelength is tuned to a nearby region that is weakly or not absorbed. The lidar return from the "off" laser wavelength provides a reference signal for the atmospheric scattering from molecules and aerosols and for the slowly varying "background" atmospheric absorption that is common to both lidar wavelengths. The retrieval is executed using the DIAL approximation

$$N_{WV}(R) = -\frac{1}{2\sigma}\frac{d}{dR}\ln\frac{P_{on}(R)}{P_{off}(R)} \tag{4.6}$$

where σ is the difference between the online and offline water-vapor absorption coefficients. P_{on} and P_{off} are the online and offline signal return powers, respectively. Obviously, no calibration of the DIAL system is required, the accuracy is mainly determined by laboratory measurements of the water-vapor absorption cross section in the wavelength range of interest.

Error analyses can be performed for each profile using

$$\frac{\sigma_{WV}}{N_{WV}} = \frac{\sqrt{2}}{2\Delta\tau}\sqrt{\left(\frac{\sigma_{on}}{I_{on}}\right)^2 + \left(\frac{\sigma_{off}}{I_{off}}\right)^2} \tag{4.7}$$

by exploiting the SNR of the return signals. Here, $\Delta\tau$ is differential optical thickness of water-vapor in a range cell. Alternatively, error profiles can be determined by the analysis of the autocovariance function or the spectra of the high-resolution water-vapor time series at each range level (Wulfmeyer, 1999a; Lenschow et al., 2000; Wulfmeyer et al., 2010).

Obviously, water-vapor DIAL measurements can be performed under a variety of atmospheric conditions even if the atmosphere is very dry, as long as the strength of the differential water-vapor absorption cross section is adapted. The signal-to-noise ratio of the signals is significantly higher in comparison to Raman signals, as elastic backscatter is used. Therefore, if a high-power laser transmitter is used at the same efficiency of the receiver and same laser power, better daytime performance of DIAL can be expected but the range may be limited. This makes DIAL appropriate tool for high-resolution, turbulence resolving daytime measurements in the ABL (Wulfmeyer, 1999a,b) and for daytime upper tropospheric measurements. Additionally, if a low-power, compact DIAL system is used, the error equation demonstrates that the same temporal-spatial resolution of Raman lidar can be achieved during daytime. Further details are discussed and extensive performance analyses are presented in Wulfmeyer and Walther (2001a,b).

4.4 State of the Technology

4.4.1 DIAL Systems

Differential absorption lidar systems have a long heritage having been demonstrated only one year after the first elastic lidar system (Schotland, 1964). Limited primarily by the availability of tunable sources of laser radiation, ground based DIAL systems have been demonstrated for water vapor and are now quasi-operational (Wulfmeyer, 1998; Wulfmeyer and Bösenberg, 1998; Behrendt et al., 2009; Lazzaroto, 1999; Nehrir et al., 2011; Repasky et al., 2011; Vogelmann et al., 2011). Suitable water vapor vibrational-rotational bands are located around 820-840nm, 920-940 nm and longer wavelength regions of the IR.

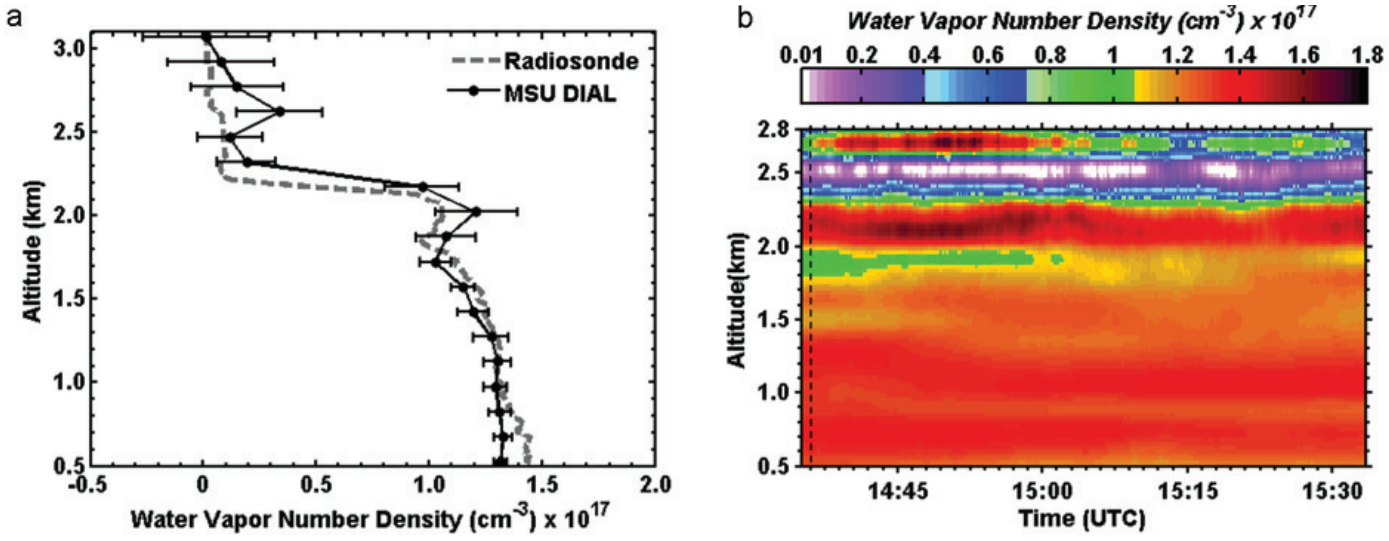

Figure 4-3. Results from a compact, all solid state DIAL system developed at Montana State University that utilizes a low pulse rate, high pulse rate transmitter. Integration time for the measurement was 30 minutes.

The main challenge of the DIAL technique is the development and operation of a suitable laser transmitter. In the DIAL approximation, it is assumed that the laser transmitter spectrum can be considered as a delta function with respect to the water-vapor absorption line. This leads to stringent requirements with respect to frequency stability, bandwidth, and spectral purity (Wagner et al., 2011). High frequency stability in H_2O DIAL systems has been accomplished by Alexandrite lasers (Wulfmeyer and Bösenberg, 1995, 1996), optical parametric oscillators (Fix et al., 1998) and other high power mixing systems. These lasers are expensive and typically require significant scientific technical expertise. This is a limitation to the technique that has been a barrier to the use of DIAL in observational systems, except for a few meteorological agencies. One example of a quasi-operational DIAL system is the Institute for Meteorology and Climate Research-Atmospheric Environmental Research (IMK-IFU) instrument deployed at the Scheefernerhaus Observatory on the Zugspitze in Germany (Vogelmann et al., 2008). This instrument utilizes two single mode optical parametric oscillators to seen a flashlamp-pumped Ti:Sapphire laser. Pulse energies of 250 mJ enable vertical measurements to heights of 12 km, approximately five times per week, to investigate changes in upper tropospheric water vapor.

Recently, work has focused on development of low energy, high pulse repetition rate DIAL instruments for water vapor profiling. Initial work was done by Machol et al. (2004), who demonstrated a DIAL system using a high pulse rate, low pulse energy diode laser source, and solid state flared amplifier to measure water vapor in the boundary layer at nighttime. The technique demonstrated by Machol et al. (2004) has been extended in recent years to daytime by including transmitter-amplifier combinations with higher pulse energy, as shown in a poster presentation by Repasky (see Nehrir et al., 2009, 2001; Repasky et al., 2011) of Montana State University (MSU). The workshop presentation presented results obtained from a DIAL system utilizing the low power, high repetition rate, diode laser source methodology. Such a system is likely to be nearly an order of magnitude less expensive than prior high power systems. Figure 4.3 shows results from the MSU instrument, indicating good agreement with a sonde and excellent temporal stability. Work is ongoing to increase laser pulse energy, a necessary improvement to enable daytime operation in regions of high water vapor. Because of its potential for low cost and high reliability, this technology has promise for application in a surface-based network.

Figure 4.4 demonstrates the current daytime performances of a state of art ground-based DIAL at the University of Hohenheim. Measurements in the lower to the middle troposphere are possible with a resolution of 10 s and 60 m, respectively. In the near-range measurements are possible even with a resolution of 1 s and 15 m, respectively. Turbulent processes are clearly resolved in the convective PBL (between 300-800 m). Also above the PBL, highly

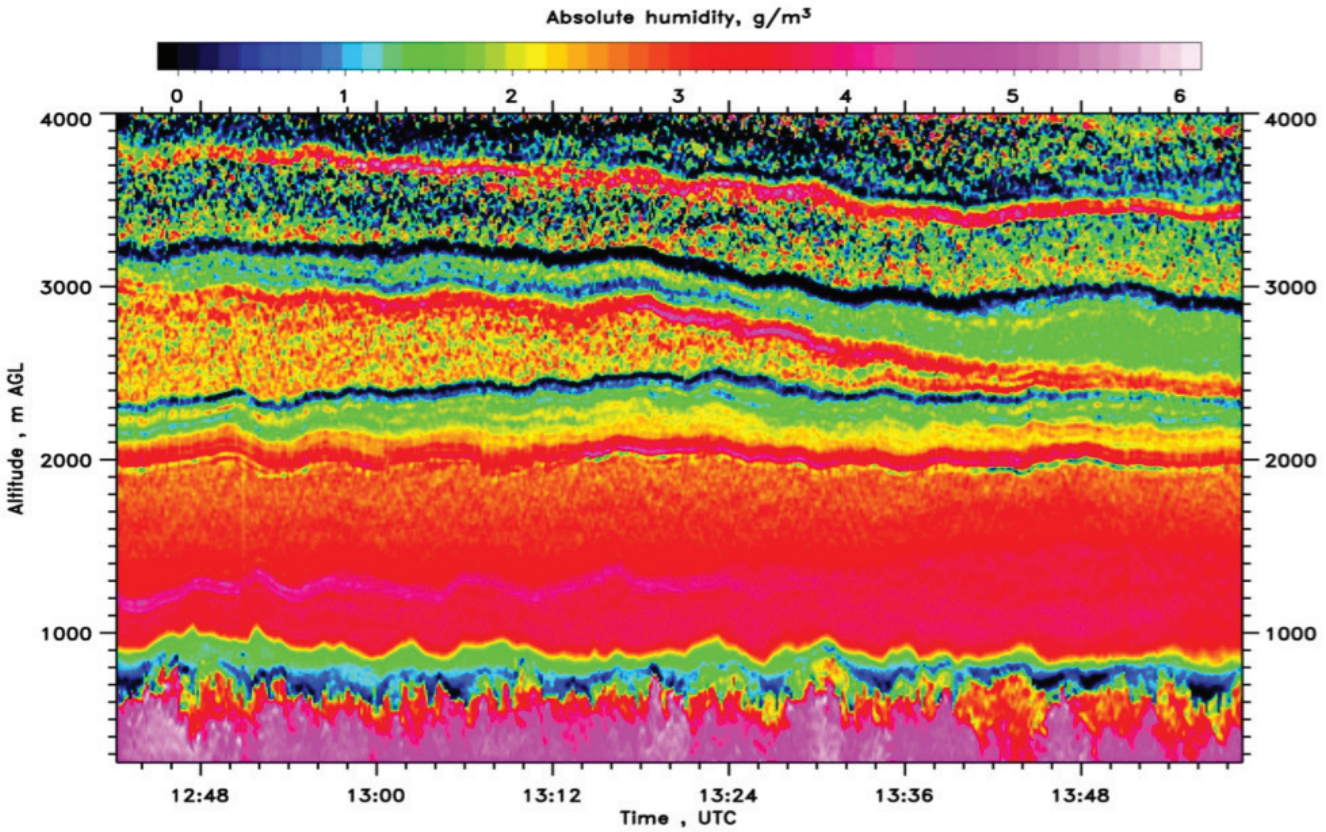

Figure 4-4. Time-height cross section of water-vapor measurement using the IPM system during COPS on July 26, 2007. The temporal-vertical resolution of the profiles is 10s and 60 m, respectively, throughout the lower troposphere.

accurate measurements are possible resolving a complex vertical structure of the water-vapor field including wavelike activities.

Solar Radiation Influence

As water vapor DIAL operates in the near infrared, solar radiation background is important and operation at night will have higher performance than daytime. Narrow interference filters are required for DIAL and this mitigates solar background as does the NIR wavelength where Rayleigh scattering is decreased dramatically from visible wavelengths.

Calibration of the Water Vapor Mixing Ratio

The DIAL technique has the advantage that the water vapor absorption coefficient at these wavelengths is well known and only moderately affected by temperature and pressure as the profile is retrieved at high altitudes. The water vapor line strengths are listed in the HITRAN database (Rothman et al., 2008). The water vapor spectrum contains considerable absorption between lines in the IR spectrum and the source of such "continuum" absorption is an active research topic. It not only affects retrievals of water vapor and temperature, but is important for other trace gas retrievals such as CO.

Eye Safety

At these near IR wavelengths, eye safety is an issue and may limit the use of the lidar systems if mitigation procedures are not employed. While slant use of Raman systems has been used to give horizontal resolution for water vapor (Eichenger et al., 2006), DIAL would be more restricted from use in this mode because the direct beam would be more likely to be viewed in slant path. Low power systems, such as that demonstrated by Nehrir et al., (2001), have the advantage that the power level of exposure can be controlled to be eye-safe by expansion of the outgoing laser beam.

4.4.2 Raman Water Vapor Profiling Systems

Raman lidar systems are based on mature technologies and are being used routinely for both research and operational purposes. Raman lidars have achieved a turnkey operational capability to continuously probe the PBL (Goldsmith et al., 1998; Calpini et al., 2011). Some of these systems require minimal intervention and maintenance for routine day and night operations. The fact that the technology has been demonstrated in over 10-years of operational setting together with the minimal intervention required as compared to the DIAL technique has made it a preferred choice by many national weather services and agencies around the world (Germany in Lindenberg, MeteoSwiss in Payerne, several sites within the DOE/ARM network, and others are examples).

During nighttime, many operating Raman systems can provide water vapor mixing ratio data from near the ground to more than 10-12 km at night using averaging time in the order of 1-5 minutes. The altitude range can be extended by using longer averaging times and the error reduced by using statistical treatments. During daytime, the vertical range is about 4-6 km but longer averages have been used to extend the usable range.

Solar Radiation Interference

One of the main difficulties in the Raman-based water vapor profiling technique is the weak Raman backscatter; it is about four orders of magnitude lower than combined Mie plus Rayleigh backscatter. With signals that are extremely low, detection and isolating the water vapor signal from all other signals requires a very narrow bandwidth filter. Raman operation in the daytime PBL is severely impacted by solar radiation background; which affects the efficiency of the detection statistics. Because of this solar radiation interference, the daytime profiling capability is limited; for most systems this maximum daytime altitude for the water vapor mixing ratio profile for 1-minute averaging time is about 4-6 km. This is comparable or better than what can be achieved from passive systems.

Calibration of Mixing Ratio

Raman systems provide profiles of water vapor mixing ratio (g/kg) and these measurements are traditionally calibrated using an external sensor. Water vapor mixing ratio value at a given altitude (typically from a radiosonde) or an integrated quantity like the integrated precipitable water vapor (IPW) amount that can be derived from a GPS network, microwave radiometer, or sunphotometer is used. The calibration factors derived from such standard techniques give very stable values, usually with changes that are less than 3-5% over several months to years (Turner et al., 2000).

Recently, a technique have been developed that uses a NIST-traceable lamp as a calibration source and has shown great promise that allow for the independent determination of the water vapor mixing ratio calibration factor for a Raman lidar system (Venable et al., 2011). This technique utilizes a procedure whereby a light source of known spectral characteristics is scanned across the aperture of the lidar system's telescope and the overall optical efficiency of the system is determined. The method leads to a stable, theoretical determination of the water vapor mixing ratio calibration factor. A comparison of the theoretical and experimentally determined values agrees to better than 5%.

Eye Safety

The outgoing laser beam is expanded many times to achieve eye safety. The eye safety is an important consideration for an automated system and the reason why the fundamental and the second harmonic wavelengths of the laser are generally not transmitted. Typically, eye safety considerations are dealt with by expanding the outgoing beam.

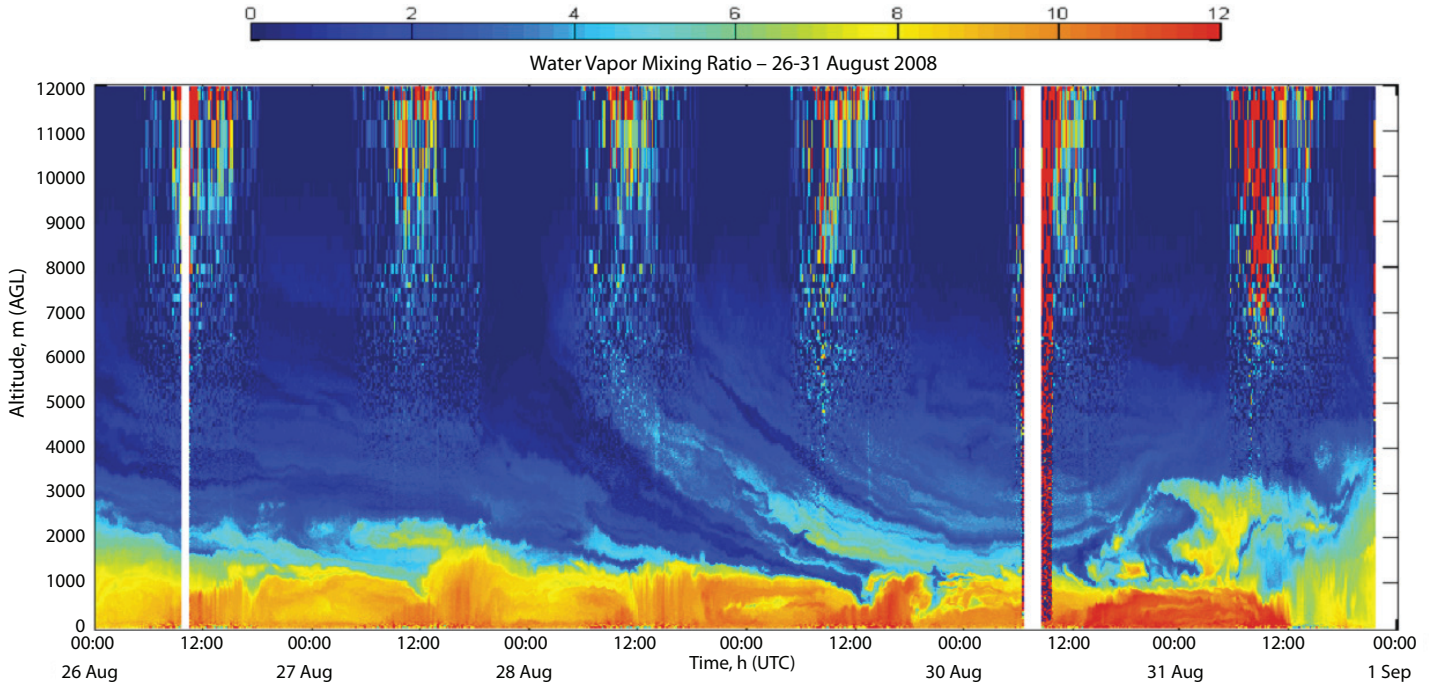

Figure 4-5. An example of a time-height false color plot of 6-day sequence of water vapor mixing ratio (g/kg) from the MeteoSwiss Raman lidar system (RALMO). A detailed picture of the PBL and nighttime UT is clearly captured. Note also the daytime-noise signature starting about 5-6km around 12UTC.

State of the Art Systems

Two examples that demonstrate the state of the art in continuous day-night and operational profiling of the PBL in use are the RALMO (Raman Lidar for meteorological observations, SWISS Meteorological Service (MeteoSwiss), http://eflum.epfl.ch/research/lidars/ralmo) at Payerne, Switzerland, and the DOE/ARM CARL (Goldsmith et al., 1998; Ferrare et al., 2006).

RALMO is fully automated, self-contained, eye-safe instrument for day and night-time vertical profiling of water vapor mixing ratio, aerosol backscatter, and extinction within the troposphere. The system uses a variable resolution with height for water vapor mixing ratio: 2-minutes and 15 m in the boundary layer changing to 30-minutes and 100–450 m in the free troposphere for time and vertical resolution, respectively. Similar resolutions hold for aerosol extinction and backscatter coefficients. RALMO's highest altitude range during daytime is 5 km while at night measurements are given to 10 km altitude. The lowest altitude of usable data for RALMO is 50 m, made possible by the unique multi-telescope design of the system. The water vapor mixing ratio detection limit for RALMO is 0.2 g/kg. Data from RALMO is automatically processed and prepared for upload to MeteoSwiss for operational use.

The Central Oklahoma ARM Raman Lidar (CARL) is located at the Southern Great Plains (SGP) central facility in north-central Oklahoma and has operated since 1996. The system uses a frequency tripled Nd:YAG laser, transmitting nominally 350 mJ pulses of 355 nm light into the atmosphere at 30 Hz. The backscattered light is collected with a 61-cm telescope. The system measures backscattered light at the laser wavelength (aerosol return), as well as 408 and 387 nm (water vapor and nitrogen Raman shifted returns, respectively). CARL has 10 detection channels giving aerosol backscatter, depolarization, water vapor, temperature, and experimental channels for liquid/ice water content. The aerosol return is split into co-polarized and cross-polarized channels with respect to the laser's output in order to compute the linear depolarization ratio. Recent modifications and details on the configuration of the Raman lidar can be found in (Goldsmith et al., 1998; Ferrare et al., 2006). CARL is operated in weather controlled housing through an optical window that adds an all-weather capability leading to profiles of water vapor mixing ratio in light rain and virga conditions. Figure 4.6 shows CARL uptime over a 4-year period indicating high overall reliability.

CARL Raman Atmospheric Temperature

A routine measurement of the temperature profile is also available from the CARL Raman lidar. It uses the anti-stokes regime (353.3 and 354.3nm) for detection and operates continuously (Newsom and Turner, 2011). Data reduction is automated and calibration of overlap is made using radiosondes. Complete overlap is achieved at about 4km. Raw data is collected at 10 s and 7.5 m resolution but temperature data is derived and provided at 300m in height and 60 min time averaging. The calibration constant is relatively stable with a variation of about 2.3%. The a mean nighttime temperature error is about 1.5°K or about 0.5% and daytime errors vary from

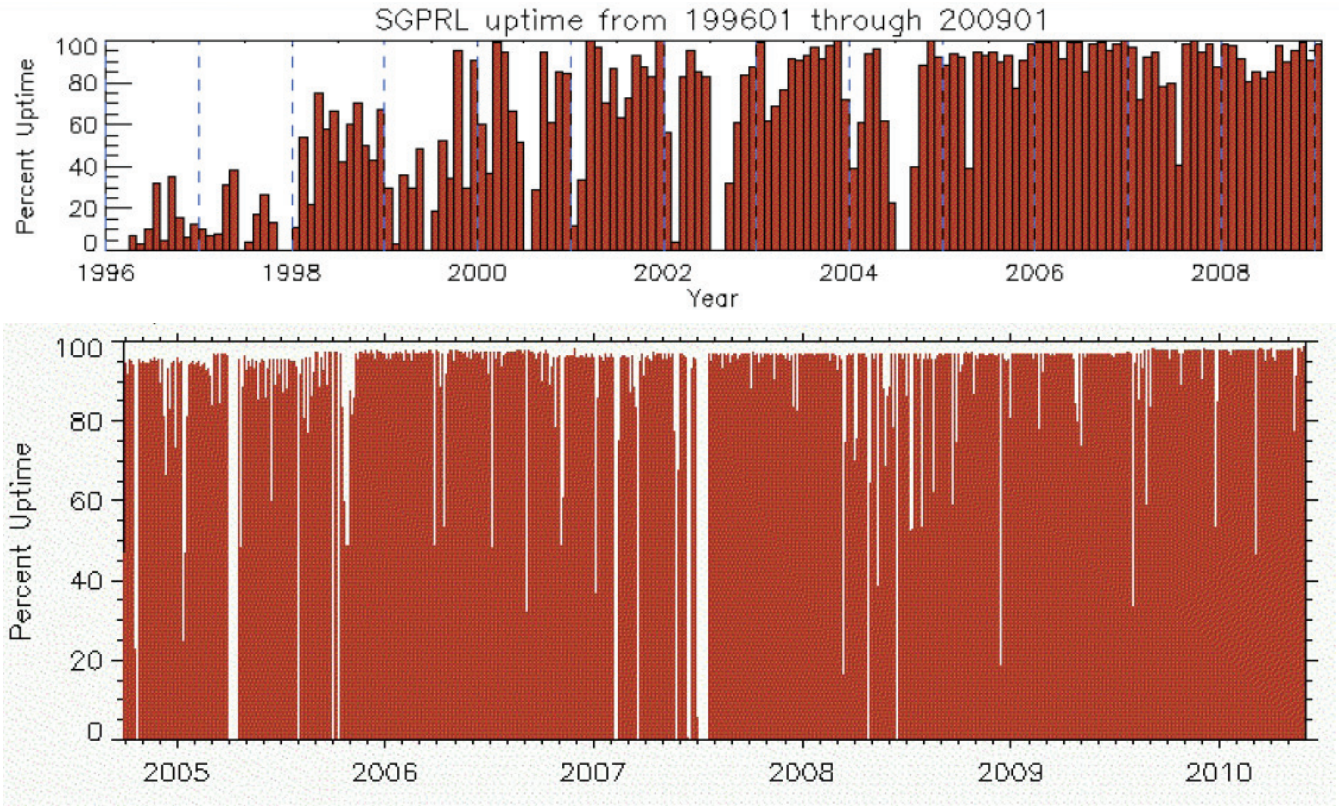

Figure 4-6. CARL Raman lidar uptime for January 1996 to May 2010. The uptime significantly improved and data availability improved. Data was available about 89% of the time (courtesy of D. Turner, unpublished).

1.5 to 2°K below 6 km and increases to >5°K above. The temperature data is only valid below clouds and when a good overlap correction is determined with a comparison with AERI observations showed correlation coefficients > 0.96 below 3km (AERI limit) and a median difference of +/−0.5 %.

4.5 Strengths, Weaknesses

DIAL and Raman lidar-based profiling of temperature and water vapor have many strengths and weaknesses that are directly relevant to suitability for network deployment.

4.5.1 Strengths of Raman Lidar

History of continuous operation: Unlike many passive remote-sensing instruments that require inversion schemes, the Raman lidar technique allows for a direct method of profiling water vapor mixing ratio amounts. Furthermore, for each profile, accurate estimates of the error covariance matrix can be determined in dependence of weather conditions. This makes Raman lidar a nearly ideal remote sensing system for data assimilation (Grzeschik et al., 2008). The Raman lidar system gives very high vertical and temporal resolution of water in the PBL.

Ease of operation: Raman lidars are relatively easy to operate and can be remotely controlled. Even at their worst, daytime performance, Raman lidars outperform passive sensors both in temporal resolution as well as altitude coverage.

Error analysis: The noise error covariance matrix can be retrieved for each profile in dependence of weather conditions. Error analysis is easily quantifiable and variables are usually known, unlike passive sensors that have to depend in a complicated covariance matrix.

Adaptability and expansion: Raman lidars can be designed to include receivers for rotational channels and be used to simultaneously retrieve temperature and water vapor profiles. In fact, many of the Raman lidars mentioned above do include simultaneous temperature and water vapor sensing.

4.5.2 Weaknesses of Raman Lidar

Solar radiation interference: An inherent difficulty in the Raman-based water vapor profiling technique is the weak Raman backscatter signal. As discussed above, a good detection of these signals and isolation from the solar background requires very narrow bandwidth and high out-of-band-rejection filters as well as high-power laser transmitters and large receivers. The current capability in filter technology and solar radiation error rejection techniques limit daytime water vapor mixing ratio profiling to 4-5 km at 1 minute resolution. However, although reported here as limitation, this daytime capability is superior to most passive sensors.

Calibration of mixing ratio: Raman systems provide profiles of water vapor mixing ratio (g/kg) and these measurements are traditionally calibrated using an external sensor although recent work by Venable et al (2011) have demonstrated calibration without an external WV reference. When using an external source, water vapor mixing ratio value at a given altitude (typically from a radiosonde) or an integrated quantity like the Integrated Precipitable Water vapor (IPW) amount that can be derived from a GPS network is used. The calibration factors derived from such standard techniques give very stable values, usually with changes that are less than 3-5% over several months or even years (Turner et al., 2000).

Overlap correction: As with all lidars, the incomplete overlap of the laser beam and the receiver telescope field of view in the immediate distances above the lidar significantly affects the performance of lidars. This incomplete overlap distance depends on the design properties of each lidar and amounts to about 100's of meters depending on the width of the field of view of the telescope. Most lidar designs attempt to minimize the effect by smart optical (telescope) design. Central to most of these corrections is the assumption of vertically homogenous atmosphere within the overlap region. However, this can be avoided by a scanning lidar.

Laser maintenance: The laser source in all lidar systems is a large portion of the installation and running cost. While laser lifetimes have improved, especially with diode pumped lasers over flashlamp pumped lasers, mean-time-between-failure (MTBF) for lasers in continuous mode is still an issue. If rapid field support is not commercially available for the laser source, redundancy in laser sources will be required to maintain continuous operations.

Environmental issues: *Weather controlled Housing*: Most day-night operational lidars use Nd:YAG or Ti:Sapphire lasers. These laser systems require temperature controlled housing for optimal operation. Other protective designs from rain and/or hail need to be installed to safeguard the telescope and associated electronics. Other than the eye safety issue, there are no other environmental effects that a lidar network will introduce on the environment.

Eye Safety Issues: Although the laser beam output can be designed to be "eye-safe", the system should be constructed in such a way that it is not possible for humans to stare into the beam directly from close distances. This is mostly accomplished by fencing the lidar system and/or having the beam outlet high and out of reach of the public. Further, the standard laser safety precautions and warnings must be met and the necessary FAA and other regulatory coordination are required.

4.5.3 Strengths of DIAL

Solar radiation interference: The sensitivity with respect to daylight background is strongly reduced in comparison to Raman lidar. Some differences in performance may remain, however, the extraordinary combination of temporal and spatial resolution is superior to passive remote sensing and superior to Raman lidar during daytime.

Calibration: The DIAL technology is a "self-calibrating" remote sensing technology. Typically, a systematic error of <5% can be expected throughout the troposphere.

Temporal and spatial resolution: High-power DIAL systems demonstrated the highest accuracy and resolution of all water-vapor remote sensing technologies yet. The combination of spatial and temporal resolution up to the upper troposphere (few 100 m and min) fulfills the requirements for data assimilation in mesoscale models during daytime and nighttime (Wulfmeyer et al., 2006). As during daytime the SNR of a low-power DIAL is still high enough for profiling in the lower troposphere, low-power compact DIAL systems are very interesting and affordable options for future water-vapor remote sensing networks.

Error analysis: The noise error covariance matrix can be retrieved for each profile in dependence of weather conditions. The bias is usually that low that bias correction in any data assimilation system is not necessary (Wulfmeyer et al., 2006).

Scanning capability: It is possible to operate scanning DIAL systems during daytime so that the profiles can be extended to the ground closing an important gap to the surface. Because of eye safety issues and compliance with FAA regulations in the U.S., scanning an infrared system is more challenging than an ultraviolet system as some jurisdictions do not accept radar interlocks to protect overflying aircraft.

4.5.4 Weaknesses of DIAL

Complexity of laser transmitter: The DIAL technique requires a laser transmitter with high frequency stability, low bandwidth, and high spectral purity. It is challenging to maintain all these requirements, simultaneously, and at high average power. Critical laser technology includes fully diode-laser pumped, frequency doubled Nd:YAG lasers for driving Ti:Sapphire, OPOs, or mixed Garnet transmitters.

Overlap correction: Same as Raman lidar (see above). However, measurements close to the ground are possible with scanning systems (Behrendt et al., 2009).

Environmental issues: *weather controlled housing:* Same as Raman lidar except that better vibrational control is useful for the operation of DIAL transmitters.

Eye-Safety Issues: As DIAL is operating in the near-IR, eye-safety is a more difficult issue than for Raman lidar. However, if low-

power operation of DIAL is considered, this system can be made fully eye-safe as well.

4.6 Readiness for Deployment in a Network

The routine and operational Raman lidars mentioned above (e.g., RALMO, CARL) are rather "large" and may be costly to be considered as network ready. They are less complicated, however, than the existing NWS operational Weather Surveillance Radar (WSR-88D) instruments.

A recent development that has made the compact DIAL closer to a reality is the progress made by researchers at Montana State University (Nehrir et al., 2011). They have demonstrated the feasibility of using commercially available low energy, high pulse repetition frequency diode laser based seed sources and amplifiers for retrievals of lower tropospheric water vapor and aerosol extinction profiles with integration periods of 20 minutes and 1 minute, respectively. Recent improvements in this technology indicate the possibility of retrieval of boundary layer water vapor and aerosol extinction profiles at resolutions approaching 10 minutes and 1 second, respectively. Daytime profiling of water vapor to about 3 km and nighttime profiles to about 6 km with a resolution of 150 m or less appears potentially feasible.

Figure 4-7. A picture of the DOE/ARM Raman lidar located at the Central Oklahoma Facility in Lamont, Oklahoma.

4.6.1 Deployment Scenarios

The most feasible deployment scenario for lidars, at the moment, is distributed zenith profiling with each lidar co-located with other passive and in-situ sensors. This co-location with microwave systems will compensate for data loss from lidars during rain/clouds.

A recent report (Turner et al., 2011) assumes 140 Raman lidars at the NWS WSR-88 locations. Such a network would be capable of capturing the synoptic scale variability of the water vapor and temperature variations but will miss much of the mesoscale and sub-mesoscale water vapor variability important for convection and quantitative precipitation forecasting as investigated in IHOP_2002, COPS2007 and other field sites (Weckwerth, 2004; Wulfmeyer et al., 2008).

Additional Benefits of Scanning

Data derived by scanning lidar systems can be applied to many different atmospheric applications. These include the study of spatial variations of aerosols and the BL dynamics (Piironen and Eloranta, 1995; Mayor and Spuler, 2004), near surface moisture transport due to turbulence, heterogeneity of evaporation, and application in complex train flow studies (see Behrendt et al., 2009 for extended discussion). By scanning the system rapidly, flow of aerosol and water vapor structures can be visualized. It is possible to mitigate the overlap issues discussed above by obtaining near surface data to the side of the lidar.

Unfortunately, there are very few water vapor and temperature lidar systems that operate in scanning mode. Scanning a laser beam is commonly avoided because of eye-safety considerations. In addition, scanning DIAL systems would limit the altitude and range of the probed water mixing ratio (because of beam attenuation in the thicker PBL) and make its use questionable. Further, scanning systems tend to be operationally complex and unstable compared to zenith profiling systems. The UHOH scanning RRL system (Radlach et al., 2008) and the DIAL system (Behrendt et al., 2009) are the most advanced operational scanning RRL and water vapor lidar systems. Although these systems have expanded the application of lidar data into many different types of study (farm animal effluent dispersion; spatio-temporal aerosol variability, low-level moisture variability; see Behrendt et al., 2011a; Valdebenito et al., 2011), they still require extensive attention during operation.

4.6.2 Approximate Costs

Water vapor and temperature profiling lidars are not commercially available yet. But, there are a number of systems in operation and the approximate costs are given in the table below. In the estimate below, estimates of costs of some promising systems that are under development and may appear in the market in the coming year or two, if not months, are also included. *The statement that is "game changer" here is that the lidar community is poised for breakthrough systems that may be cost competitive with available commercial passive systems.*

Table 4-1. Table showing costs and operating parameters for current and future lidar systems. Costs and performance for the Montana State DIAL system are projected for the next generation version of the instrument.

Name	Approximate Initial Cost ($K USD)	Operating Cost ($K USD)	Auton-omous	Variable Measured	Resolution		Accuracy	Maximum Range
					Vertical	Temporal		
Raman Lidars								
CARL	1500	15-20	Y	Temperature	30m	15m	<1.5 K	4km Daytime; 10km Night
				Water Vapor	30m	10s	<5%	
Comment: Turner and Goldsmith, 1999; Ferrare et al., 2006; Newsom and Turner, 2011.								
RALMO	600-700	15-20	Y	Water Vapor	Variable: < 4km-15m; < 6.5km-30m; < 9km-100m; > 9km-300m	Variable: < 4km-10min; > 4km-30min	<5%	5km Daytime; 12km Night
				Temperature			~0.5 K	
Comment: Material cost is 500K CHF (~$634 USD). Contact: valentin.simeonov@epfl.ch								
HURL	250	15-20	N	Water Vapor	30m	1min	~5%	4km Daytime; 10km Night
Comment: Material cost only. HURL is a research and teaching Raman lidar.								
DIAL								
MSU-DIAL	<100**	10	N	Water Vapor	< 150m	5min	N/A	3km Night 6km Daytime
*Comment: Montana State University DIAL lidar: **Estimated material cost only. Nehrir et. al. (2011).*								
IMK-IFU	>600	10	Y	Water Vapor	50-250	41s	5% (to 5 km)	~12km
Comments: Five profiles per week.								

4.7 Research Needed

The challenges facing the lidar community for networking lidars can be divided into the following three main categories.

4.7.1 Laser and Associated Technology

The first can be classified as of technological nature, e.g., the general lack of availability of affordable laser technology that would yield a consistent and stable power and bandwidth as well as frequency stability. This lack of appropriate laser technology specifically targeted for atmospheric lidar remote sensing affects both the DIAL and Raman lidar techniques. The critical laser technologies are high-power diode lasers for laser pumping and for direct operation as water-vapor DIAL as well as high-power diode-laser pumped Nd:YAG laser technology for improving laser stability, minimizing maintenance costs and cooling power, and for increasing the SNR of the backscatter signals (Ostermeyer et al., 2006). For Raman lidar but also for pumping DIAL laser transmitters, these diode-pumped Nd:YAG lasers should have an average power of 100 W in the IR at repetition rates of 50-500 Hz. A research input into such lasers and associated technology will yield a large payoff towards making routine operation of lidar-based water vapor and temperature profiles and the realization of lidar networks in a cost effective manner.

Automated calibration systems have begun to be developed for lidar (Venable et al., 2011). The ability to determine and correct the overlap function for these lidars also needs automation, if extension of lidar data down to the surface is planned.

4.7.2 Lidar for Data Assimilation

The second area of research needed is of atmospheric application and network design. A rigorous and detailed Observation System Simulation Experiment (OSSE) that takes into consideration the different lidar technologies involved and an accurate characterization of the error characteristics for each system is lacking. A recent work by Otkin et al. (2011) published such a study that attempted to compare and quantify the benefits of assimilating an AERI, MWR, and Raman lidar and the resulting combinations. However, the study was made for a single case and was not comprehensive. Further, there have not been research investigations specifically designed to enumerate the cost-benefit analysis of scanning versus no scanning systems in numerical weather forecasting models. In particular, data assimilation impact and process studies with a combination of different sensors need to be investigated. Most of these questions can also be addressed using existing data of ground-based Raman lidar and DIAL systems in combination with OSEs on the convection-permitting scale. It is very timely to use these data for more extended OSE impact studies, as error covariance matrices can easily be constructed and ingested in data assimilation systems in combination with Rapid Update Cycle (RUC) models.

4.7.3 Commercialization and Packaging

The third area that is very much in need of research is the packaging and commercialization of small lidar systems. Research funding through a Small Business Innovation Research initiative has been started by NWS (Facundo et al., 2011). This call defined requirements, needs, and boundaries of the data needed by NWS for a continuous water vapor profiling system. Such specifications provide a framework for future operational systems and allow the commercial companies what to aim for in terms of the capability of the lidar systems. The multi-instrument integration with lidars, GPS-MET, and surface observations instruments will provide a needed boost for more improvements. Such opportunities for commercialization and integration of synergistic instruments should be expanded.

4.8 Synergy with Other Instruments

A very important aspect of lidar is its synergy with other remote sensing instrumentation. Mixing ratio profiles from a lidar typically made at 1-minute resolution are easily combined with temperature profiles measured either with a microwave radiometer (MWR) or Atmospheric Emitted Radiance Interferometer (AERI) measured temperature profiles to reveal a more complete picture of the thermodynamics of the low level boundary layer (e.g., the dryline passage or frontal passages in Turner et al., 2000). In addition, lidars have an important synergy with radars in cloud boundary and cloud-microphysics studies. A combination of radar-lidar-radiometer profiling has resulted in the derivation of many bulk cloud microphysics properties (Comstock et al., 2011).

4.9 Contributions for Air Quality Applications

One of the main data products from lidars is the elastic backscatter return. This elastic signal contributes to air quality applications in a number of ways

Monitoring the boundary layer: Knowledge of BL characteristics is crucial in developing an understanding of air pollution dynam-

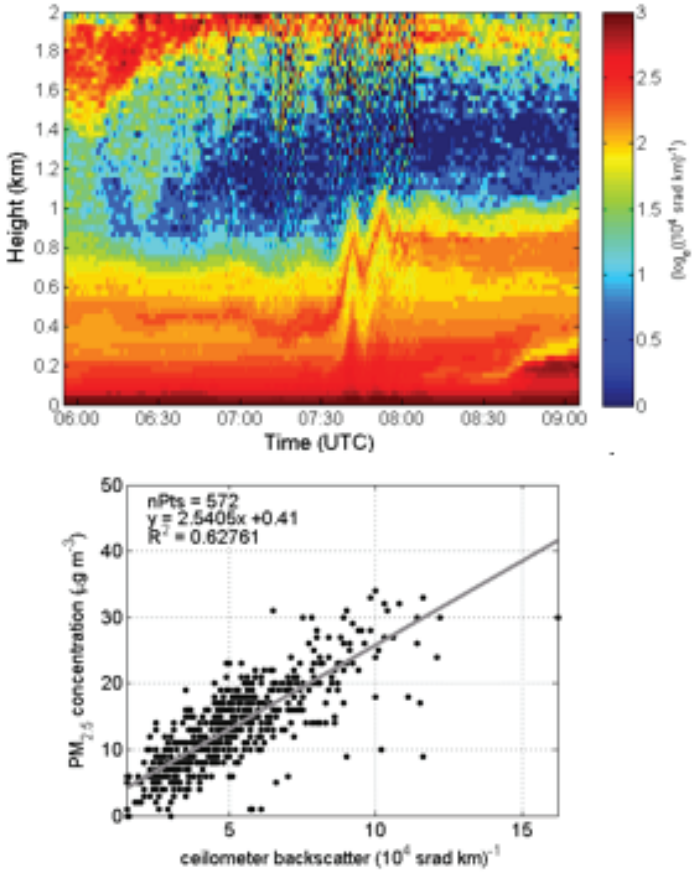

Figure 4-8. Examples of (top) a well resolved transient atmospheric wave: the undular bore. The design of ceilometers is ideal for capturing such dynamic and transient atmospheric phenomena. (Bottom) A correlation of particulate matter versus ceilometer derived backscatter at Howard University Beltsville Research Center.

ics and forecasting pollution using numerical weather models. The lidar is an excellent instrument in monitoring the routine diurnal evolution of the BL. A number of methods for retrieving mixing layer height from lidar backscatter profiles have been demonstrated and compared to radiosonde and other instrumentation and models (see Menut et al., 1999; Steyn et al., 1999; Cohn and Angevine, 2000; Davis et al., 2000; Munkel et al., 2007; Pal et al., 2009). Lidar-derived BL heights are part of NASA-NOAA high resolution model verification study (McQueen et al., 2010 and an overview is available at http://www.emc.ncep.noaa.gov/mmb/aq/pbl/; accessed July 10, 2011).

Lidar remote sensing for aerosol, dust, and volcanic ash monitoring: There are a number of sites and networks involved in monitoring the aerosol loading in the troposphere and transport of pollution. These include lidar networks like the European EARLINET (Pappalardo et al., 2004) the Asian Dust Network (Murayama et al., 2001), NASA's Micro Pulse Lidar Network (MPLNET, Welton et al., 2010 (visit http://mplnet.gsfc.nasa.gov/), the ceilometers network of the German Meteorological Service (Flentje et al., 2010), and the current GALION initiative of the WMO (WMO, 2007) (available at the WMO site: http://www.wmo.int/pages/prog/arep/gaw/gaw-reports.html). These activities and network sites demonstrate the high-quality and mature stages that lidar profiling has reached. An interesting blog of such activities and networks is available at http://alg.umbc.edu/usaq/. Recent investigations have focused on multi-wavelength and multi-polarization lidar profiling efforts to measure the aerosol concentration and size (Veselovskii et al., 2009) as well as detailed study of the correlations of lidar extinction to measurements of aerosol (PM_{10}) concentration and evolution (Van der Kamp and McKendry, 2010; Munkel et al., 2007; Raut and Chazette, 2009).

SECTION 5. OTHER METHODS

The remaining techniques providing thermodynamic information broadly fall in the category of active microwave remote sensing. There are a variety of approaches available that primarily constrain moisture, and most of them are relatively insensitive to weather conditions. The information retrieved is however generally insufficient, but it can add value to that provided by other techniques.

5.1 Refractive Index or Time of Travel Measurements

The average refractive index of air along a path can be derived by measuring the time of travel of electromagnetic waves between two points: one with a transmitter, and another where the signal is either received or reflected back towards the transmitter that will then also act as a receiver. The delay in the time of travel compared to an expected value in vacuum hence provides one constraint on path-integrated pressure, temperature and vapor pressure (Bean and Dutton, 1968; Rüeger, 2002). While the measurement only provides one constraint for three variables and is hence incomplete, it is relatively easy to make and can be achieved in most weather conditions.

Three technologies rely on this approach: 1) the measurement of refractive index profiles using a Global Navigation Satellite Systems (GNSS) satellite as a signal source and a low-orbiting satellite as a receiver, 2) the estimation of precipitable water vapor (or total slant delay) using GNSS satellites and receivers at the ground, and 3) the radar measurement of refractivity. The satellite-to-satellite technique (Ware et al., 1996) is booming with the deployment of several satellites systems just for that purpose such as COSMIC/FORMOSAT-3 (e.g., Anthes et al., 2008; Figure 5.1). It is already exploited by many weather forecasting centers (Cucurull and Derber 2008) but its information is currently not of high-enough resolution for mesoscale work at this time, especially in the lower troposphere at this time. In the second technique, ground based receivers measure precisely the small delay caused by the atmosphere on a satellite-ground path. That delay is the sum of a dry delay due to the path-integrated density, or the weight, of the atmosphere, and a wet delay that is a function of $\int e/T^2$, e being the partial pressure of water vapor and T being temperature. In hydrostatic equilibrium, surface pressure is a function of the weight of the atmosphere above, and this can be used to estimate the dry delay, leaving us with an estimate of the wet delay between the surface and the dozen of GNSS satellites in view at any one time (Braun et al., 2001; Braun et al., 2003; Bengsson et al., 2003). The technology is well proven. At about $15K per site, it is also the cheapest of all the techniques presented in this document. SuomiNet (Ware et al., 2000, http://www.suominet.ucar.edu/; Figure 5.2) is an example of a network of ground-based GNSS receivers designed for the purpose of estimating precipitable water. Data assimilation of slant delays has shown positive impact on QPF (Poli et al., 2002; Zus et al., 2008; Bauer et al., 2011; Zus et al., 2011). The third technique uses radar and fixed targets to measure refractive index between each radar-target pair (Fabry et al., 1997; Fabry, 2004; Weckwerth et al., 2005; Roberts et al., 2008). With enough targets, horizontal maps of refractive index can be built up to a range of approximately

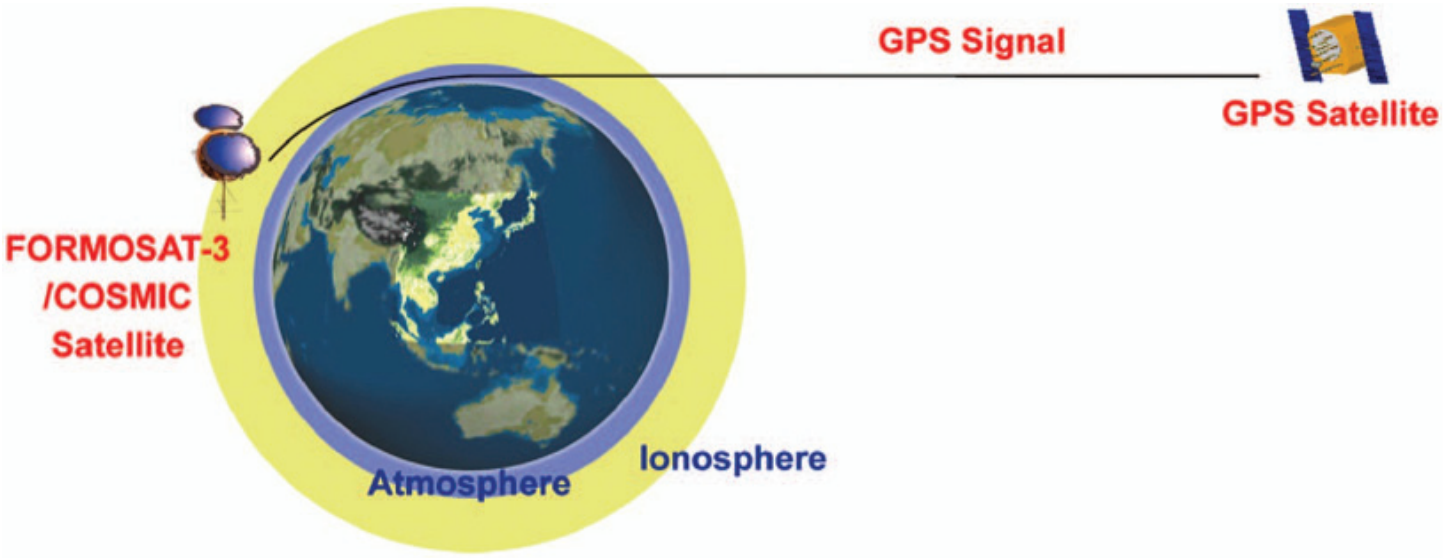

Figure 5-1. Schematic diagram illustrating the radio occultation of GPS signals (Anthes et al., 2008).

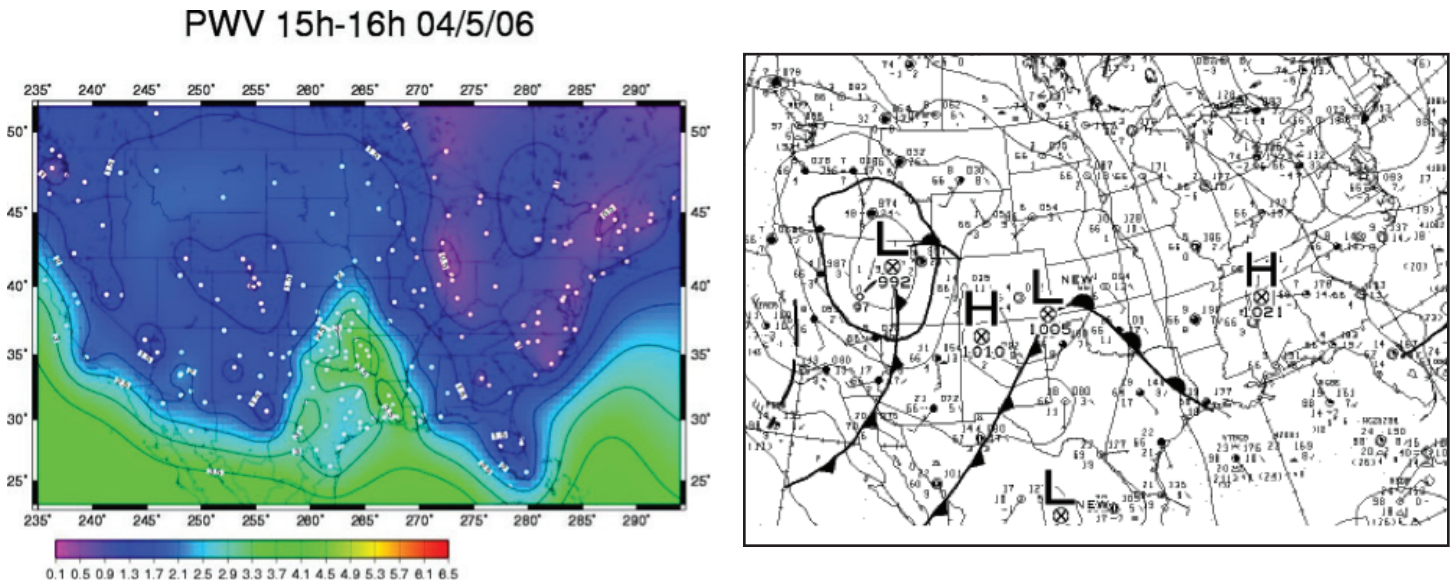

Figure 5-2. Precipitable water (in cm) map derived from GPS receivers of the SuomiNet network (white dots on the left image) showing the warm and humid sector of a growing low pressure system observed at the surface (right) in the southern U.S. on 5 April 2006.

40 km from a scanning radar (Figure 5.3). However, only data a few tens of meters above the surface can be derived. The technique nevertheless could provide information with the existing radar infrastructure, and is being deployed for operational use in France and the United Kingdom.

5.2 Radio Acoustic Sounding System

When matched with an acoustic source, wind profilers can measure the speed of sound waves as a function of height, from which a virtual temperature profile can be derived (Marshall et al., 1972; North et al., 1973; Wilczak et al., 1996; Figure 5.4). This radio acoustic sounding system, or RASS, is used in most current wind profilers of the National Profiler Network (http://www.profiler.noaa.gov/npn/). While RASS provides one of the best range-resolved constraint on (virtual) temperature, its reliance on a sound source that can disturb neighbors was seen negatively by many workshop participants. Also, the height up to which RASS can get temperature is limited for UHF profilers.

5.3 Other Radar-Only Methods

In addition to the previous active microwave methods that have all been used in operational settings, more experimental techniques

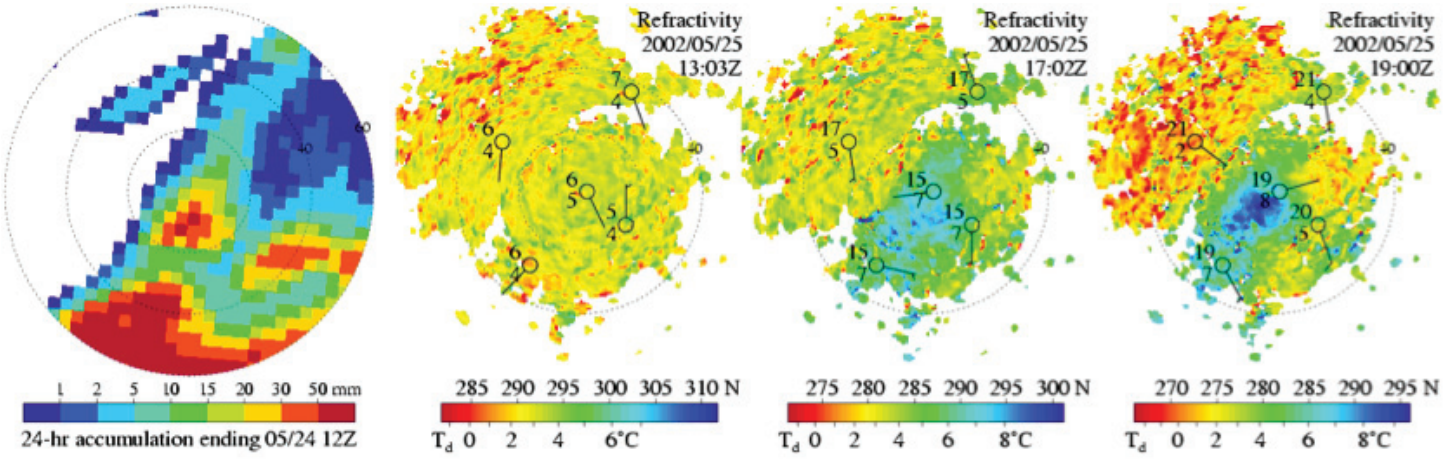

Figure 5-3. Rainfall accumulation over a 24-hr period (first image) responsible for the time evolution of refractivity (N, following images) and dew point temperatures (T_d) on the first sunny morning following the rain. Thanks to very weak winds, we observe the gradual appearance of regions of different humidity, with more humid regions corresponding to areas of heavy rain on the previous days. Range rings are every 20 km (Fabry, 2003).

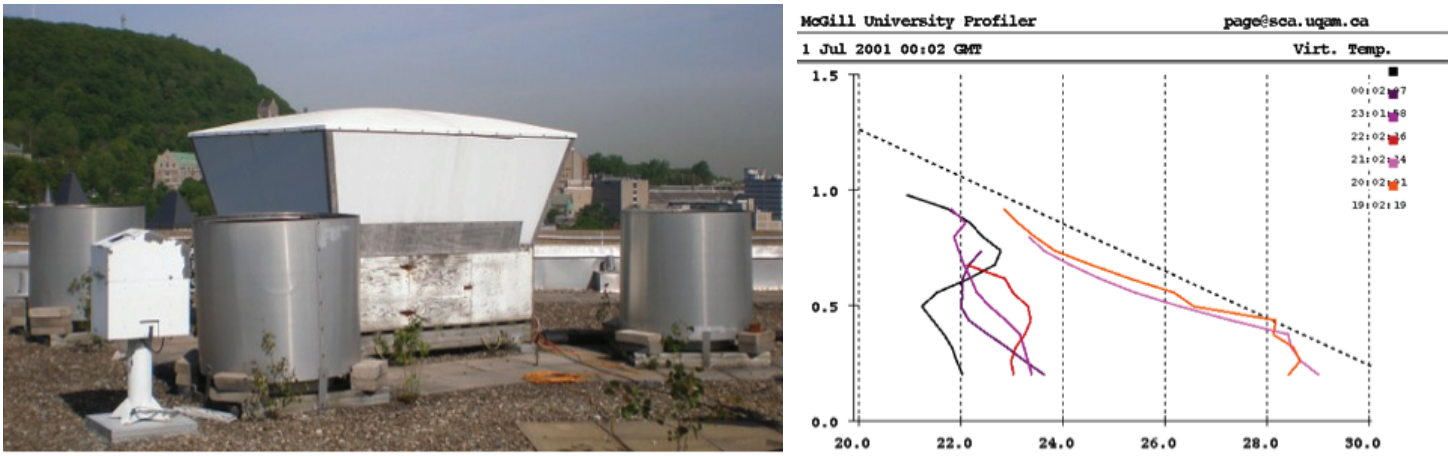

Figure 5-4. The UHF profiler of McGill (left) University surrounded by four sound producers to provide RASS capability measured the passage of a cold front between 20 and 21 UTC (right).

have been devised. The same wind profilers that are used with RASS can also be used to detect clear air echoes caused by temperature and especially moisture discontinuities (Figure 5.5). One can then use this gradient detection capability in combination with lower resolution sensors such as GNSS receivers (Gossard et al., 1999; Stankov et al., 2003) or microwave radiometers (Bianco et al., 2005) to build a more accurate and higher resolution profile of refractive index or of humidity.

Finally, in the same way that two laser frequencies can be used to make a DIAL, two radar frequencies can be used to make a DIfferential Attenuation Radar (DIAR) if the atmosphere attenuates the signal differently at the two frequencies. This works provided that the target has properties that do not change significantly between these two frequencies. It has recently been attempted by Ellis and Vivekenandan (2010) using the edge of precipitation trails as targets for an S-band (10-cm) and a Ka-band (8.6 mm) radar to retrieve a humidity profile (Figure 5.6). DIAR sampling depends on the presence of a distribution of background targets at various ranges to recover water vapor profile information, so the profile depth of retrieved water vapor may be limited, particularly in precipitation-free conditions.

5.4 Beyond the Remote Sensing of Electromagnetic Waves

While the focus of the workshop was primarily on techniques using the remote sensing of light and radio waves, other methods have been used to obtain temperature and humidity profiles. Currently, one operational system involves soundings from commercial aircraft, such as Aircraft Meteorological Data Reports (AMDAR; Moninger et al., 2003) and Tropospheric Aircraft Meteorological Data Reports (TAMDAR, Moninger et al., 2010). Other experimental techniques have been utilized, such as tethered balloons, unmanned aerial vehicles (Holland et al., 1992), dropsondes launched from research airplanes (Hock and Franklin, 1999) or from stratospheric balloons, and sodars (Coulter and Kallistratova, 2004, Bradley, 2008). However, in-situ measurements remain difficult to make with the needed density while sodars have limited height coverage (typically <1 km AGL) and usefulness for thermodynamic profiling. Among other problems, regulation agencies such as the FAA put severe limits to the operations of in-situ sensors such as unmanned aerial vehicles (UAVs) .

5.5 Enhancing Profiling Technologies

None of the technology presented above can, on their own, fulfill the mandate of providing the needed thermodynamic information. At least two reasons can be invoked. First, none of the technologies profile temperature and humidity at the needed resolution under all weather conditions. Second, the density of proposed profiling sites is still low for many applications. To mitigate these problems, two solutions must be explored: how can we best combine different technologies, and can we make more measurements than simply profiling thermodynamic variables.

5.5.1 Possible Synergies and Their Basis

In order to determine the best, or at least a good, profile of temperature and humidity in all weather conditions, one is forced to consider how best to combine the different technologies and to look for synergies. Several examples of synergies were presented in previous sections. While valuable, these combinations were driven more by what instruments were available at a given site than by any systematic approach. In the context of a deployment of a thermodynamic profiling network, we must attack the synergy issue in a more formal manner.

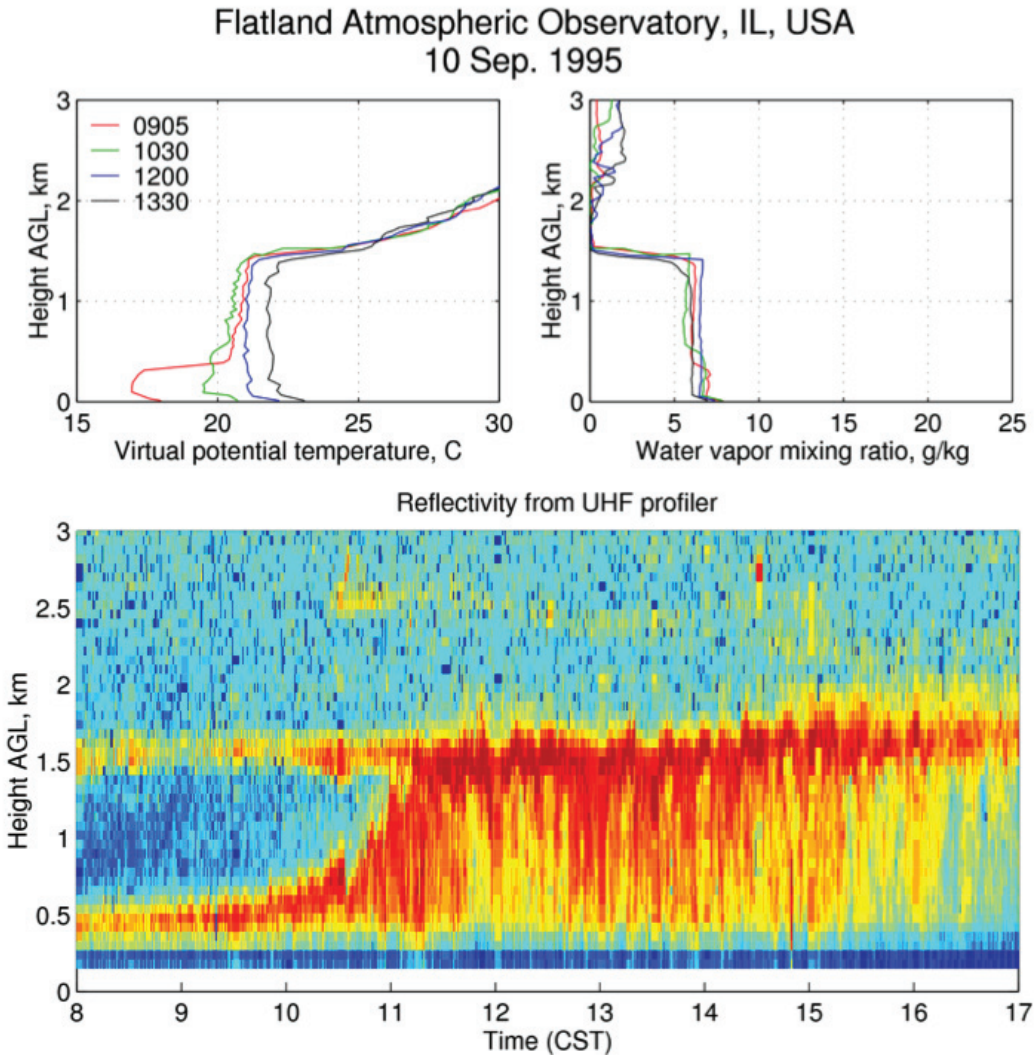

Figure 5-5. Virtual potential temperature and water vapor mixing ratio from four soundings at the times shown are plotted in the upper panels. The lower panel shows a time-height section of reflectivity from a UHF profiler (arbitrary intensity scale). Layers of echoes correspond to levels where the potential temperature and the absolute humidity change rapidly. Adapted from Angevine et al. (1998).

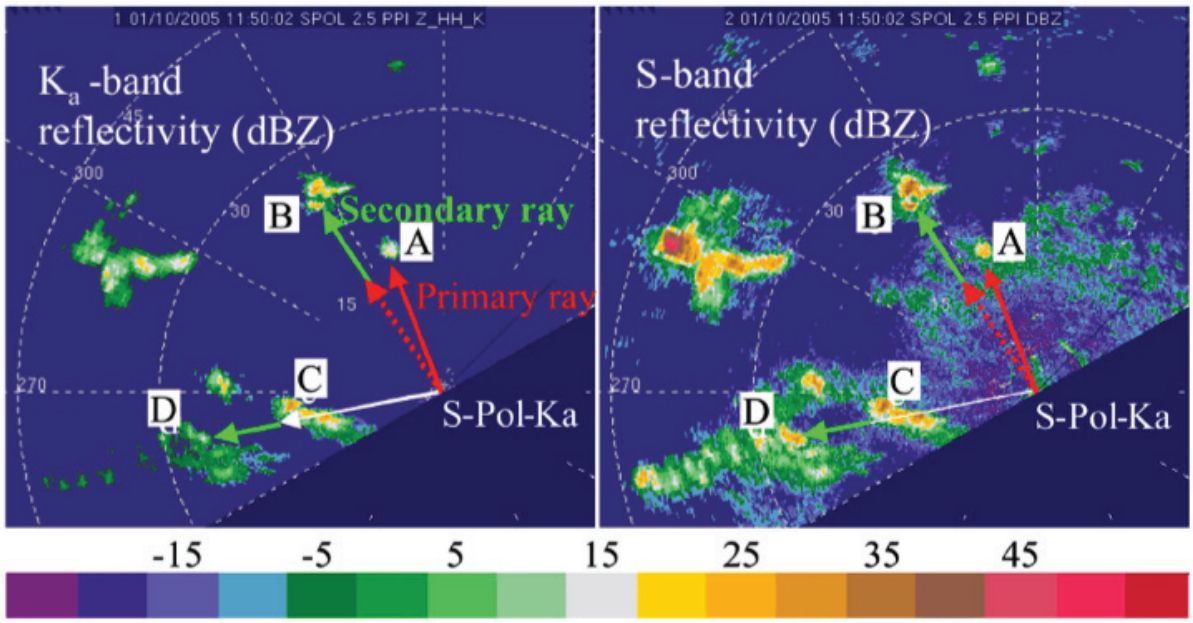

Figure 5-6. PPI plots of (left) K_a-band and (right) S-band reflectivity values. Differential attenuation is measured along the path of the arrows and is used to retrieve path-integrated humidity (Ellis and Vivekenandan, 2010).

Strictly speaking, given *n* possible types of instruments, one can devise $[2^n - 1]$ combinations of sensors in a site. There are clearly too many permutations to consider each systematically. One must hence look at complementarity between sensors in terms of their characteristics (Table 5.1).

A possible method to approach the search for synergies is as follows. If we limit ourselves to search for possible rationales to pair two technologies, we must find ways to combine the strengths of those different technologies. Two possible examples:

Combining instruments with low-resolution but complete information with instruments detecting gradients: Some instruments provide good reference information but have too low a resolution to be complete (e.g., IR and microwave radiometers, GNSS receivers). Other instruments are capable of detecting gradients, but do not provide absolute values of humidity or temperature (e.g., wind profilers). Together, they can be used to both detect gradients such as fronts and boundary layer tops as well as determine layer-mean values.

Combining the high resolution information of a technology requiring long dwell times and the low resolution information from a technology requiring short-enough dwell times to be able to scan: Optical-based technologies (lidars, infrared radiometers) tend to provide higher-resolution information than microwave-based ones, but often have longer dwell times and higher weather sensitivity; they however make great vertically pointing instruments. Microwave-based approaches (microwave radiometers) have lower weather sensitivity and generally shorter dwell times, making them capable of scanning and of constraining temperature and humidity over a larger region. Together, they would considerably improve our ability to make thermodynamic measurements at the mesoscale.

There have been attempts to combine information from multiple sensors for thermodynamic profiling. In addition to the already-mentioned work of Gossard et al. (1999), Stankov et al. (2003), and Bianco et al. (2005) on combining wind profilers with other instruments, methods have been developed to combine optimally information from different instruments such as a microwave radiometer, a cloud radar, a ceilometer, the nearest operational radiosonde, surface measurements, and statistics from a cloud model (Löhnert et al., 2004) or by using IR and microwave radiometers (Löhnert et al., 2009). A debate still rages as to whether one should use the retrievals obtained from these techniques or instead assimilate all data streams into a numerical model and let the assimilation system sort out how to best reconcile and combine all measurements and physics constraints. A significant number of workshop attendants viewed the real-time, comprehensive integration of measurements as a highly desirable feature.

The search for the best combination of instrumentation is bound to be complex, as one searches for the best combination of resolution, accuracy, coverage, weather insensitivity, and affordability. There is no magic bullet, and specific combinations of instruments may depend on climatology. For example, climatic regimes with frequent low-level clouds would likely require the all weather capability of microwave radiometers, whereas infrared devices would be more advantageous in semi-arid environments. Because of the limited number of researchers working on each of these many technologies, there have been few opportunities to look for such synergies. This will have to be a major undertaking in the near future. And the search for these synergies may be best done in a simulation environment such as OSSE mentioned in Section 1.

5.5.2 To Scan or Not To Scan

What should we do in between sites? Because we cannot afford a much denser network, we have either to rely on past or other information to interpolate the data between sites or try to make some measurements in between sites, for example by having some sensors scan.

Table 5-1. A brief summary of the relative strengths and weaknesses of many of the technologies presented in this document. For the relative assessment, infrared radiometry was used as the benchmark.

Technology	Relative Strengths	Relative weaknesses
Infrared radiometry (passive optical)	- Commercially available	- No information above cloud base
Raman and DIAL lidars (active optical)	- Highest resolution information	- Weather sensitivity - Costs
Microwave radiometry (passive radiowave)	- Commercially available - Mostly weather insensitive	- Few constraints; limited resolution
Ground-based GPS receivers	**- Lowest cost** **- Weather insensitive**	- Lowest information content (precipitable water only)
Wind profilers (active radiowave)	- High resolution gradient detection - All-weather winds measurements	- Least quantitative - Costs

A great deal of discussion arose as to whether some of the instruments should scan in elevation and azimuth or simply stare vertically. To scan or not to scan is a complex question with a blend of scientific, technical, and logistical considerations. It was also a polarizing topic among workshop participants as some instruments can scan more easily than others, giving these technologies a perceived edge in the context of a measurement network designed for mesoscale uses but with 100-km distance between stations.

Why might an instrument scan? At least four reasons can be invoked.

1) *To increase the representativeness of the measurement*: Measurements from profiling instruments have small horizontal footprints that sample only a tiny fraction of the horizontal area covered by a model grid point (see the blue dot on the horizontal sections of Figure 5.7). These "soda straw" measurements are not representative of the conditions within the model grid point, and this introduces an error. Only by scanning in many directions may one hope to properly sample the average temperature and humidity conditions within a gridpoint;
2) *To increase the information content of a passive measurement*: Some instruments such as radiometers can constrain temperature and humidity better if measurements at multiple elevation angles can be made to receive emissions from different atmospheric thicknesses;
3) *As part of the measurement process*: Some instruments benefit from scanning in elevation as part of the calibration process, such as microwave radiometers using the tipping calibration technique;
4) *To increase measurement coverage*: In the same way radars scan to make measurements over large mesoscale areas, so can other instruments, allowing them to constrain thermodynamic variables over a much larger region than fixed pointing instruments (Figure 5.7).

In order to scan, an instrument must both have a small enough beam width and a short enough dwell time. If we consider a cycle time typical of that of radar-based weather surveillance (say, five minutes), an instrument that can make several tens of measurements can make one scan in azimuth or in elevation; only if they can make several hundreds of measurements (or have a dwell time of less than 1 s) can crude scanning in both elevation and azimuth be usefully considered. Microwave-based instruments that do not suffer as much from attenuation can make measurements at further ranges and can provide more additional information by scanning than optical-based instruments.

There are however costs to scanning. The instruments must be more complex and more costly. The site must be appropriate with minimum blockage. And the data use and interpretation will also be more involved. As a rule of thumb, the costs and complexity of scanning remain fairly low for elevations larger than about 10°, but in many ways so may be its usefulness because not many more model pixels would be constrained (Figure 5.7). Costs escalate quickly if we want to scan below 10°, both because of higher instrument costs (narrower beamwidth) and especially because of higher site costs (harder to find, more costly to set-up, though it is a one-time cost for all instruments). Yet at the same time, most of the benefits of scanning are at low elevation angles given the expected distance between instruments.

Whether an instrument should scan or not will hence involve a trade-off between the costs and the usefulness of the measurement. Its advisability requires a science-driven cost-benefit analysis that has yet to be done.

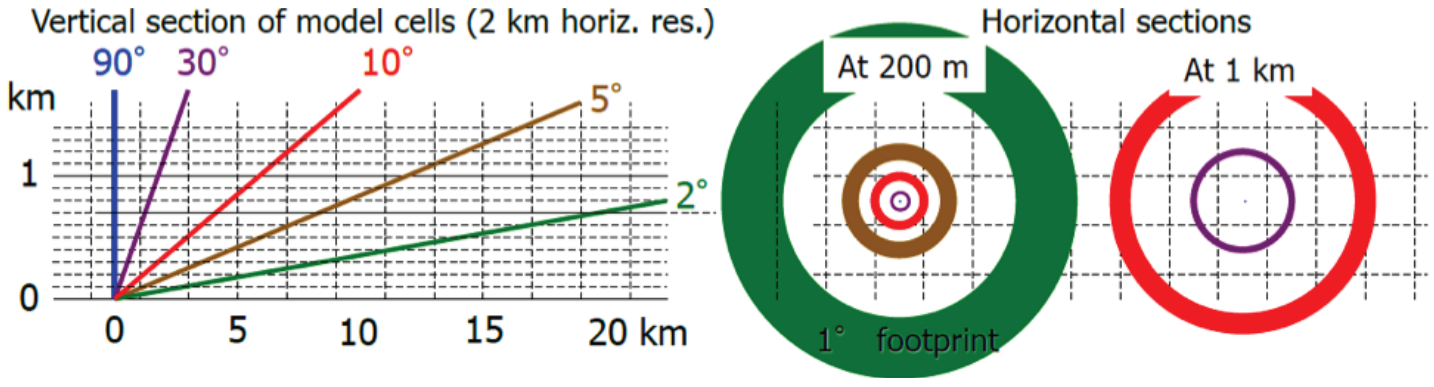

Figure 5-7. Illustration of how measurements made at different elevations constrain the gridpoints from a model at 2 km horizontal resolution and 100 m vertical resolution. Left: vertical cross-section of model grid points with the path sampled by instruments pointing at different elevation angles; right: horizontal sections at 200 m and 1 km altitude of the region sampled by an instrument with a 1° beamwidth at different elevation angles.

SECTION 6. TPT TESTBEDS

6.1 Testbed Fundamentals

Generally speaking, networks exist because information from multiple locations is required to solve a need. Information falls into two categories: providing observations used to derive the information for a system for which the processes are well understood, and providing observations used to derive information for a system for which the processes not well understood. A monitoring network typically falls into the former category; a research network falls into the latter category. Both monitoring and research networks allow for continual, spatial, and temporal measurements. However, testbeds allow for rigorous, transparent, and replicable testing of scientific theories, computational tools, and new technologies.

For a monitoring network, information may be needed for warning that an unsafe threshold has been detected and warning is required. A simple example is the use of a network of smoke and heat alarms in a building that when activated, sends a signal to the local fire department that an emergency has been detected. In this case, heat and smoke detectors have been used to provide information about parameters that are needed to identify a fire, to warn occupants to evacuate, and to notify in a timely manner closest local emergency officials that there is a problem that requires their response. In this example, what information is needed is sufficiently known, instruments that provide the required information are well developed, the computational and data networking infrastructure is well developed, and the timeliness of warning for safety and emergency response is sufficient. In a sense, the establishment of a monitoring network is the "end game".

For a physical system for which there is insufficient understanding, observations are needed in a continuous and iterative process to first generate sufficient information that adequately describe the physical system and then provide reliable information in a timely manner to provide warning of a changing and unsafe condition. In this case, the establishment of a research network is the "beginning game" to solving a problem.

Because there is insufficient description of our Earth's physical system, observations are first needed to understand the physical processes and/or statistical representations of those processes. Then, these processes need to be validated by using continuous observations. Models of the physical system can be constructed to test the relationship between the various processes. Model output can be validated against the continuing observations. This iterative process may well identify processes for which more information is needed to bring closure to the uncertainty between model output and validation. This iteration is required until the information provided is sufficiently known, so that the instruments that provide the required information are appropriate, and that the computational and data networking infrastructure are well developed, so that the timeliness of warning for safety and emergency response is sufficient.

Therefore, research networks are not static. The need for additional sites and/or instrumentation will evolve until the processes and/or statistical representations of those processes are sufficiently known and able to meet the need of the intended information.

Testbeds are generally subsets of networks that have a specific purpose that are typically used to intercompare instruments and their observations to determine a best methodology for a particular set of measurements. Testbeds can also be used to evaluate the accuracy of a process, an algorithm, or a model output. Testbeds can also be used to evaluate uncertainty of observations and model outputs.

6.2 Types and Roles of Testbeds

The presentations by Ackerman (Lessons learned by ARM) and Helms (NOAA/NWS implementation) at the workshop were particularly insightful and provided discussions about concepts of testbeds and networks. Networks allow for continual, spatial and temporal measurements. Testbeds allow for rigorous, transparent, and replicable testing of scientific theories, computational tools, and new technologies.

The Atmospheric Radiation Measurement Climate Research Facility is an example shown in Figure 6.1, which includes fixed sites and mobile facilities..

Testbeds can be used to intercompare instruments and their observations to determine a best methodology or reference for a particular set of measurements. In the early years of the ARM program, for example, the Southern Great Plains Site hosted a number of field campaigns to intercompare instruments that provided water vapor and liquid water in an atmospheric column. Microwave radiometers, Raman Lidars, radiosondes, and other instruments were intercompared to identify a stable and reliable water vapor reference. However, the National Weather Service might use a testbed to intercompare the reliability and operational costs of remote sensing systems that provide thermodynamic properties of the troposphere. Before installing a network of instruments, it is more cost effective to install a suite of new instruments at one location to gain confidence of instrument performance and reliability. In this case, a single location can serve as a testbed for new instrumentation. Use of an exiting testbed is an opportunity to test reliability of the instrument in a real-world, operational setting.

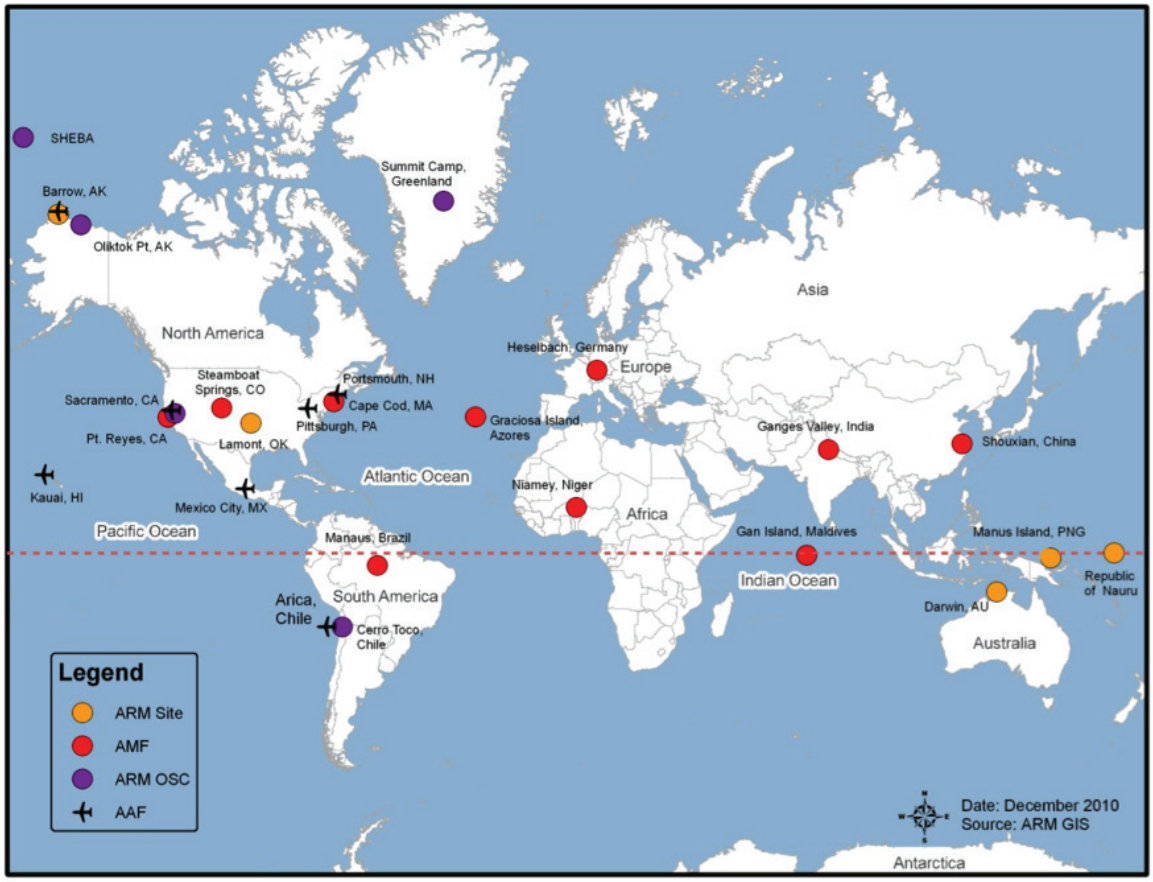

Figure 6-1. The ARM Climate Research Facility fixed and mobile site deployment locations.

Testbeds can also be used to evaluate the accuracy of a model and or a process. The ARM sites continue to be a testbed to determine, among other meteorological parameters, improvements to a line-by-line radiative transfer code used in climate models. In this case, improvements in the code to either improve the predictive capability of the model and/or reduce the uncertainty of the model forecast are the objective. One or more new measurements or observations can be tested for overall improvements in model forecasts in a single testbed of current instruments at one fixed location.

Although not specifically stated, the impetus for the network of networks is to improve the accuracy of timing and location of atmospheric phenomena (e.g., unusual or severe weather events) that affect society. Therefore, the primary users of the data are the national weather service model developers (NCEP) and forecasters that are charged with early warning.

Because the focus of this Workshop was thermodynamic profiling, it is assumed that the improvements to weather models and forecasts will come from better (than currently provided) representation of thermodynamic properties that are assimilated by the models. But the cost and application of specific instrument types is an economic issue.

The specific thermodynamic parameters that need to be improved were not specifically stated, but based on the discussions of earlier sessions, it can be inferred that surface fluxes, boundary layer heights, and profiles of wind, temperature, and humidity of the lower troposphere need to be more accurately measured with sufficient detail, spatial, and temporal resolution to provide better information about the instability that drives convective instability.

Therefore, a single testbed of various instruments types that provide measurements of parameters that potentially improve model forecast can be developed to determine the optimum condition of model forecast improvement and to assess cost. Although a ceilometer may be less accurate than a micropulse lidar for cloud base measurements, the improvement to the forecast realized through use of the lidar may be only marginal, and may not justify the potentially substantial deployment cost differential. Cost effective instruments that meet operational reliability and accuracy could then be tested on location before procuring many instruments for all network sites.

An interesting concept discussed with enthusiasm was that a testbed may not have to be fixed: a mobile testbed (similar to the ARM concept) would allow a core set of instruments to be deployed at different locations for sufficient time periods to asses the improvement of regional forecasts, and then moved to another location.

Figure 6-2. The first ARM Mobile Facility (AMF1) deployed during 2005 in Germany for COPS.

The deployment of the first ARM Mobile Facility (AMF1) in Germany during the 2005 the Convective and Orographically-induced Precipitation Study (COPS) field campaign is shown in Figure 6.2.

While the ARM program uses its mobile facilities to essentially deploy the core suite of instruments found at their fixed sites, the NWS might consider a mobile facility approach to deploy a candidate suite of instruments at different NWS sites for a period of time to evaluate the improvements to local forecasts with one or more of the candidate instruments. It may be that different observations make better improvements to forecasts in different regions of a large network. A set of measurements to improve short-term forecasts for severe thunderstorms in the central region of the U.S. than may be different than one to improve wildfire forecasts for the western region of the U.S. or snowstorm forecasts in the north and eastern regions of the U.S. It is not likely that one new instrument deployed at every NWS will improve predicative capability equally everywhere. In this case, mobile site could be deployed as a testbed to different regions of a network for some period of time to assess which instruments provide the greatest improvement to regional and local forecasts.

A potential drawback to such a strategy is not having a long-term, continuous testbed data set at any one location. Long-term data sets provide validation to model forecasts and should be maintained. The importance of having quality assured data for validation of retrievals and more forecasts cannot be understated.

6.3 Data Quality and Other Issues

The quality of and representativeness of measurements is critical. Clearly, calibrations and data checks must be part of the routine of a network. As instruments become more robust and complex, data quality assessment becomes more challenging. Testbeds can host multiple instruments that have some overlap in measurements because they are useful to assess the quality in near-real time of primary measurement systems. Also, multiple instruments may be required to provide the value-added measurements needed to improve model forecasts. But multiple instruments may not be required at all sites.

Traditionally, NOAA does not save the data and metadata (data about the data) used for forecast model input. Ackerman's presentation, the panel, and input from the audience favored saving the data, even though there are costs associated with data archiving (the ARM experience suggested less than 10% of the operating budget) and potentially reprocessing.

Saving the data has value to NOAA and other business enterprises that want to sell to clients freely obtained NOAA data, but also to non-weather researchers. Numerical Weather Prediction shouldn't be overemphasized; non-weather research communities often need atmospheric data and are very grateful for the help. Forging partnerships is valuable and can pay dividends in the long run!

Change is inevitable, so a network or testbed should plan and budget for change. Therefore, the cost of a testbed needs to include planning for aging or end of life instrumentation. Also, improvements to sensors, new applications of established sensors, or technological breakthroughs must also be allowed to take place because new observations and measurements push new breakthroughs in understanding and modeling processes. Testbeds need to anticipate the unexpected (technological advances) for new data needs that improve model forecasts.

New instruments can be added to testbeds to be thoroughly tested before they are brought on-line operationally. To maintain data continuity, intercomparisons are needed to determine the uncertainties and offsets that need to be part of the metadata to ensure no interruption to the continuity of long-term data sets. Again, testbeds made up of instruments with overlapping measurements are quite useful.

6.4 Role of Field Experiments

There is a strong role for field campaigns and aircraft (manned and unmanned) platforms, as well as data from other platforms (ships and oil rigs, etc.) that provide cost effective supplemental measurements or insights into processes. OSEs and OSSEs can certainly improve the understanding of surface based measurements.

Currently, it is not possible to provide vertical profiles with sufficient accuracy and resolution of the overlaying state of the atmosphere for all situations without in-situ observations. Field campaigns give us a chance to use new technology to provide better observations that can be used to improve the processes and algorithms that models employ to provide forecasts.

6.5 Value Added Data Products

The data obtained will likely need to be processed to provide usable retrievals by the weather modeling community. Instrument scientists are not data assimilation experts and vice versa, so the National Weather Service will need to obtain a particular category of individuals with a specialized skill set to translate measurements to standardized retrievals. This is not a trivial task. Measurements from various instruments may be needed to provide a complete profile of a particular parameter. Therefore, data streams from individual instruments will need to be merged for higher-level data products. Such algorithms require high levels of data completeness from the individual instruments. Nevertheless, they fill the void of observations that cannot be measured directly by a single instrument system.

6.6 Forging a Community

It is advantageous to seek synergism, not duplication, to leverage spatial distribution of instruments, testbeds, and networks. In conceiving a testbed, developers should be intentional about encouraging interactions with other user groups, i.e., build a clientele. The true improvement to instrumentation and measurement needs takes place more quickly when researchers can provide feedback into improvements for network and testbed infrastructure.

While NOAA may not intend to develop a research network, having NOAA and NSF scientists leveraging NOAA and NSF data for science studies gives opportunity for discovery, which advances the science and has a positive feedback that provides more accurate retrievals that improve forecasts. Although it is recognized that we all have to live within our means, a long-term effect will be that NOAA really feels ownership of the results, which improves quality and ultimate utility of future operational network data.

SECTION 7. THE WAY FORWARD

The Thermodynamic Profiling Workshop was planned to be a continuation of the NRC assessment of needs for lower atmospheric continuous profiling (NRC, 2009). The state-of-the-art of remote sensing and in-situ measurements has progressed in the last decade to a point where demonstrations on a research basis and over scales up to 100km have been possible. The ARM experience and experiments, such as the IHOP_2002 and the COPS study in Germany, show that a suite of measurements can provide data that show promise of improving forecast skill. The next steps in the utilization of such technology will be to combine a longer-term observation period where assimilation of such data into forecast models can be evaluated and is worth the expense of building such an assimilation system.

7.1 Recommendations

7.1.1 Improvement in the Utilization of Existing Technology

Ceilometers are underutilized for potential application in a TPT testbed. ASOS data is only now retained hourly with a one-minute observation at the top of each hour. The operation of ASOS instruments throughout the hour is lost and needs to be rectified. Data volumes from ASOS and transmission of those data should not be an issue with modern internet and satellite communications.

7.1.2 NOAA Should Consider Implementing a Regional Testbed

In order to scope the cost and feasibility of scaling up remote sensing measurements to a national observing system, a testbed of instruments should be developed in a region that has significant orographic, land use (i.e., urbanization), and weather differences. The choice of the region should be guided by difficulty in forecasting. Land-sea contrast, mountain-plain changes, convective storms, etc., should be considerations in choosing a region for such a testbed. The testbed should contain identical instrumentation at sites roughly placed 150km apart.

7.1.3 Data Capture Should be into the NOAA MADIS System

Because a long-term national improvement to its lower tropospheric observing system will be operational in nature, NOAA will need to evaluate a testbed for such observations within its operational data framework. The NEXTGEN analysis of the future of NWS's observation should include provision for acquisition of surface remote sensing sites. MADIS will clearly be absorbed into NEXTGEN and this will provide a research to operations path.

7.1.4 Data Assimilation of the Remote Sensing Data Should be a Goal for the Testbed

Inclusion of new data sources into a 3DVAR or 4DVAR data assimilation system is expensive and may not improve the forecast commensurate with its cost. The value of assimilating data from a testbed of limited spatial scale needs to be assessed and can be tested with OSSEs. Research has indicated that there is positive value in assimilation ground-based remote sensing data (Turner et al., 2010) but only a few instruments were included in that study and for a limited case study. This needs to be expanded to cover a range of passive and active sensors that can credibly be placed within a testbed.

Existing data should be used for performing OSEs in combination with RUCs. These studies will provide essential insight in the impact of additional remote sensing observations.

7.2 Initial Steps

NOAA should begin a planning process for the testbed concept and implement one or more regional testbeds as funding allows. Consensus exists that passive instruments such as the microwave radiometer and AERI can be robustly distributed through a testbed. Clearly, ceilometers can be placed at testbed sites at relatively low cost. Several of the testbed sites should have more sophisticated lidars (Raman or DIAL) to obtain water vapor vertical cross-sections and provide higher resolution than the passive sensors. Radar windprofilers have been demonstrated on national scale and should be deployed at each site. Use of rawinsondes for validation should be included at testbed sites.

Because the NWS and its WFOs will be the users of this system, NOAA should extend the "Proving Ground" concept currently being used for GOES-R and JPSS to TPT sensors. This would involve training, WFO demonstrations, and user feedback to the observing system about how the data is being used or could be improved. The National Hurricane Center, the Alaska Weather Office, and the National Severe Storms Laboratory have all been involved in recent Proving Ground demonstrations and infrastructure exists for moving new observations into the forecast environment.

7.3 R&D Priorities

The workshop reflected existing preconceptions that TPT observations are expensive and in some cases, too expensive to implement. Research and development should both work on new techniques to measure water, pressure, temperature, and winds in the lowest 3 km of the atmosphere at high resolution, and, importantly, incorporate new technology which can dramatically reduce the costs of existing techniques. The active visible remote sensing section (Section 3) showed that fiber-laser based systems for DIAL are being developed within a research lab. Such fiber-laser technologies are widely used in communications and costs are considerably less than high power transmitters. There must be a mechanism whereby such research is encouraged to lower operational observational costs.

Phased array technology in radar shows promise to improved both vertical profiling as well as micro-radars for systems such as CASA. The ability to use differential absorption radar to give species dependent returns is novel and should be promoted.

Hybrid systems which combine remote sensing and aircraft sensors show promise for the observing system. ACARS has been an excellent example of using commercial platforms for sensing and incorporation into the observing system. There is a continuing need to validate such profiles to determine thermal hysteresis in descent measurements from ACARS. In addition, such descents are not vertical and ingest full three-dimensional coordinate data into the numerical models. Approaches which are over water and then land in a coastal city have notable artifacts in the profile.

NOAA has ceilometers which will be widely used for cloud base profiling and which are now proposed to obtain aerosol and PBL profiles. Various ceilometer manufacturers and models will lead to problems in intercomparibility between systems. There is a need for systematic study of what these instruments really measure.

OSSEs and OSEs are in the nascent development stage for ground-based observations. They will be valuable tools to help answer questions of instrument synergy and whether some of the instruments should scan or not. Numerical experiments testing the value of combining different technologies should be a priority and should have been completed prior to a large-scale (as opposed to a prototype-scale) deployment of the network. Development of accurate observation operators for each technology will also be critical to the success of these numerical experiments.

7.4 Follow Up for Other Atmospheric Variables

The NRC Report was not limited to TPT variables. Atmospheric composition in the troposphere is important for climate, air quality, agriculture, and human health. It was recognized at the outset that a single workshop to cover all the other species in the atmosphere would be overwhelming. A second workshop is recommended and may focus on supporting observations for other agencies such as NASA, DHS, and EPA.

REFERENCES

Ackerman, T.P., and G.M. Stokes, 2003: The Atmospheric Radiation Measurement Program. *Phys. Today*, **56**, 38-44, doi: 10.1063/1.1554135.

Adam M., B.B. Demoz, D.D. Venable, E. Joseph, R. Connell, D.N. Whiteman, A. Gambacorta, J. Wei, M.W. Shephard, L.M. Miloshevich, C.D. Barnet, R.L. Herman, and J. Fitzgibbon, 2010: Water vapor measurements by Howard University Raman lidar during the WAVES 2006 Campaign. *J. Atmos. Oceanic Technol.*, **27**, 42–60. doi: 10.1175/2009JTECHA1331.1.

Angevine, W.M., P.S. Bakwin, and K.J. Davis, 1998: Wind profiler and RASS measurements compared with measurements from a 450-m-tall tower. *J. Atmos. Oceanic Technol.*, **15**, 818–825, doi: 10.1175/1520-0426(1998)015<0818.

Ansmann, A., M. Riebesell, U. Wandinger, C. Weitkamp, E. Voss, W. Lahmann, and W. Michaelis, 1992: Combined Raman elastic-backscatter LIDAR for vertical profiling of moisture, aerosol extinction, backscatter, and LIDAR ratio. *Appl. Phys.*, **B55,** 18–28, doi: 10.1007/BF00348608.

Anthes, R.A., D. Ector, D.C. Hunt, Y-H. Kuo, C. Rocken, W.S. Schreiner, S.V. Sokolovskiy, S. Syndergaard, T-K. Wee, Z. Zeng, P.A. Bernhardt, K.F. Dymond, Y. Chen, H. Liu, K. Manning, W.J. Randel, K.E. Trenberth, L. Cucurull, S.B. Healy, S-P. Ho, C. McCormick, T.K Meehan, D.C. Thompson, and N.L. Yen, 2008: The COSMIC/FORMOSAT-3 Mission: Early results. *Bull. Amer. Meteor. Soc.*, **89**, 313–333, doi: 10.1175/BAMS-89-3-313.

Arshinov, Y., S. Bobrovnikov, I. Serikov, A. Ansmann, U. Wandinger, D. Althausen, I. Mattis, and D. Müller, 2005: Daytime operation of a pure rotational Raman lidar by use of a Fabry-Perot interferometer. *Appl. Optics*, **44**, 3593–3603, doi: 10.1364/AO.44.003593.

Bauer, H.-S., T. Weusthoff, M. Dorninger, V. Wulfmeyer, T. Schwitalla, T. Gorgas, M. Arpagaus, and K. Warrach-Sagi, 2011: Predictive skill of a subset of models participating in D-PHASE in the COPS region. COPS Special Issue of the *Q. J. Roy. Meteor. Soc.*, **137**, 287-305, doi: 10.1002/qj.715.

Bean, B.R., and E.J. Dutton. *Radio Meteorology*, Dover Publications, New York, 435 pp., 1968.

Behrendt, A., and J. Reichardt, 2000: Atmospheric temperature profiling in the presence of clouds with a pure rotational Raman lidar by use of an interference-filter-based polychromator. *Appl. Optics*, **39**, 1372–1378, doi: 10.1364/AO.39.001372.

Behrendt, A., V. Wulfmeyer, H.-S. Bauer, T. Schaberl, P. Di Girolamo, D. Summa, C. Kiemle, G. Ehret, D.N. Whiteman, B.B. Demoz, E.V. Browell, S. Ismail, R. Ferrare, S. Kooi, and J. Wang, 2007a: Intercomparison of water vapor data measured with lidar during IHOP_2002, Part I: Airborne to ground-based lidar systems and comparisons with chilled-mirror hygrometer radiosondes. *J. Atmos. Oceanic Technol.*, **24**, 3–21, doi: 10.1175/JTECH1924.1.

Behrendt, A., V. Wulfmeyer, T. Schaberl, H.-S. Bauer, C. Kiemle, G. Ehret, C. Flamant, S. Kooi, S. Ismail, R. Ferrare, E.V. Browell, and D.N. Whiteman, 2007b: Intercomparison of water vapor data measured with lidar during IHOP_2002. Part II: Airborne-to-airborne systems. *J. Atmos. Oceanic Technol.*, **24**, 22–39, doi: 10.1175/JTECH1925.1.

Behrendt, A., S. Pal, V. Wulfmeyer, Á.M. Valdebenito B., and G. Lammel, 2011: A novel approach for the characterisation of transport and optical properties of aerosol particles near sources, Part I: Measurement of particle backscatter coefficient maps with a scanning UV lidar. *Atmos. Environ.*, **45**, 2795–2802, doi: 10.1016/j.atmosenv.2011.02.061.

Behrendt, A.: Temperature Measurements with Lidar, Chapter 10, in: *Lidar: Range-Resolved Optical Remote Sensing of the Atmosphere*, C. Weitkamp, ed., Springer, New York, 480 pp., 2005.

Bengsson, L., G. Robinson, R. Anthes, K. Aonashi, A. Dodson, G. Elgered, G. Gendt, R. Gurney, M. Jietai, C. Mitchell, M. Mlaki, A. Rhodin, P. Silvestrin, R. Ware, R. Watson, and W. Wergen, 2003: The use of GPS measurements for water vapor determination. *Bull. Amer. Meteor. Soc.*, **84**, 1249–1258, doi: 10.1175/BAMS-84-9-1249.

Bianco, L., D. Cimini, F.S. Marzano, and R. Ware, 2005: Combining microwave radiometer and wind profiler radar measurements for high-resolution atmospheric humidity profiling. *J. Atmos. Oceanic Technol.*, **22**, 949–965, doi: 10.1175/JTECH1771.1.

Bösenberg, J., 1998: Ground-based differential absorption lidar for water-vapor and temperature profiling: Methodology. *Appl. Optics*, **37**, 3845–3860, doi: 10.1364/AO.37.003845.

Bradley, S.: *Atmospheric Acoustic Remote Sensing: Principles and Applications*, CRC Press, Boca Raton, Florida, 296 pp., 2007.

Braun, J., C. Rocken, and J. Liljegren, 2003: Comparisons of line-of-sight water vapor observations using the Global Positioning System and a pointing microwave radiometer. *J. Atmos. Oceanic Technol.*, **20**, 606–612, doi: 10.1175/1520-0426(2003)20<606.

Braun, J., C. Rocken, and R. Ware, 2001: Validation of line-of-sight water vapor measurements with GPS. *Radio Sci.*, **36**, 459–472, doi: 10.1029/2000RS002353.

Cadeddu M.P., V.H. Payne, S.A. Clough, K. Cady-Pereira, and J.C. Liljegren, 2007: Effect of the oxygen line-parameter modeling on temperature and humidity retrievals from ground-

based microwave radiometers, *IEEE Trans. Geosci. Rem. Sens.*, **45**, 2216-2223, doi: 10.1109/TGRS.2007.894063.

Cadeddu, M.P., and D.D. Turner, 2011: Evaluation of water permittivity models from ground-based observations of cold clouds at frequencies between 23 and 170 GHz. *IEEE Trans. Geosci. Rem. Sens.*, **49**, 2999–2008, doi: 10.1109/TGRS.2011.2121074.

Calpini, B., V. Hentsch, P. Huguenin, D. Ruffieux, T. Dinoev, and V. Simeonov, 2009: Water vapor upper air observations at MeteoSwiss Payerne, Proceedings of the 8th International Symposium on Tropospheric Profiling, 19-23 October 2009, Delft, Netherlands. Weblink accessed in November 2011 at http://www.meteosuisse.admin.ch/web/en/research/completed_projects/lidar.Par.0020.DownloadFile.tmp/extabstractcalpiniistp2009vf.pdf.

Cardinali, C., L. Isaksen, and E. Andersson, 2003. Use and impact of automated aircraft data in a global 4DVAR data assimilation system. *Mon. Wea. Rev.*, **131**, 1865–1877, doi: 10.1175//2569.1.

Cimini, D., E. Campos, R. Ware, S. Albers, G. Giuliani, J. Oreamuno, P. Joe, S.E. Koch, S. Cober, and E. Westwater, 2011: Thermodynamic atmospheric profiling during the 2010 Winter Olympics using ground-based microwave radiometry. *IEEE Trans. Geosci. Rem. Sens.*, **49**, 4959–4969, doi: 10.1109/TGRS.2011.2154337.

Cimini, D., E.R. Westwater, and A.J. Gasiewski, 2010: Temperature and humidity profiling in the Arctic using ground-based millimeter-wave radiometry and 1DVAR. *IEEE Trans. Geosci. Rem. Sens.*, **48**, 1381–1388, doi: 10.1109/TGRS.2009.2030500.

Cimini, D., E.R. Westwater, Y. Han, and S.J. Keihm, 2003: Accuracy of ground-based microwave radiometer and balloonborne measurements during WVIOP2000 field experiment. *IEEE Trans. Geosci. Rem. Sens.*, **41**, 2605–2615, doi: 10.1109/TGRS.2003.815673.

Cimini, D., T.J. Hewison, L. Martin, J. Güldner, C. Gaffard, and F.S. Marzano, 2006: Temperature and humidity profile retrievals from ground-based microwave radiometers during TUC. *Meteorol. Z.*, **15**, 45–56., doi: 10.1127/0941-2948/2006/0099.

Clough, S.A., M.W. Shephard, E.J. Mlawer, J.S. Delamere, M.J. Iacono, K. Cady-Pereira, S. Boukabara, and P.D. Brown, 2005: Atmospheric radiative transfer modeling: A summary of the AER codes. *J. Quant. Spectrosc. Radiat. Trans.*, **91**, 233–244, doi: 10.1016/j.jqsrt.2004.05.058.

Cohn, S.A., and W.M. Angevine, 2000: Boundary layer height and entrainment zone thickness measured by lidars and wind-profiling radars. *J. Appl. Meteor.,* **39,** 1233–1247. doi: 10.1175/1520-0450(2000)039<1233.

Comstock, J.M., A. Protat, S. McFarlane, J. Delanoë, and M. Deng, 2011: Intercomparison of multi-sensor retrievals of cloud microphysical properties–Results using ARM data at Darwin, Australia. Presented at the 5th Symposium on Lidar Atmospheric Applications, 91st American Meteorological Society Annual Meeting, 22-27 January 2011, Seattle Washington.

Cooney, J., 1972: Measurement of atmospheric temperature profiles by Raman backscatter. *J. Appl. Meteor.*, **11**, 108–112, doi: 10.1175/1520-0450(1972)011<0108.

Coulter, R.L., and M.A. Kallistratova, 2004: Two decade of progress in SODAR techniques: A review of 11 ISARS proceedings. *Meteorol. Atmos. Phys.*, **85,** 3–19, doi: 10.1007/s00703-003-0030-2.

Crewell S., K. Ebell, U. Löhnert, and D.D. Turner, 2009: Can liquid water profiles be retrieved from passive microwave zenith observations? *Geophys. Res. Lett.*, **36**, L06803, doi:10.1029/2008GL036934.

Crewell, S., and U. Löhnert, 2003: Accuracy of cloud liquid water path from ground-based microwave radiometry, 2. Sensor accuracy and synergy. *Radio Sci.*, **38**, 8042, doi: 10.1029/2002RS002634.

Crewell, S., and U. Löhnert, 2007: Accuracy of boundary layer temperature profiles retrieved with multifrequency multiangle microwave radiometry. *IEEE Trans. Geosci. Rem. Sens.*, **45**, 2195–2201, doi: 10.1109/TGRS.2006.888434.

Crewell, S., H. Czekala, U. Löhnert, C. Simmer, T. Rose, R. Zimmermann, and R. Zimmermann, 2001: Microwave radiometer for cloud carthography: A 22-channel ground-based microwave radiometer for atmospheric research. *Radio Sci.*, **36**, 621–638.

Crook, N.A., 1996: Sensitivity of moist convection forced by boundary layer processes to low-level thermodynamic fields. *Mon. Wea. Rev.*, **124**, 1767–1785, doi: 10.1175/1520-0493(1996)124<1767.

Cucurull, L., and J.C. Derber, 2008: Operational implementation of COSMIC observations into NCEP's Global Data Assimilation System. *Wea. Forecasting*, **23**, 702–711, doi: 10.1175/2008WAF2007070.1.

Davis, K.J., N. Gamage, C.R. Hagelberg, C. Kiemle, D.H. Lenschow, and P.P. Sullivan, 2000: An objective method for deriving atmospheric structure from airborne lidar observations. *J. Atmos. Oceanic Technol.,* **17**, 1455–1468. doi: 10.1175/1520-0426(2000)017<1455

Dierer, S., M. Arpagaus, A. Seifert, E. Avgoustoglou, R. Dumitrache, F. Grazzini, P. Mercogliano, M. Milelli, and K. Starosta, 2009: Deficiencies in quantitative precipitation fore-

casts: Sensitivity studies using the COSMO model. *Meteorol. Z.*, **18**, 631–645, doi: 10.1127/0941-2948/2009/0420.

Di Girolamo, P., R. Marchese, D.N. Whiteman, and B. Demoz, 2004: Rotational Raman lidar measurements of atmospheric temperature in the UV. *Geophys. Res. Lett.,* **31**, L01106, doi:10.1029/2003GL018342.

Ducrocq, V., J.-P. Lapore, J.-L. Redelsperger, and F. Orain, 2000: Initialization of a fine-scale model for convective-system prediction: A case study. *Q. J. Roy. Meteor. Soc*., **126**, 3041–3065, doi: 10.1002/qj.49712657004.

Eichinger W.E., D.I. Cooper, L.E. Hipps, W.P. Kustas, C.M.U. Neale, and J.H. Prueger, 2006: Spatial and temporal variation in evapotranspiration using Raman lidar. *Adv. Water Res*., **29**, 369–381, doi: 10.1016/j.advwatres.2005.03.023.

Ellis, S.M., and J. Vivekanandan, 2010: Water vapor estimates using simultaneous dual-wavelength radar observations. *Radio Sci.*, **45,** RS5002, doi:10.1029/2009RS004280.

Fabry, F., 2003: Seeing air humidity with radar. *Bull. Amer. Meteor. Soc.*, **84**, 1508–1509.

Fabry, F., 2004: Meteorological value of ground target measurements by radar. *J. Atmos. Oceanic Technol*., **21**, 560–573, doi: 10.1175/1520-0426(2004)021<0560.

Fabry, F., C. Frush, I. Zawadzki, and A. Kilambi, 1997: On the extraction of near-surface index of refraction using radar phase measurements from ground targets. *J. Atmos. Oceanic Technol.*, **14**, 978–987, doi: 10.1175/1520-0426(1997)014<0978.

Facundo, J., 2011: Update on the integrated upper air water vapor system. Presented at the 5th Symposium on Lidar Atmospheric Applications, 91st American Meteorological Society Annual Meeting, 22-27 January 2011, Seattle, Washington.

Feltz, W.F., and J.R. Mecikalski, 2002: Monitoring high-temporal-resolution convective stability indices using the ground-based Atmospheric Emitted Radiance Interferometer (AERI) during the 3 May 1999 Oklahoma–Kansas tornado outbreak. *Wea. Forecasting*, **17**, 445–455.

Feltz, W.F., W.L. Smith, H.B. Howell, R.O. Knuteson, H. Woolf, and H.E. Revercomb, 2003: Near-continuous profiling of temperature, moisture, and atmospheric stability using the Atmospheric Emitted Radiance Interferometer (AERI). *J. Appl. Meteor.*, **42**, 584–597, doi: 10.1175/1520-0450(2003)042<0584.

Feltz, W.F., H.B. Howell, R.O. Knuteson, H.M. Woolf, D.D. Turner, R. Mahon, T.D. Halther, and W.L. Smith, 2005: Retrieving Temperature and Moisture Profiles from AERI Radiance Observations: AERIPROF Value-Added Product Technical Description, DOE/SC-ARM/TR-066, U.S. Department of Energy, Washington, D.C.

Feltz, W.F., W.L. Smith, R.O. Knuteson, H.E. Revercomb, H.M. Woolf, and H.B. Howell, 1998: Meteorological applications of temperature and water vapor retrievals from the ground-based Atmospheric Emitted Radiance Interferometer (AERI). *J. Appl. Meteor.*, **37**, 857–875, doi: 10.1175/1520-0450(1998)037<0857.

Ferrare, R., D. Turner, M. Clayton, B. Schmid, J. Redemann, D. Covert, R. Elleman, J. Ogren, E. Andrews, J.E.M. Goldsmith, and H. Jonsson, 2006: Evaluation of daytime measurements of aerosols and water vapor made by an operational Raman lidar over the Southern Great Plains. *J. Geophys. Res.,* **111**, D05S08, doi: 10.1029/2005JD005836.

Fix A., V. Weiss, and G. Ehret, 1998: Injection-seeded optical parametric oscillator for airborne water vapor DIAL. *Pure Appl. Optics*, **7**, 837–852 doi: 10.1088/0963-9659/7/4/019.

Flentje, H., B. Heese, J. Reichardt, and W. Thomas, 2010: Aerosol profiling using the ceilometer network of the German Meteorological Service. *Atmos. Meas. Tech. Discuss*., **3**, 3643–3673, doi:10.5194/amtd-3-3643-2010. Available at www.atmos-meas-tech-discuss.net/3/3643/2010/.

Gero, P.J., and D.D. Turner, 2011: Long-term trends in downwelling spectral infrared radiance over the U.S. Southern Great Plains. *J. Climate.*, **24**, 4831–4843, doi: 10.1175/2011JCLI4210.1.

Goldsmith, J.E.M., F.H. Blair, S.E. Bisson, and D.D. Turner, 1998: Turn-key Raman lidar for profiling atmospheric water vapor, clouds, and aerosols. *Appl. Optics*, **37**, 4979–4990, doi: 10.1364/AO.37.004979.

Gossard, E.E., S. Gutman, B.B. Stankov, and D.E. Wolfe, 1999: Profiles of radio refractive index and humidity derived from radar wind profilers and the Global Positioning System. *Radio Sci.,* **34,** 371–383.

Grzeschik, M., H.-S. Bauer, V. Wulfmeyer, D. Engelbart, U. Wandinger, I. Mattis, D. Althausen, R. Engelmann, M. Tesche, and A. Riede, 2008: Four-dimensional variational data analysis of water vapor Raman lidar data and their impact on mesoscale forecasts. *J. Atmos. Oceanic Technol.*, **25**, 1437–1453, doi: 10.1175/2007JTECHA974.1.

Hair, J.W., L.M. Caldwell, D.A. Krueger, and C.-Y. She, 2001: High-spectral-resolution lidar with iodine-vapor filters: Measurement of atmospheric-state and aerosol profiles. *Appl. Optics*, **40**, 5280–5294, doi: 10.1364/AO.40.005280.

Han, Y., and E.R.Westwater, 2000: Analysis and improvement of tipping calibration for ground-based microwave radiometers. *IEEE Trans. Geosci. Rem. Sens.*, **38**, 1260–1276, doi: 10.1109/36.843018.

Hewison, T.J., 2006: *Profiling Temperature and Humidity by Ground-based Microwave Radiometers*, Ph.D. Thesis, Department of Meteorology, University of Reading. Available online at http://tim.zymurgy.org/hewison/Thesis.pdf.

Hewison, T.J., 2007: 1D-VAR retrieval of temperature and humidity profiles from a ground-based microwave radiometer. *IEEE Trans. Geosci. Rem. Sens.*, **45**, 2163–2168, doi: 10.1109/TGRS.2007.898091.

Hock, T.F., and J.L. Franklin, 1999: The NCAR GPS dropwindsonde. *Bull. Amer. Meteor. Soc.*, **80,** 407–420, doi: 10.1175/1520-0477(1999)080<0407.

Holland, G.J., T. McGeer, and H. Youngren, 1992: Autonomous aerosondes for economical atmospheric soundings anywhere on the globe. *Bull. Amer. Meteor. Soc.*, **73**, 1987–1998, doi: 10.1175/1520-0477(1992)073<1987.

Hua, D., M. Uchida, and T. Kobayashi, 2005: Ultraviolet Rayleigh-Mie lidar for daytime-temperature profiling of the troposphere. *Appl. Optics*, **44**, 1315–1322, doi: 10.1364/AO.44.001315.

Huang, D., Y. Liu, and W. Wiscombe, 2008: Cloud tomography: Role of constraints and a new algorithm. *J. Geophys. Res.*, **113**, D23203, doi: 10.1029/2008JD009952.

Kadygrov, E.N., and D.R. Pick, 1998: The potential for temperature retrieval from an angular-scanning single-channel microwave radiometer and some comparisons with in situ observations. *Meteorol. Appl.*, **5**, 393–404, doi: 10.1017/S1350482798001054.

Kneifel, S., S. Crewell, U. Löhnert, and J. Schween, 2009: Investigating water vapor variability by ground-based microwave radiometry: Evaluation using airborne observations. *IEEE Geosci. Remote Sens. Letts.*, **6**, 157–161, doi: 10.1109/LGRS.2008.2007659.

Kneifel, S., U. Löhnert, A. Battaglia, S. Crewell, and D. Siebler, 2010: Snow scattering signals in ground-based passive microwave radiometer measurements. *J. Geophys. Res.*, **115**, D16214, doi: 10.1029/2010JD013856.

Knuteson, R.O., H.E. Revercomb, F.A. Best, N.C. Ciganovich, R.G. Dedecker, T.P. Dirkx, S.C. Ellington, W.F. Feltz, R.K. Garcia, H.B. Howell, W.L. Smith, J.F. Short, and D.C Tobin, 2004a: Atmospheric Emitted Radiance Interferometer, Part I: Instrument design. *J. Atmos. Oceanic Technol.*, **21**, 1763–1776, doi: 10.1175/JTECH-1662.1.

Knuteson, R.O., H.E. Revercomb, F.A. Best, N.C. Ciganovich, R.G. Dedecker, T.P. Dirkx, S.C. Ellington, W.F. Feltz, R.K. Garcia, H.B. Howell, W.L. Smith, J.F. Short, and D.C Tobin, 2004b: Atmospheric Emitted Radiance Interferometer: Part II, Instrument performance. *J. Atmos. Oceanic Technol.*, **21**, 1777–1789, doi: 10.1175/JTECH-1663.1.

Koch, S.E., and W.L. Clark, 1999: A nonclassical cold front observed during COPS-91: Frontal structure and the process of severe storm initiation. *J. Atmos. Sci.*, **56**, 2862–2890, doi: 10.1175/1520-0469(1999)056<2862.

Lazzarotto, B., P. Quaglia, V. Simeonov, G. Larchevêque, H. van den Bergh, and B. Calpini, 1999: A Raman differential absorption lidar for ozone and water vapor measurement in the lower troposphere. *Int. J. Environ. Anal. Chem.*, **74**, 255–261, doi: 10.1080/03067319908031430.

Lenschow, D.H., V. Wulfmeyer, and C. Senff, 2000: Measuring second- through fourth-order moments in noisy data. *J. Atmos. Oceanic Technol.*, **17**, 1330–1347, doi: 10.1175/1520-0426(2000)017<1330.

Li, Jun, Jinlong Li, J. Otkin, T.J. Schmit, and C.-Y. Liu, 2011: Warning information in a preconvection environment from the Geostationary Advanced Infrared Sounding System–A simulation study using the IHOP Case. *J. Appl. Meteor. Climatol.*, **50**, 776–783, doi: 10.1175/2010JAMC2441.1.

Liljegren J.C., S.-A. Boukabara, K. Cady-Pereira, and S.A. Clough, 2005: The effect of the half-width of the 22-GHz water vapor line on retrievals of temperature and water vapor profiles with a 12-channel microwave radiometer. *IEEE Trans. Geosci. Rem. Sens.*, **43**, 1102–1108, doi: 10.1109/TGRS.2004.839593.

Lin, P.-F., P.-L. Chang, B.J.-D. Jou, J.W. Wilson, and R.D. Roberts, 2011: Warm season afternoon thunderstorm characteristics under weak synoptic-scale forcing over Taiwan Island. *Wea. Forecasting*, **26**, 44–60, doi: 10.1175/2010WAF2222386.1.

Liu, H., and M. Xue, 2008: Prediction of convective initiation and storm evolution on 12 June 2002 during IHOP_2002: Part I, Control simulation and sensitivity experiments. *Mon. Wea. Rev.,* **136,** 2261–2282, doi: 10.1175/2007MWR2161.1.

Löhnert, U., and S. Crewell, 2003: Accuracy of cloud liquid water path from ground-based microwave radiometry, 1, Dependency on cloud model statistics. *Radio Sci.*, **38**, 8041, doi: 10.1029/2002RS002654.

Löhnert, U., S. Crewell, and C. Simmer, 2004: An integrated approach toward retrieving physically consistent profiles of temperature, humidity, and cloud liquid water. *J. Appl. Meteor.*, **43**, 1295–1307, doi: 10.1175/1520-0450(2004)043<1295.

Löhnert U., E. van Meijgaard, H.K. Baltink, S. Groß, and R. Boers, 2007: Accuracy assessment of an integrated profiling technique for operationally deriving profiles of temperature, humidity, and cloud liquid water. *J. Geophys. Res.*, **112**, D04205, doi: 10.1029/2006JD007379.

Löhnert, U., S. Crewell, O. Krasnov, E. O'Connor, and H. Russ-

chenberg, 2008: Advances in continuously profiling the thermodynamic state of the boundary layer: Integration of measurements and methods. *J. Atmos. Oceanic Technol.*, **25**, 1251–1266, doi: 10.1175/2007JTECHA961.1.

Löhnert, U., D.D. Turner, and S. Crewell, 2009: Ground-based temperature and humidity profiling using spectral infrared and microwave observations: Part I. Simulated retrieval performance in clear-sky conditions. *J. Appl. Meteor. Climatol.*, **48**, 1017–1032, doi: 10.1175/2008JAMC2060.1.

Machol, J.L., T. Ayers, K.T. Schwenz, K.W. Koenig, R.M. Hardesty, C.J. Senff, M.A. Krainak, J.B. Abshire, H.E. Bravo, and S.P. Sandberg, 2004: Preliminary measurements with an automated compact differential absorption lidar for the profiling of water vapor. *Appl. Optics,* **43**, 3110–3121, doi: 10.1364/AO.43.003110 .

Marshall, J.M., A.M. Peterson, and A.A. Barnes, Jr., 1972: Combined radar-acoustic sounding system. *Appl. Optics*, **11**, 108–112, doi: 10.1364/AO.11.000108.

Marsham, J.H., S.B. Trier, T.M. Weckwerth, and J.W. Wilson, 2011: Observations of elevated convection initiation leading to a surface-based squall line during 13 June IHOP_2002. *Mon. Wea. Rev.*, **139**, 247–271, doi: 10.1175/2010MWR3422.1.

Martin, W.J., and M. Xue, 2006: Sensitivity analysis of convection of the 24 May 2002 IHOP case using very large ensembles. *Mon. Wea. Rev.*, **134**, 192–207, doi: 10.1175/MWR3061.1.

Mayor, S.D., and S.M. Spuler, 2004: Raman-shifted eye-safe aerosol lidar. *Appl. Optics*, **43**, 3915–3924, doi: 10.1364/AO.43.003915.

McMillan, W.W., R.B. Pierce, L.C. Sparling, G. Osterman, K. McCann, M.L. Fischer, B. Rappenglück, R. Newsom, D. Turner, C. Kittaka, K. Evans, S. Biraud, B. Lefer, A. Andrews, and S. Oltmans, 2010: An observational and modeling strategy to investigate the impact of remote sources on local air quality: A Houston, Texas, case study from the Second Texas Air Quality Study (TexAQS II). *J. Geophys. Res.*, **115**, D01301, doi: 10.1029/2009JD011973.

McQueen, J.T., Y. Zhu, C.M. Tassone, M. Tsidulko, S. Liu, L. Cucurull, G. DiMego, S. Lu, M.B. Ek, W. Pendergrass, E.J. Welton, E.L. Joseph, M. Hicks, and R.M. Hoff, 2010: An overview of the NOAA/NWS/NCEP Real-Time Mesoscale Analysis (RTMA) system with extensions for the atmospheric boundary layer. Presented at the 16th Conference on Air Pollution Meteorology, 90th American Meteorological Society Annual Meeting, 17–21 January 2010, Atlanta, Georgia.

Menut, L., C. Flamant, J. Pelon, and P.H. Flamant, 1999: Urban boundary-layer height determination from lidar measurements over the Paris Area. *Appl. Optics*, **38**, 945–954, doi: 10.1364/AO.38.000945.

Miao, Q., and B. Geerts, 2007: Finescale vertical structure and dynamics of some dryline boundaries observed in IHOP. *Mon. Wea. Rev.,* **135**, 4161–4184, doi: 10.1175/2007MWR1982.1.

Minnett, P.J., R.O. Knuteson, F.A. Best, B.J. Osborne, J.A. Hanafin, and O.B. Brown, 2001: The Marine-Atmospheric Emitted Radiance Interferometer: A high-accuracy, seagoing infrared spectroradiometer. *J. Atmos. Oceanic Technol.*, **18**, 994–1013, doi: 10.1175/1520-0426(2001)018<0994.

Moninger, W.R., R.D. Mamrosh, and P.M. Pauley, 2003: Automated meteorological reports from commercial aircraft. *Bull. Amer. Meteor. Soc.*, **84**, 203–216, doi: 10.1175/BAMS-84-2-203.

Moninger, W.R., S.G. Benjamin, B.D. Jamison, T.W. Schlatter, T.L. Smith, and E.J. Szoke, 2010: Evaluation of regional aircraft observations using TAMDAR. *Wea. Forecasting*, **25**, 627–645, doi: 10.1175/2009WAF2222321.1.

Münkel, C., N. Eresmaa, J. Räsänen, and A. Karppinen, 2007: Retrieval of mixing height and dust concentration with lidar ceilometer. *Boundary-Layer Meteor.*, **124**, 117-128, doi: 10.1007/s10546-006-9103-3.

Murayama, T., N. Sugimoto, I. Uno, K. Kinoshita, K. Aoki, N. Hagiwara, Z. Liu, I. Matsui, T. Sakai, T. Shibata, K. Arao, B.-J. Sohn, J.-G. Won, S.-C. Yoon, T. Li, J. Zhou, H. Hu, M. Abo, K. Iokibe, R. Koga, and Y. Iwasaka, 2001: Ground-based network observation of Asian dust events of April 1998 in east Asia. *J. Geophys. Res.*, **106**, 18,345–18,359, doi: 10.1029/2000JD900554.

Murphey, H.V., R.M. Wakimoto, C. Flamant, and D.E. Kingsmill, 2006: Dryline on 19 June 2002 during IHOP, Part I. Airborne Doppler and LEANDRE II analyses of the thin line structure and convection initiation. *Mon. Wea. Rev.*, **134**, 406–430, doi: 10.1175/MWR3063.1.

National Research Council, 2008, Committee on Developing Mesoscale Meteorological Observational Capabilities to Meet Multiple National Needs, *Observing Weather and Climate from the Ground Up: A Nationwide Network of Networks*, National Academies Press, Washington D.C., ISBN: 13 978-0-309-12986-2.

Nehrir, A.R., K.S. Repasky, J.L. Carlsten, M.D. Obland, and J.A. Shaw, 2009: Water vapor profiling using a widely tunable, amplified diode-laser-based Differential Absorption Lidar (DIAL). *J. Atmos. Ocean. Technol.*, **26**, 733–745 doi: 10.1175/2008JTECHA1201.1.

Nehrir, A.R., K.S. Repasky, and J.L. Carlsten, 2011: Eye-safe diode-laser-based micropulse Differential Absorption Lidar (DIAL) for water vapor profiling in the lower troposphere. *J. Atmos. Oceanic Technol.*, **28**, 131–147 doi: 10.1175/2010JTECHA1452.1.

Newsom, R.K., and D.D. Turner, 2011: Long-term evaluation of Raman lidar temperature profiles. Presented at the 5th Symposium on Lidar Atmospheric Applications, 91st American Meteorological Society Annual Meeting, 22–27 January 2011, Seattle, Washington.

North, E.M., A.M. Peterson, and H.D. Parry, 1973: RASS, a remote sensing system for measuring low-level temperature profiles. *Bull. Amer. Meteor. Soc.*, **54**, 912–919, doi: 10.1175/1520-0477(1973)054<0912.

Obland, M.D., 2007: Water vapor profiling using a widely tunable amplified diode laser differential absorption lidar (DIAL), Ph.D. Dissertation, Montana State University, Bozeman, Montana. Available at http://etd.lib.montana.edu/etd/2007/obland/OblandM0507.pdf.

Obland, M.D., K.S. Repasky, A.R. Nehrir, J.L. Carlsten, and J.A. Shaw, 2010: Development of a widely tunable amplified diode laser differential absorption lidar for profiling atmospheric water vapor. *J. Appl. Rem. Sens.*, **4**, 043515, doi: 10.1117/1.3383156.

Ostermeyer, M., P. Kappe, R. Menzel, and V. Wulfmeyer, 2005: Diode-pumped Nd:YAG master oscillator power amplifier with high pulse energy, excellent beam quality, and frequency-stabilized master oscillator as a basis for next-generation lidar system. *Appl. Optics,* **44**, 582–590, doi: 10.1364/AO.44.000582.

Padmanabhan, S., S.C., Reising, J. Vivekanandan, F. Iturbide-Sanchez, 2009, Retrieval of atmospheric water vapor density with fine spatial resolution using three-dimensional tomographic inversion of microwave brightness temperatures measured by a network of scanning compact radiometers. *IEEE Trans. Geosci. Rem. Sens.*, **47**, 3708–3721, doi: 10.1109/TGRS.2009.2031107.

Pal, S., A. Behrendt, and V. Wulfmeyer, 2010: Elastic-backscatter-lidar-based characterization of the convective boundary layer and investigation of related statistics. *Ann. Geophys.*, **28**, 825–847, doi: 10.5194/angeo-28-825-2010.

Pappalardo, G., A. Amadeo, M. Pandolfi, U. Wandinger, A. Ansmann, J. Bösenberg, V. Matthias, V. Amiridis, F. De Tomasi, M. Frioud, M. Iarlori, L. Komguem, A. Papayannis, F. Rocadenbosch, and X. Wang, 2004: Aerosol lidar intercomparison in the framework of the EARLINET Project, 3. Raman lidar algorithm for aerosol extinction, backscatter, and lidar ratio. *Appl. Optics*, **43**, 5370–5385, doi: 10.1364/AO.43.005370.

Payne V.H., J.S. Delamere, K.E. Cady-Pereira, R.R. Gamache, J.-L. Moncet, E.J. Mlawer, and S.A. Clough, 2008: Air-broadened half-widths of the 22- and 183-GHz water-vapor lines. *IEEE Trans. Geosci. Rem. Sens.*, **46**, 3601–3617, doi: 10.1109/TGRS.2008.2002435.

Payne, V.H., E.J. Mlawer, K.E. Cady-Pereira, and J. Moncet, 2011: Water vapor continuum absorption in the microwave. *IEEE Trans. Geosci. Rem. Sens.*, **49**, 2194–2208, doi: 10.1109/TGRS.2010.2091416.

Piironen, A.K., and E.W. Eloranta, 1995: Convective boundary layer mean depths and cloud geometrical properties obtained from volume imaging lidar data. *J. Geophys. Res.,* **100**, D12, 25,569–25,576, doi: 10.1029/94JD02604.

Poli, P., J. Joiner, and E.R. Kursinski, 2002: 1DVAR analysis of temperature and humidity using GPS radio occultation refractivity data. *J. Geophys. Res.*, **107**, 4448, doi: 10.1029/2001JD000935.

Radlach, M., A. Behrendt, and V. Wulfmeyer, 2008: Scanning rotational Raman lidar at 355 nm for the measurement of tropospheric temperature fields. *Atmos. Chem. Phys*. **8**, 159–169, doi: 10.5194/acp-8-159-2008.

Rall, J.A.R., 1994: Differential absorption lidar measurements of atmospheric water vapor using a pseudonoise code modulated AlGaAs laser, NASA Technical Memorandum 104610, NASA Center for AeroSpace Information, Linthicum Heights, Maryland.

Raut, J.-C., and P. Chazette, 2009: Assessment of vertically-resolved PM_{10} from mobile lidar observations. *Atmos. Chem. Phys.*, **9**, 8617–8638, doi: 10.5194/acp-9-8617-2009.

Repasky K.S., J.A. Reagan, A.R. Nehrir, D.S. Hoffman, M.H. Thomas, J.L. Carlsten, J.A. Shaw, and G.E. Shaw, 2011: Observational studies of atmospheric aerosols over Bozeman, Montana, using a two-color lidar, a water vapor DIAL, a solar radiometer, and a ground-based nephelometer over a 24-h period. *J. Atmos. Oceanic Technol.*, **28**, 320–336, doi: 10.1175/2010JTECHA1463.1.

Revercomb, H.E., H. Buijs, H.B. Howell, D.D. LaPorte, W.L. Smith, and L.A. Sromovsky, 1988: Radiometric calibration of IR Fourier transform spectrometers: Solution to a problem with the High-Resolution Interferometer Sounder. *Appl. Optics*, **27**, 3210–3218, doi: 10.1364/AO.27.003210.

Richardson, Y.P., K.K. Droegemeier, and R.P. Davies-Jones, 2007: The influence of horizontal environmental variability on numerically simulated convective storms, Part I. Variations in vertical shear. *Mon. Wea. Rev*., **135**, 3429–3455, doi: 10.1175/MWR3463.1.

Roberts, R.D., E. Nelson, J.W. Wilson, N. Rehak, J. Sun, S. Ellis, T. Weckwerth, F. Fabry, P.C. Kennedy, J. Fritz, V. Chandrasekar, S. Reising, S. Padmanabhan, J. Braun, T. Crum, L. Mooney, and R. Palmer, 2008: REFRACTT 2006 Real-time retrieval of high-resolution, low-level moisture fields from operational NEXRAD and research radars. *Bull. Amer. Meteor. Soc.*, **89**, 1535–1548, doi: 10.1175/2008BAMS2412.1.

Rodgers, C.D., *Inverse Methods for Atmospheric Sounding: Theory and Practice*, World Scientific, 256 pp., ISBN: 978-981-02-2740-1, 2000.

Rothman, L.S., I.E. Gordon, A. Barbe, D.C. Benner, P.F. Bernath, M. Birk, V. Boudon, L.R. Brown, A. Campargue, J.-P. Champion, K. Chance, L.H. Coudert, V. Dana, V.M. Devi, S. Fally, J.-M. Flaud, R.R. Gamache, A. Goldman, D. Jacquemart, I. Kleiner, N. Lacome, W.J. Lafferty, J.-Y. Mandin, S.T. Massie, S.N. Mikhailenka, C.E. Miller, N. Moazzen-Ahmadi, O.V. Naumenko, A.V. Nikitin, J. Orphal, V.I. Perevalov, A. Perrin, A. Predoi-Cross, C.P. Rinsland, M. Rotger, M. Šimečhková, M.A.H. Smith, K. Sung, S.A. Tashkun, J. Tennyson, R.A. Toth, A.C. Vandaele, and J. Vander Auwera, 2009: The HITRAN 2008 molecular spectroscopic database. *J. Quant. Spectrosc. Radiat. Trans.*, **110**, 533–572, doi: 10.1016/j.jqsrt.2009.02.013.

Rüeger, J.M., Refractive index formulae for radio waves. XXII International Congress of the International Federation of Surveyors (FIG), Washington, D.C., 19–26 April 2002, Technical Program Session J28, 2000.

Russo, F., 2007: *An investigation of Raman lidar measurements and their application to the study of the aerosol indirect effect*, Ph.D. Thesis, University of Maryland, Baltimore County, Baltimore, Maryland.

Schwitalla, T., H.-S. Bauer, V. Wulfmeyer, and F. Aoshima, 2011: High-resolution simulation over central Europe: Assimilation experiments during COPS IOP9c. COPS Special Issue of the *Q. J. R. Meteor. Soc.*, **137**(S1), 156–175, doi: 10.1002/qj.721.

Smith, W.L, W.F. Feltz, R.O. Knuteson, H.E. Revercomb, H.M. Woolf, and H.B. Howell, 1999: The retrieval of planetary boundary layer structure using ground-based infrared spectral radiance measurements. *J. Atmos. Oceanic Technol.*, **16**, 323–333, doi: 10.1175/1520-0426(1999)016<0323.

Stankov, B.B., E.E. Gossard, B.L. Weber, R.J. Lataitis, A.B. White, D.E. Wolfe, D.C. Welsh, and R.G. Strauch, 2003: Humidity gradient profiles from wind profiling radars using the NOAA/ETL advanced signal processing system (SPS). *J. Atmos. Oceanic Technol.*, **20,** 3–22, doi: 10.1175/1520-0426(2003)020<0003.

Steyn, D.G., M. Baldi, and R.M Hoff, 1999: The detection of mixed layer depth and entrainment zone thickness from lidar backscatter profiles. *J. Atmos. Oceanic Technol.*, **16**, 953–959, doi: 10.1175/1520-0426(1999)016<0953.

Sun, J., and Y. Zhang, 2008: Analysis and prediction of a squall line observed during iHOP using multiple WSR-88D observations. *Mon. Wea. Rev.*, **136**, 2364–2388.

Tobin, D.C., F.A. Best, P.D. Brown, S.A. Clough, R.G. Dedecker, R.G. Ellingson, R.K. Garcia, H.B. Howell, R.O. Knuteson, E.J. Mlawer, H.E. Revercomb, J.F. Short, P.F.W. van Deist, and V.P. Walden, 1999: Downwelling spectral radiance observations at the SHEBA ice station: Water vapor continuum measurements from 17 to 26 μm. *J. Geophys. Res.*, **104**, D2, 2081–2092, doi: 10.1029/1998JD200057.

Turetsky, M.R., E.S. Kane, J.W. Harden, R.D. Ottmar, K.L. Manies, E. Hoy, and E.S. Kasischke, 2011: Recent acceleration of biomass burning and carbon losses in Alaskan forests and peatlands, *Nature Geosci.*, **4**, 27–31, doi: 10.1038/ngeo1027.

Turner, D.D., 2005: Arctic mixed-phase cloud properties from AERI lidar observations: Algorithm and results from SHEBA. *J. Appl. Meteor.*, **44**, 427–444, doi: 10.1175/JAM2208.1.

Turner, D.D., 2007: Improved ground-based liquid water path retrievals using a combined infrared and microwave approach. *J. Geophys. Res.*, **112**, D15204, doi: 10.1029/2007JD008530.

Turner, D.D., 2008: Ground-based infrared retrievals of optical depth, effective radius, and composition of airborne mineral dust above the Sahel. *J. Geophys. Res.*, **113**, D00E03, doi: 10.1029/2008JD010054.

Turner, D.D., and J.E.M. Goldsmith, 2005: The refurbishment and upgrade of the Atmospheric Radiation Measurement Raman lidar. Proceedings of the Fifteenth Atmospheric Radiation Measurement (ARM) Science Team meeting, 14–18 March 2005, Daytona Beach, Florida.

Turner, D.D., and P.J. Gero, 2011: Downwelling 10 μm radiance temperature climatology for the Atmospheric Radiation Measurement Southern Great Plains site. *J. Geophys. Res.*, **116**, D08212, doi: 10.1029/2010JD015135.

Turner, D.D., W.F. Feltz, and R.A. Ferrare, 2000: Continuous water profiles from operational ground-based active and passive remote sensors. *Bull. Amer. Meteor. Soc.*, **81**, 1301–1317, doi: 10.1175/1520-0477(2000)081<1301.

Turner, D.D., R.A. Ferrare, L.A. Heilman Brasseur, W.F. Feltz, and T.P. Tooman, 2002: Automated retrievals of water vapor and aerosol profiles from an operational Raman lidar. *J. Atmos. Oceanic Technol.*, **19**, 37–50.

Turner, D.D., R.O. Knuteson, H.E. Revercomb, C. Lo, and R.G. Dedecker, 2006: Noise reduction of Atmospheric Emitted Radiance Interferometer (AERI) observations using principal component analysis. *J. Atmos. Oceanic Technol.*, **23**, 1223–1238, doi: 10.1175/JTECH1906.1.

Van der Kamp, D., and I.G. McKendry, 2010: Comparison of tethered balloon vertical profiles of particulate matter size distributions with lidar ceilometer backscatter in the nocturnal urban boundary layer. *Int. J. Environ. Pollut.*, **41**, 155–165, doi: 10.1504/IJEP.2010.032251.

Venable, D.D., D.N. Whiteman, M.N. Calhoun, A.O. Dirisu, R.M. Connell, and E. Landulfo, 2011: Lamp mapping technique for independent determination of the water vapor mixing ratio calibration factor for a Raman lidar system. *Appl. Optics*, **50**, 4622–4632, doi: 10.1364/AO.50.004622.

Veselovskii, I., D.N. Whiteman, A. Kolgotin, E. Andrews, and M. Korenskii, 2009: Demonstration of aerosol property profiling by multiwavelength lidar under varying relative humidity conditions. *J. Atmos. Oceanic Technol.*, **26**, 1543–1557, doi: 10.1175/2009JTECHA1254.1.

Vogelmann, H., and Tricki, T., 2008. Wide-range sounding of free-tropospheric water vapor with a differential-absorption lidar (DIAL) at a high-altitude station. *Appl. Optics*, **47**(12), 2116–2132.

Vogelmann, H., R. Sussmann, T. Tricki, and T. Borsdorff, 2011. Intercomparison of atmospheric water vapor soundings from the differential absorption lidar (DIAL) and the solar FTIR system on Mt. Zugspitze. *Atmos. Meas. Tech.,* **4**, 835–841, doi: 10.5194/amt-4-835-2011.

Wagner, T.J., W.F. Feltz, and S.A. Ackerman, 2008: The temporal evolution of convective indices in storm-producing environments. *Wea. Forecasting*, **23**, 786–794, doi: 10.1175/2008WAF2007046.1.

Wakimoto, R.M., and H.V. Murphey, 2010: Analysis of convergence boundaries observed during IHOP_2002. *Mon. Wea. Rev.*, **138**, 2737–2760, doi: 10.1175/2010MWR3266.1.

Ware, R., C. Rocken, F. Solheim, M. Exner, W. Schreiner, R. Anthes, D. Feng, B. Herman, M. Gorbunov, S. Sokolovskiy, K. Hardy, Y. Kuo, X. Zou, K. Trenberth, T. Meehan, W. Melbourne, and S. Businger, 1996: GPS sounding of the atmosphere from low earth orbit: Preliminary results. *Bull. Amer. Meteor. Soc.*, **77**, 19–40, doi: 10.1175/1520-0477(1996)077<0019.

Ware, R.H., D.W. Fulker, S.A. Stein, D.N. Anderson, S.K. Avery, R.D. Clark, K.K. Droegemeier, J.P. Kuettner, J.B. Minster, and S. Sorooshian, 2000: SuomiNet: A real-time national GPS network for atmospheric research and education. *Bull. Amer. Meteor. Soc.*, **81**, 677–694, doi: 10.1175/1520-0477(2000)081<0677.

Weckwerth, T.M., 2000: The effect of small-scale moisture variability on thunderstorm initiation. *Mon. Wea. Rev*., **128**, 4017–4030, doi: 10.1175/1520-0493(2000)129<4017.

Weckwerth, T.M., V. Wulfmeyer, R.M. Wakimoto, R.M. Hardesty, J.W. Wilson, and R.M. Banta, 1999: NCAR-NOAA lower-tropospheric water vapor workshop. *Bull. Amer. Meteor. Soc.*, **80**, 2339–2357, doi: 10.1175/1520-0477(1999)080<2339.

Weckwerth, T.M., D.B. Parsons, S.E. Koch, J.A. Moore, M.A. LeMone, B.B. Demoz, C. Flamant, B. Geerts, J. Wang, and W.F. Feltz, 2004: An overview of the International H_2O Project (IHOP_2002) and some preliminary highlights. *Bull. Amer. Meteor. Soc.*, **85**, 253–277, doi: 10.1175/BAMS-85-2-253.

Weckwerth, T.M., C.R. Pettet, F. Fabry, S.J. Park, M.A. LeMone, and J.W. Wilson, 2005: Radar refractivity retrieval: Validation and application to short-term forecasting. *J. Appl. Meteor.*, **44**, 285–300, doi: 10.1175/JAM-2204.1.

Welton, E.J., J.R. Campbell, J.D. Spinhirne, and V.S. Scott, 2001: Global monitoring of clouds and aerosols using a network of micro-pulse lidar systems, in *Lidar Remote Sensing for Industry and Environmental Monitoring*; U.N. Singh, T. Itabe, N. Sugimoto, (eds.); Proc. SPIE, **4153**, 151-158.

Whiteman, D.N., 2003a: Examination of the traditional Raman lidar technique, I. Evaluating the temperature-dependent lidar equations. *Appl. Optics*, **42**, 2571-2592, doi: 10.1364/AO.42.002571.

Whiteman, D.N., 2003b: Examination of the traditional Raman lidar technique: II. Evaluating the ratios for water vapor and aerosols. *Appl. Optics*, **42**, 2593–2608, doi: 10.1364/AO.42.002593.

Whiteman, D.N., B. Demoz, K. Rush, G. Schwemmer, B. Gentry, P. Di Girolamo, J. Comer, I. Veselovskii, K. Evans, S.H. Melfi, Z. Wang, M. Cadirola, B. Mielke, D. Venable, and T. Van Hove, 2006: Raman lidar measurements during the International H_2O Project: Part I. Instrumentation and analysis techniques. *J. Atmos. Oceanic Technol.,* **23**, 157–169, doi: 10.1175/JTECH1838.1.

Wilczak, J.M., E.E. Gossard, W.D. Neff, and W.L. Eberhard, 1996: Ground-based remote sensing of the atmospheric boundary layer: 25 years of progress. *Boundary-Layer Meteorol.*, **78**, 321–349, doi: 10.1007/BF000120940.

Wilson, J.W., and W.E. Schreiber, 1986: Initiation of convective storms at radar-observed boundary-layer convergence lines. *Mon. Wea. Rev*., **114**, 2516–1536, doi: 10.1175/1520-0493(1986)114<2516.

Wilson, J.W., and R.D. Roberts, 2006: Summary of convective storm initiation and evolution during IHOP: Observational and modeling perspective. *Mon. Wea. Rev.*, **134**, 23–47, doi: 10.1175/MWR3069.1.

WMO: Plan for the implementation of the GAW Aerosol Lidar Observation Network: GALION, GAW Report No. 178, 45 pp., Hamburg, Germany, 27–29 March 2007.

Wulfmeyer, V., 1998: Ground-based differential absorption lidar for water-vapor and temperature profiling: Development and specifications of a high-performance laser transmitter. *Appl. Optics*, **37**, 3804–3824, doi: 10.1364/AO.37.003804.

Wulfmeyer, V., 1999a: Investigation of turbulent processes in the lower troposphere with water vapor DIAL and Radar-RASS. *J. Atmos. Sci*., **56**, 1055–1076, doi: 10.1175/1520-0469(1999)056<1055.

Wulfmeyer, V., 1999b: Investigations of humidity skewness and variance profiles in the convective boundary layer and comparison of the latter with large eddy simulation results. *J. Atmos. Sci*. **56**, 1077–1087, doi: 10.1175/1520-0469(1999)056<1077.

Wulfmeyer, V., and J. Bösenberg, 1998: Ground-based differential absorption lidar for water-vapor profiling: Assessment of accuracy, resolution, and meteorological applications. *Appl. Optics*, **37**, 3825–3844, doi: 10.1364/AO.37.003825.

Wulfmeyer, V., and C. Walther, 2001a: Future performance of ground-based and airborne water-vapor differential absorption lidar, I. Overview and theory. *Appl. Optics*, **40**, 5304–5320, doi: 10.1364/AO.40.005304.

Wulfmeyer, V., and C. Walther, 2001b: Future performance of ground-based and airborne water-vapor differential absorption lidar: II. Simulations of the precision of a near-infrared, high-power system. *Appl. Optics*, **40**, 5321–5336, doi: 10.1364/AO.40.005321.

Wulfmeyer, V., H.-S. Bauer, M. Grzeschik, A. Behrendt, F. Vandenberghe, E.V. Browell, S. Ismaikl, and R.A. Ferrare, 2006: Four-dimensional variational assimilation of water vapor differential absorption lidar data: The first case study within IHOP_2002. *Mon. Wea. Rev.*, **134**, 209–230, doi: 10.1175/MWR3070.1.

Wulfmeyer, V., A. Behrendt, and H.-S. Bauer, C. Kottmeier, U. Corsmeier, A. Blyth, G. Craig, U. Schumann, M. Hagen, S. Crewell, P. Di Girolamo, C. Flamant, M. Miller, A. Montani, S. Mobbs, E. Richard, M.W. Rotach, M. Arpagaus, H. Russchenberg, P. Schlüssel, M. König,, V. Gärtner, R. Steinacker, M. Dorninger, D.D. Turner, T. Weckwerth, A. Hense, and C. Simmer, 2008: Reserach Campaign: The Convective and Orographically Induced Precipitation Study: A research and development project of the World Weather Research Program for improving quantitative precipitation forecasting in low-mountain regions. *Bull. Amer. Meteor. Soc*., **89**, 1477–1486, doi: 10.1175/2008BAMS2367.1

Wulfmeyer, V., D.D. Turner, S. Pal, and E. Wagner, 2010: Can Water Vapor Raman Lidar Resolve Profiles of Turbulent Variables in the Convective Boundary Layer? *Boundary-layer Meteorol.* **136**, 253-284, doi:10.1007/s10546-010-9494-z.

Wulfmeyer, V., A. Behrendt, Ch. Kottmeier, U. Corsmeier, C. Barthlott, G.C. Craig, M. Hagen, D. Althausen, F. Aoshima, M. Arpagaus, H.-S. Bauer, L. Bennett, A. Blyth, C. Brandau, C. Champollion, S. Crewell, G. Dick, P. Di Girolamo, M. Dorninger, Y. Dufournet, R. Eigenmann, R. Engelmann, C. Flamant, T. Foken, T. Gorgas, M. Grzeschik, J. Handwerker, C. Hauck, H. Höller, W. Junkermann, N. Kalthoff, C. Kiemle, S. Klink, M. König, L. Krauss, C.N. Long, F. Madonna, S. Mobbs, B. Neininger, S. Pal, G. Peters, G. Pigeon, E. Richard, M.W. Rotach, H. Russchenberg, T. Schwitalla, V. Smith, R. Steinacker, J. Trentmann, D.D. Turner, J. van Baelen, S. Vogt, H. Volkert, T. Weckwerth, H. Wernli, A. Wieser, and M. Wirth, 2011: The Convective and Orographically Induced Precipitation Study (COPS): The scientific strategy, the field phase, and first highlights. COPS Special Issue of the *Q. J. R. Meteor. Soc.,* **137**, 3–30, doi: 10.1002/qj.752.

Yan, X., V. Ducrocq, G. Jaubert, P. Brousseau, P. Poli C. Champollion, C. Flamant, and K. Boniface, 2009: The benefit of GPS zenith delay assimilation to high-resolution quantitative precipitation forecasts: A case-study from COPS IOP 9. *Q. J. Roy. Meteor. Soc.*, **135**, 1788–1800, doi: 10.1002/qj.508.

Yurganov, L., W. McMillan, C. Wilson, M. Fischer, S. Biraud, and C. Sweeney, 2010: Carbon monoxide mixing ratios over Oklahoma between 2002 and 2009 retrieved from Atmospheric Emitted Radiance Interferometer spectra. *Atmos. Meas. Tech.*, **3**, 1319–1331, doi: 10.5194/amt-3-1319-2010.

Ziegler, C.L., E.R. Mansell, J.M. Straka, D.R. MacGorman, and D.W. Burgess, 2010: The impact of spatial variations of low-level stability on the life cycle of a simulated supercell storm. *Mon. Wea. Rev*., **138**, 1738–1766, doi: 10.1175/2009MWR3010.1.

Zus, F., M. Grzeschik, H.-S. Bauer, V. Wulfmeyer, G. Dick, and M. Bender, 2008: Development and optimization of the IPM MM5 GPS slant path 4DVAR system. *Meteorol. Z.*, **17**, 867–885, doi: 10.1127/0941-2948/2008/0339.

Acknowledgements

The workshop organizers would like to thank the following NCAR Earth Observing Laboratory (EOL) staff for their excellent work in preparing for and executing the workshop.

Geoff Cheesemann
Tammy Kepple
Patricia Kidd
Sara Metz
Julie Petro
Jan Wilmesmeier
Shelley Zucker

We also thank Sue Schauffler for her unwavering support as the Acting EOL Director and Debra Dailey-Fisher of NOAA Earth System Research Laboratory Chemical Sciences Division for her diligence in completing the graphic design and layout of this report.

Sponsorship of the National Science Foundation was provided in part by Facilities for Atmospheric and Earth Science Research (FAESR). FAESR is the online resource of facilities and instruments used by the atmospheric and earth system research communities.

Appendix A

Workshop Participation List
Boulder, Colorado
12-14 April 2011

Tom Ackerman	University of Washington ackerman@atmos.washington.edu	USA
Phillip Acott	Ophir Corporation phila@ophir.com	USA
Robert Banta	NOAA ESRL Chemical Sciences Division robert.banta@noaa.gov	USA
Idar Barstad	Bjerknes Centre for Climate Research Idar.Barstad@uni.no	Norway
Angela Benedetti	European Centre for Medium-Range Weather Forecasts Angela.Benedetti@ecmwf.int	United Kingdom
Don Berchoff	National Weather Service Office of Science and Technology don.berchoff@noaa.gov	USA
Kristen Bond	Metropolitan State University kbond8@mscd.edu	USA
Jean-Pierre Bouchard	INO jean-pierre.bouchard@ino.ca	Canada
Thomas Bourcy	Météo-France thomas.bourcy@meteo.fr	France
William Brown	National Center for Atmospheric Research Earth Observing Laboratory wbrown@ucar.edu	USA
C. Baker Bruce	NOAA - Atmospheric Turbulence and Diffusion Division Bruce.Baker@noaa.gov	USA
Loren Caldwell	Ophir Corporation caldwell@ophir.com	USA
William Callahan	Earth Networks bcallahan@earthnetworks.com	USA
Rit Carbone	National Center for Atmospheric Research carbone@ucar.edu	USA
Gregory Carmichael	University of Iowa gcarmich@engineering.uiowa.edu	USA
Fred Carr	University of Oklahoma fcarr@ou.edu	USA
Laurent Cazenave	Délégation Générale pour l'Armement laurent-cazenave@wanadoo.fr	France
Phillip Chilson	University of Oklahoma, School of Meteorology chilson@ou.edu	USA
Domenico Cimini	IMAA-CNR Istituto di Metodologie per l'Analisi Ambientale (IMAA), Department of Earth and Environment of the Italian National Research Council (CNR) nico.cimini@aquila.infn.it	Italy
Steve Cohn	National Center for Atmospheric Research cohn@ucar.edu	USA
Jaime Compton	University of Maryland, Baltimore County compton1@umbc.edu	USA
William Cottingame	Northrop Grumman Aerospace Systems william.cottingame@ngc.com	USA
Susanne Crewell	Universität zu Köln crewell@meteo.uni-koeln.de	Germany
Walter Dabberdt	Vaisala Group walter.dabberdt@vaisala.com	Finland
Belay Demoz	Howard University bbdemoz@howard.edu	USA

Frederic Fabry	McGill University frederic.fabry@mcgill.ca	Canada
Joseph Facundo	NOAA National Weather Service Joseph.Facundo@noaa.gov	USA
Wayne Feltz	University of Wisconsin at Madison, Cooperative Institute for Meteorological Satellite Studies (CIMSS) Space Science and Engineering Center (SSEC) wayne.feltz@ssec.wisc.edu	USA
George Frederick	Falcon Consultants, LLC george.frederick@vaisala.com	USA
Bart Geerts	University of Wyoming geerts@uwyo.edu	USA
Gary Gimmestad	Georgia Institute of Technology gary.gimmestad@gtri.gatech.edu	USA
Ismail Guiltepe	Environnement Canada Ismail.Gultepe@ec.gc.ca	Canada
John Hanesiak	University of Manitoba john_hanesiak@umanitoba.ca	Canada
Michael Hardesty	NOAA Earth System Reseaboratory Chemical Sciences Division Mike.Hardesty@noaa.gov	USA
David Helms	NOAA National Weather Service david.helms@noaa.gov	USA
Michel Hicks	Howard University and NOAA National Weather Service Mhicks2011@gmail.com	USA
Raymond Hoff	University of Maryland, Baltimore County hoff@umbc.edu	USA
Chin Huang	Bureau of Ocean Energy Management chester.huang@mms.gov	USA
Syed Ismail	NASA Langley Research Center syed.ismail-1@nasa.gov	USA
Everette Joseph	Howard University ejosgm@gmail.com	USA
Vivekanandan Jothiram	National Center for Atmospheric Research vivek@ucar.edu	USA
Sebastian Kauczok	Selex Systems Integration GmbH s.kauczok@selex-si.de	Germany
Gene Keluche	University Corporation for Atmospheric Research Foundation, Member of the Board of Directors wintun600@aol.com	USA
Marian Klein	Boulder Environmental Sciences and Technology, LLC marian.klein@boulderest.com	USA
Kevin Knupp	University of Alabama in Huntsville kevin@nsstc.uah.edu	USA
Steven Koch	NOAA Earth System Research Laboratory Global Systems Division Steven.Koch@noaa.gov	USA
Nofel Lagrosas	Ateneo de Manila University, Physics Department nofel@observatory.ph	Philippines
Richard Lataitis	NOAA ESRL Physical Sciences Division Richard.Lataitis@noaa.gov	USA
Thierry Leblanc	Jet Propulsion Laboratory, California Institute of Technology leblanc@tmf.jpl.nasa.gov	USA
Robert Lee	Hampton University robertbenjaminleeiii@yahoo.com	USA
Eric Loew	National Center for Atmospheric Research ericloew@ucar.edu	USA
Scott McLaughlin	DeTect, Inc. scott.mclaughlin@detect-inc.com	USA
Amin Nehrir	Montana State University arnehrir@gmail.com	USA
Ralph Petersen	University of Wisconsin, Cooperative Institute for Meteorological Satellite Studies Ralph.Petersen@ssec.wisc.edu	USA

Kevin Petty	Vaisala Group kevin.petty@vaisala.com	Finland
Adrien Quesnel	Leosphere aquesnel@leosphere.fr	France
Kevin Repasky	Montana State University repasky@ece.montana.edu	USA
Luc Rochette	LR Technologies, Inc. luc.rochette@lrtech.ca	USA
Claude Roy	The ABB Group claude.b.roy@ca.abb.com	Switzerland/Sweden
Dominique Ruffieux	Federal Office of Meteorology and Climatology MeteoSwiss dominique.ruffieux@meteoswiss.ch	Switzerland
Laurent Sauvage	NRG Systems and Leosphere lsauvage@leosphere.fr	USA/France
Robert Serafin	National Center for Atmospheric Research Earth Observing Laboratory serafin@ucar.edu	USA
Nir Shiloah	IIBR (Sabbatical in NCAR/UCAR) shiloah.nir@gmail.com	USA
Doug Sisterson	Argonne National Laboratory dlsisterson@anl.gov	USA
David Sonnenfroh	Physical Sciences, Inc. sonnenfroh@psicorp.com	USA
Lisa Spaeth	Ophir Corporation lisas@ophir.com	USA
Scott Spuler	National Center for Atmospheric Research spuler@ucar.edu	USA
David Stensrud	NOAA National Severe Storms Laboratory david.stensrud@noaa.gov	USA
David Turner	NOAA National Severe Storms Laboratory dave.turner@noaa.gov	USA
Junhong Wang	National Center for Atmospheric Research junhong@ucar.edu	USA
Zhien Wang	University of Wyoming zwang@uwyo.edu	USA
Randolph “Stick” Ware	Radiometrics Corporation ware@radiometrics.com	USA
Tammy Weckwerth	National Center for Atmospheric Research Earth Observing Laboratory tammy@ucar.edu	USA
Ellsworth Welton	NASA ellsworth.j.welton@nasa.gov	USA
Allen White	NOAA ESRL Physical Sciences Division allen.b.white@noaa.gov	USA
David Whiteman	NASA Goddard Space Flight Center david.n.whiteman@nasa.gov	USA
Phillip Wiker	Department of Air Quality and Environmental Management, Clark County, Nevada wiker@clarkcountynv.gov	USA
Tim Wilfong	Tim Wilfog and Associates, LLC timwilfong@comcast.net	USA
Volker Wulfmeyer	Universität Hohenheim volker.wulfmeyer@uni-hohenheim.de	Germany
Neil Wyse	NOAA National Environmental Satellite, Data, and Information Service, Office of Systems Development Neil.Wyse@noaa.gov	USA
Masanori Yabuki	Kyoto University yabuki@rish.kyoto-u.ac.jp	Japan
Young Yee	Mkey Technologies, LLC yyee@aol.com	USA
Alexander Zucconi	Environnement Canada Alexander.Zucconi@ec.gc.ca	Canada

Appendix B

Acronyms and Abbreviations

Acronyms	Definition
1DVAR	One-Dimensional Variational Retrieval
3D	Three-Dimensional
3DVAR	Three-Dimensional Variational Retrieval
4D	Four-Dimensional
4DVAR	Four-Dimensional Variational Retrieval
ABL	Atmospheric Boundary Layer
ACARS	Aircraft Communications Addressing and Reporting System
AERI	Atmospheric Emitted Radiance Interferometer
AMDAR	Aircraft Communication Addressing and Reporting System
AMDAR	Aircraft Meteorological Data Reports
AMF	ARM Mobile Facility
AMF1	First ARM Mobile Facility
ARM	Atmospheric Radiation Measurement Program (DOE)
ASOS	Automated Surface Observing System
BL	Boundary Layer
CAPE	Convective Available Potential Energy
CARL	Cloud and Radiation Testbed Atmospheric Raman Lidar
CART	Cloud and Radiation Testbed
CASA	Collaborative Adaptive Sensing of the Atmosphere
CIN	Convective inhibition
COPS	Convective Orographically-induced Precipitation Study
COSMIC	Constellation Observing System for Meteorology, Ionosphere & Climate (UCAR)
COST	Cooperation of Scientific and Technical Research (European)t
DA	Data Assimilation
DHS	U.S. Department of Homeland Security
DIAL	Differential Absorption Lidar
DIAR	Differential Attenuation Radar
DOE	U.S. Department of Energy
DWD	German Weather Service
EARLINET	European Aerosol Research Lidar Network
EG-CLIMET	European Ground-Based Observations of Essential Variables for Climate Meteorology
EPA	U.S. Environmental Protection Agency
ESA	European Space Agency
EUMETSAT	European Organisation for the Exploitation of Meteorological Satellites
FAA	Federal Aviation Agency (USA)
FORMOSAT-3	Taiwan's Formosa Satellite Mission #3
FOV	Field of View
GALION	GAW Aerosol Lidar Observation Network (WMO)
GAW	Global Atmospheric Watch (WMO)
GNSS	Global Navigation Satellite Systems
GPS	Global Positioning System

GPS-MET	Global Positioning System Meteorology Program
GSFC	(NASA) Goddard Space Flight Center
GSM	Global System for Mobile Communications
HCRs	Horizontal Convective Rolls
HI_TRAN	High Resolution Transmission Molecular Absorption Database
HSRL	High Spectral Resolution Lidars
HURL	Howard University (USA) Raman Lidar
IF	Intermediate Frequency
IMK-IFU	Institute for Meteorology and Climate Research-Research of the Atmospheric Environment (Germany)
IHOP	International H_2O Project
IPCC	Intergovernmental Panel on Climate Change
IPM	Institute of Physics and Meteorology (Germany)
IPW	Integrated Precipitable Water Vapor
IR	Infrared
IWV	Integrated Water Vapor
JCSDA	Joint Center for Satellite Data Assimilation (NOAA)
LAUNCH-2005	International Lindenberg Campaign for Assessment of Humidity and Cloud Profiling System (WMO)
LNA	Low Noise Amplifiers
LPT	Integrated Profiling Technique
LUAMI	Lindenberg Upper-Air Method Intercomparison
LWP	Liquid Water Path
MM5 4DAR	Pennsylvania State University/NCAR Mesoscale Model 4-dimensional Variational System
MPLNET	Micro Pulse Lidar Network (NASA)
MRAD	Milliradians
MSU	Montana State University (USA)
MTBF	Mean-Time-Bewteen-Failure
MW	Microwave
MWR	Microwave Radiometers
MWRnet	Microwave Radiometer Network
MWRP	Microwave Radiometer Profile
NASA	National Air and Space Administration
NCEP	National Centers for Environmental Prediction (NOAA)
NEXRAD	Next Generation Radar
NIR	Near infrared
NIST	National Institute of Standards and Technology
NOAA	National Oceanic and Atmospheric Administration
NRC	National Research Council
NSF	National Science Foundation
NWP	Numerical Weather Prediction
NWS	National Weather Service (NOAA)
OE	Optimal Estimation Methods
OPO	Optical Parametric Oscillator
OSE	Observing Systems Experiments
OSSE	Observing Systems Simulation Experiments
PBL	Planetary Boundary Layer
PPI	Plan Position Indicator
PWV	Precipitable Water Vapor
QA/QC	Quality Assurance/Quality Control
QPF	Quantitative Precipitation Forecasting

RALMO	Raman Lidar for Meteorological Observations
RASS	Radio Acoustic Sounding System
RDP	Research and Development Project
RFI	Radio Frequency Interference
RRL	Rotational Raman Lidar
RUC	Rapid Update Cycle
SGP	Southern Great Plains (USA)
SNR	Signal-to-Noise Ratio
TAMDAR	Tropospheric Aircraft Meteorological Data Reports
TPT	Thermodynamic Profiling of the Troposphere
UAV	Unmanned Aerial Vehicles
UCAR	University Corporation for Atmospheric Research (USA)
UHF	Ultra High Frequency
UHOH	University of Hohenheim (Germany)
USWRP	U.S. Weather Research Program (a NOAA Program)
UT	Upper Troposphere
UTC	Coordinated Universal Time
UV	Ultraviolet
UW	University of Wisconsin (USA)
WFO	Weather Field Office
WMO	World Meteorological Organization
WRF	Weather Research Forecast (model)
WSR-88	Weather Surveillance Radar 88
WV	Water Vapor
WWRP	World Weather Research Program

Appendix C

List of Figures and Tables

Figures

Tables